J.P. van Wessem

Horizontal deformation of the High Speed Rail track

A study into the horizontal deformation of a sand embankment on asymmetrical soft soil for a high speed rail track

Case study HSL Rijpwetering

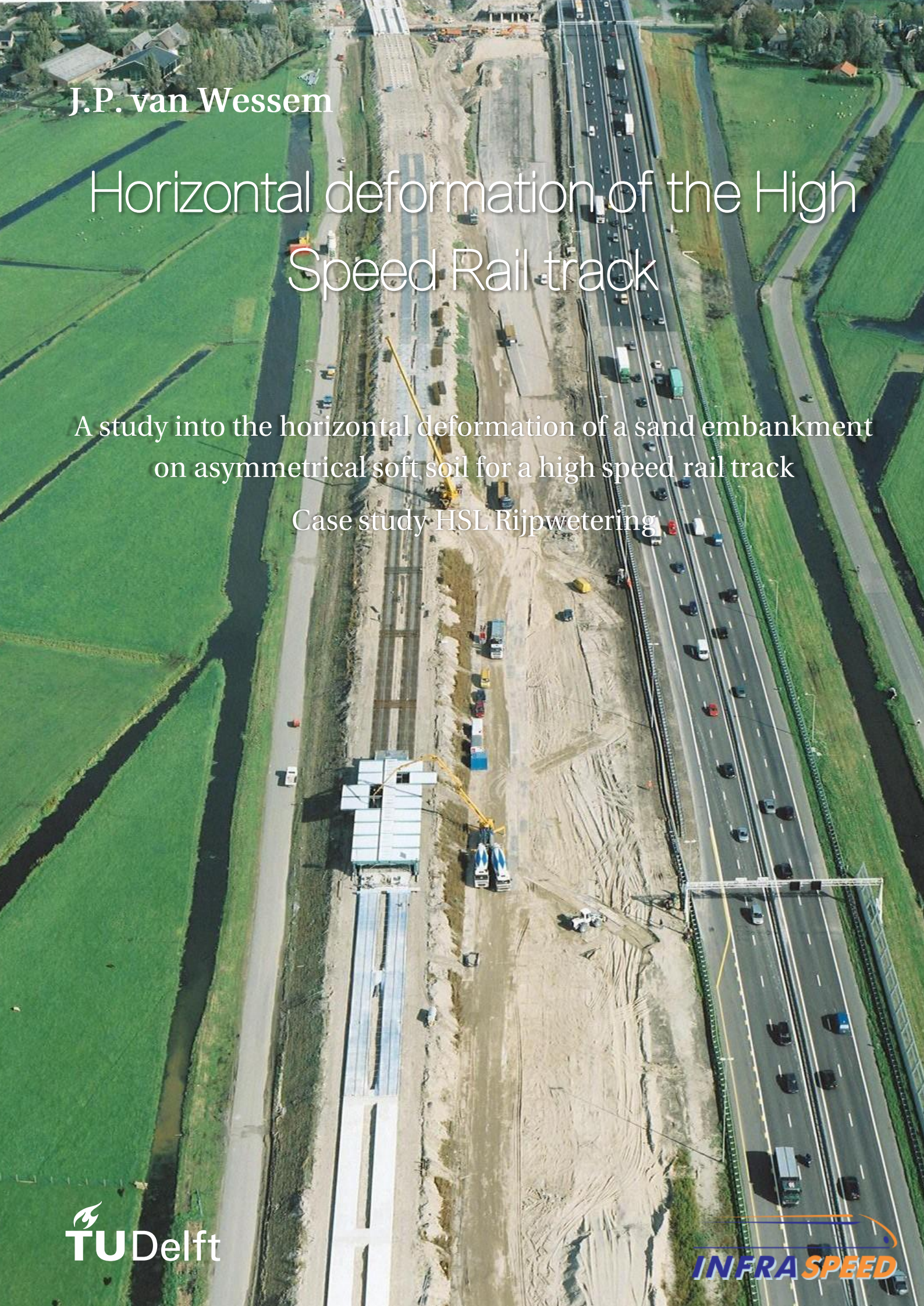

TU Delft

INFRASPEED

Horizontal deformation of the High Speed Rail track

A study into the horizontal deformation of a sand embankment on asymmetrical soft soil for a high speed rail track

Case study HSL Rijpwetering

By

J.P. van Wessem

in partial fulfilment of the requirements for the degree of

Master of Science
in Structural Engineering

with:
Road and Railway specialisation,
Railway Systems Engineering annotation
at the Delft University of Technology

Chairman:	Dr. V.L. Markine	TUDelft
Thesis committee:	Prof.dr.ir. R.P.B.J. Dollevoet	TUDelft
	Dr. X. Liu	TUDelft
	Ir. A.A. Hertogs	Infraspeed Maintenance BV
	Dr.ir. M. Dušков	InfraDelft BV

Student number: 4100727

Email: jeroen_van_wessem@hotmail.com

To be defended publicly on Thursday May 14th 2020 at 15:30

Cover image: aerial view of the construction of the HSL-zuid https://beeldbank.rws.nl/

TU Delft Delft University of Technology

INFRASPEED

Summary

The high speed rail line in the Netherlands, constructed since 2002, is built to create a fast travel connection from Amsterdam to Rotterdam and the Belgium border. The track is designed for trains with a maximum operating train speed of 300 km/h. A great part of the structure is founded on typical Dutch soft soils consisting of Holocene clay and peat layers. To ensure high speeds, mostly settlement free plates with a ballastless track structure are constructed to produce optimum track qualities. At the village Rijpwetering a part of the track, parallel to the highway, has shown lateral deformations since construction. This has resulted in the research question "What are the main factors driving the horizontal deformation mechanism in the high-speed rail settlement free plate structure and what measures can be taken to solve these horizontal deformations?"

The research consists of an analysis of the measurement results since 2005. From the measurement results a clear division can be made between the supported and the unsupported sections of the structure. The supported sections have almost stopped displacing in time with an average deformation rate of 0 to 0.5 mm per year. Unsupported sections show an ongoing deformation with a rate of 2.7 to 3.3 mm per year. This deformation will continue and lead to problems concerning structural safety due to bending moments in the top of the foundation pile.

To identify the mechanism, a finite element modelling of the track structure embankment is performed from which the deformation behaviour is assessed. Multiple geometrical variants are considered which lead to asymmetrical horizontal deformations. From the simulations an asymmetrical soil layer with a varying stiffness in the subsoil on either side has led to the highest deformation behaviour. In other words, an embankment partly founded on soft soils (peat) and partly on stiff soils (sand). This can be identified as the main factor driving the horizontal deformation mechanism. The combination of different variants leads to results corresponding to the field measurements.

To stop horizontal deformations the model is updated with 2 variants to observe the effectivity of the measures. One option is to apply a prestressed sheetpile wall, the other option is to reduce the structures weight with a low weight material (EPS). By applying a prestressed sheetpile in the slope of the embankment the resulting deformations can be stopped when applying a prestressing force of 100 to 150 kN. For the weight reduction, the EPS has to be placed in the slope on the soft soil. Reducing the weight with 144 kN/m or when applying EPS an area of 8.5mm^2 stops further deformations. Applying weight reduction on the side of the stiff soil will only increase the problem and deformations will grow.

Since weight reduction is usually a cheaper and a lower risk measure in comparison to prestressed sheetpile structures, it's a very interesting alternative to investigate more accurately. Depending on the surrounding structures and construction possibilities the best option can be chosen to reduce deformations in this structure and prevent deformations in future structures.

Preface

I proudly present to you my thesis report as a conclusion of the requirements to obtain the degree of Master of Science in Civil Engineering at the TUDelft.

The subject for this research was formulated in cooperation with Infraspeed Maintenance BV, as asset manager of the Dutch high speed rail track. As a graduate intern for BAM infra rail, the possibility to work on a current existing problem in the engineering practice was a great motivation for the topic.

I would like to thank Aad Hertogs from Infraspeed for the possibility and experience to work on this practical problem. From the first meeting Aad has always stood ready to help in every situation with guidance and experience, not just as a supervisor but also as a mentor. Secondly, I want to thank Xueyan Liu, Rolf Dollevoet and Milan Dušков for their willingness to take a seat in the committee. Their involvement, suggestions and criticism helped me greatly throughout the project. Also the opportunity to participate in expert meetings with ProRail and RoyalHaskoning DHV were a great experience. I would like to thank them for this possibility. Great thanks go to Valeri Markine as main supervisor during the project, an inspiring teacher in the railway courses and a friend since the workshops on railway technology in Berlin and Poznan.

Finally I would like to thank everyone that did not directly help me with this thesis, but with all the support and great fun throughout my study time. As an end of a great period in Delft a good moment to look back at so many memories. Many thanks go to: Raamstraat 1, Club Risk, PS Bestuur 120, Bargilde and all my other friends. Most importantly, I want to express the greatest gratitude towards my family and Iris for supporting me unconditionally.

J.P. (Jeroen) van Wessem
Den Haag, May 2020

Outline of the report

The main part of this report is subdivided in five parts.

Part I, Introduction, will start with a brief general explanation of the problem case. Afterwards the initiation of the research project will be explained. Combining the initiation and the initial problem analysis, the definition of the main research question is developed and followed by a set of sub-questions to accompany the main question. Part I will be finalized by explanation of the general research method.

Part II, Case study, concerns the analysis of the problems at the case study. First the structure and the construction process are analysed to observe what could be the cause of the problem. Afterwards the measurement data that is available will be introduced and assessed. Part II will be finalized by some hypotheses of the problem drawn from the measurements. These hypotheses will be the guideline for the simulation in part III.

Part III, Simulation, introduces the finite element modelling of several case studies. The case studies are several variants of geometrical differences which could lead to different results. The chapter starts with an explanation of the method and the model. Afterwards it introduces the different variants and shows the results of the simulation of these variants. The results of the simulation will be compared to each other and to the measurements of the case study. These results will give a conclusion of the main factors leading to the original problem (horizontal deformations). Finally, from the conclusion of the variant study the necessity of a model optimization is proposed. The model is optimized with new parameters and this is again compared to the measurements until the results match these measurements.

Part IV, Design of solutions, aims to find a practical solution to the problems faced in the case study. 2 different proposals are tested in the existing model to see the impact on the stability of the structure. The possible solutions are first introduced and afterwards the results are shown. Part IV is finalized with a conclusion to the solutions and briefly describes some practical considerations which are concerned with the solutions.

Part V, Conclusion and recommendation, summarizes the results of the different chapters into a general conclusion of the project. A recommendation is given towards the design of the solutions how the case study problem can be solved.

Table of contents

I. Introduction

1. General

Since 2009 the High Speed Line-south (HSL-Zuid) is in service. The HSL-Zuid is the high-speed rail line connecting Amsterdam to Rotterdam and towards the Belgium border, from there it connects to Brussels, Paris, London and the rest of Southern Europe. The high-speed line is a 125 km long railway track from Amsterdam to the Belgium border, where it connects to the Belgian HSL4.

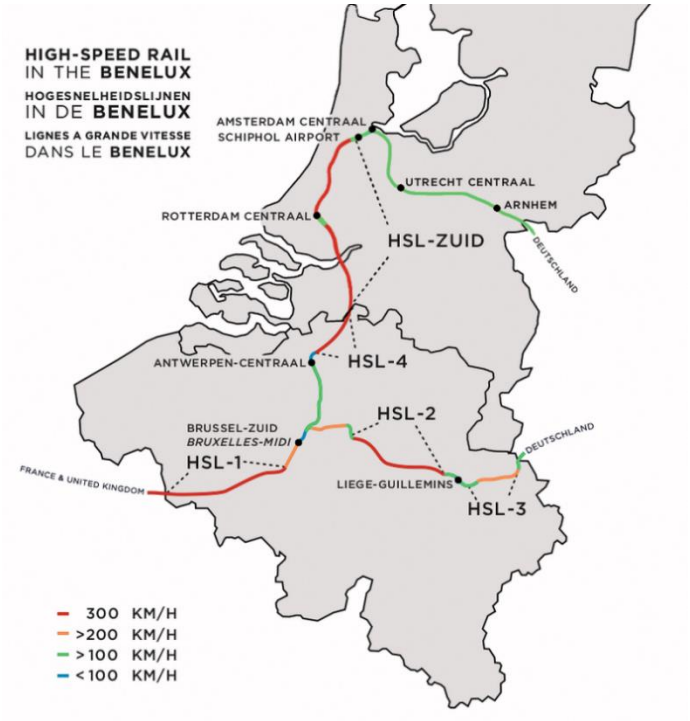

Figure 1 Schematic overview of the High-Speed Rail in the Benelux

The rail track is designed for a maximum operating train speed of 300 km/h which requires very strict rules concerning the alignment of the railway track and its supporting structure. To ensure the safety and reliability of the high-speed rail at very high speed the track structure is constructed on mostly settlement free structures and the alignment is closely monitored.

At some sections of the HSL, deformations of the structure have been acknowledged. At the section between km 131.900 and km 134.150 near the village of Rijpwetering the track is located next to the A4 highway. Here the soil structure under the track has shown settlements in both horizontal and vertical directions. The deformations have to be controlled to keep the rail track safe and reliable.

2. Initiation

The subject of the project is prepared in cooperation with Infraspeed Maintenance BV.

Infraspeed Maintenance BV is the asset manager of the High Speed Line-south (HSL-Zuid). Infraspeed is a consortium of Royal Bam Group and Siemens Mobility Nederland which is founded in 1999. Since 2001 the consortium has signed the Restated Implementation Agreement (RIA) to be responsible for the construction and maintenance of the high-speed rail. After finishing construction in 2006, Infraspeed became responsible for the maintenance of the HSL-Zuid for 25 years until 1 April 2031.

During and after construction at the section between km 131.900 and km 134.150 multiple deviations of the stability of the substructure have been acknowledged. The substructure is directly linked to the superstructure and the rail infrastructure, so deviations need to be closely monitored.

By previous studies [1] and measurements is shown that the track structure has still not stabilized. Previous studies have monitored the section but have not yet identified a mechanism causing the deviations. Multiple risks are identified which are exceeding the risk management profile of the maintenance organisation. Only by identifying the working problem mechanism an effective solution can be designed.

Figure 2 HSL rail structure at Rijpwetering

3. Research questions

From the initial problem analysis, a main research question is developed.

What are the main factors driving the horizontal deformation mechanism in the high speed rail settlement free plate structure and what measures can be taken to solve these horizontal deformations?

To systematically work towards a conclusion of this main research question a few sub-questions have been formulated:

- Is it possible to develop a suitable model to study the deformation behaviour of a settlement free plate structure on a sand embankment for a high speed rail track?

- What is the influence of geometrical surrounding conditions on the deformation mechanism?

- What is the main factor (mechanism) driving the horizontal deformations of the structure?

- What engineering measures can be taken to stop the horizontal deformations?

4. General research method

The aim of the thesis can be considered in a main objective, followed by some sub objectives.

Main objective:

- Develop a model to assess the factors driving horizontal deformation of a sand embankment on an asymmetrical soil structure for a high speed rail track.

Sub objectives:

- Represent the structure and soil conditions of the case study to study behaviour
- Validate the model with the observed deformations from the case study measurements
- Denominate the geometrical factors driving the horizontal deformations from a variant study
- Formulate designs to decrease the horizontal and vertical deformation
- Test the formulated designs in the model

Research planning

To define the planning and goal of each of the subobjectives a better planning for each objective is made. Here is shown what is expected to be the work to achieve the objective.

1. **Represent the structure and soil conditions of the case study to study behaviour**

The main goal is to develop a model to study the impact of different design possibilities on the structure for an infrastructural structure. The first task is here to define what we exactly want to model, and which results we want to receive from the modelling. If this is clear a corresponding software package for Finite Element Modelling can be chosen.

If the outline of the model and the software is chosen, the input data for the model must be considered. This includes all the sizes, material properties, loads and modelling properties to be implemented in the computer model.

2. **Validate the model with the observed deformations from the case study measurements**

From the case study, measurements are known. The goal is to match the measurements with the results from the modelling. This will certainly require numerous modifications of the model before representative values are considered.

The goal of this subobjective is to analyse the causes of the deformations which are measured in the real situation. From the causes we can learn to improve designs in the future.

3. **Denominate the geometrical factors driving the horizontal deformations from a variant study**

The modelling process of matching the model to the measurements of the case study will highlight the main factors leading to horizontal deformations. The objective is to denominate these factors such that the mechanism leading to the problem case is known.

4. Formulate designs to decrease the horizontal and vertical deformation

Resulting from the 2nd and 3rd subobjective the deformation causes are known. This brings us to the design challenge of the thesis. Here multiple possible designs will be made which are expected to improve the stability of the structure. The designs should be able to be implemented in the model and as possible engineering designs in the case study.

5. Test the formulated designs in the model

The final subobjective is to test the proposed designs in the validated model. The different designs can be evaluated on effectiveness to improve the structure. Together with some practical considerations an optimal design can be proposed to be implemented in the case study.

II. Case study

During and after construction of the track structure, multiple deformations have occurred on a part near the village of Rijpwetering just above the city of Leiden. The section under investigation is between km 131.900 and km 134.150. It is a straight section located in between two curves. On the southern side of the section the rail line crosses the highway with a concrete viaduct over the excavated highway. On the northern side the line faces a small viaduct over the Rijpwetering canal.

The location of the rail section is parallel to, on the western side, of the A4 highway. It is located in a rural area surrounded with meadows and small canals.

Figure 3 Satellite photo of the case study location (Google Maps)

5. Structure analysis

To investigate the problem situation and identify a research field the original structure is analysed.

The high-speed line near Rijpwetering is constructed on a settlement-free plate, the civil assets consist of a concrete slab on a pile foundation. The piles used are prestressed concrete foundation piles 400x400 mm. The foundation piles have a maximum bending moment resistance of 120 kNm. This value is reduced with a safety factor of 1.25.

$$\frac{120kNm}{1.25} = 96\ kNm$$

The required maximum bending moment capacity for breaking and acceleration forces are estimated at 40 kNm according to [2]. Which is estimated by finite element modelling of train loading on the piles. If we subtract this from the maximum bending moment capacity, we remain with a maximum bending moment which is remaining for soil deformation.

$$96kNm - 40kNm = 56\ kNm$$

Since the braking forces reduce over the depth, the foundation piles have a maximum working field bending moment resistance of 85 kNm and a maximum working moment in the top of the pile of 56 kNm[3].

The foundation piles are embedded a few meters in the Pleistocene-sand layer. On top of the 4 foundation piles, 2 concrete slabs are constructed. The 2 concrete slabs parallel to each other are coupled and in situ casted on the top of the embankment, as can be seen in Figure 4. They have a width of 1.5 m and a length of 30 m. At the joints the slabs are coupled in lateral direction by concrete blocks on either side and a tension anchor. This structure prevents the lateral movement between the slabs but allows the slabs to deform in longitudinal direction due to temperature changes.

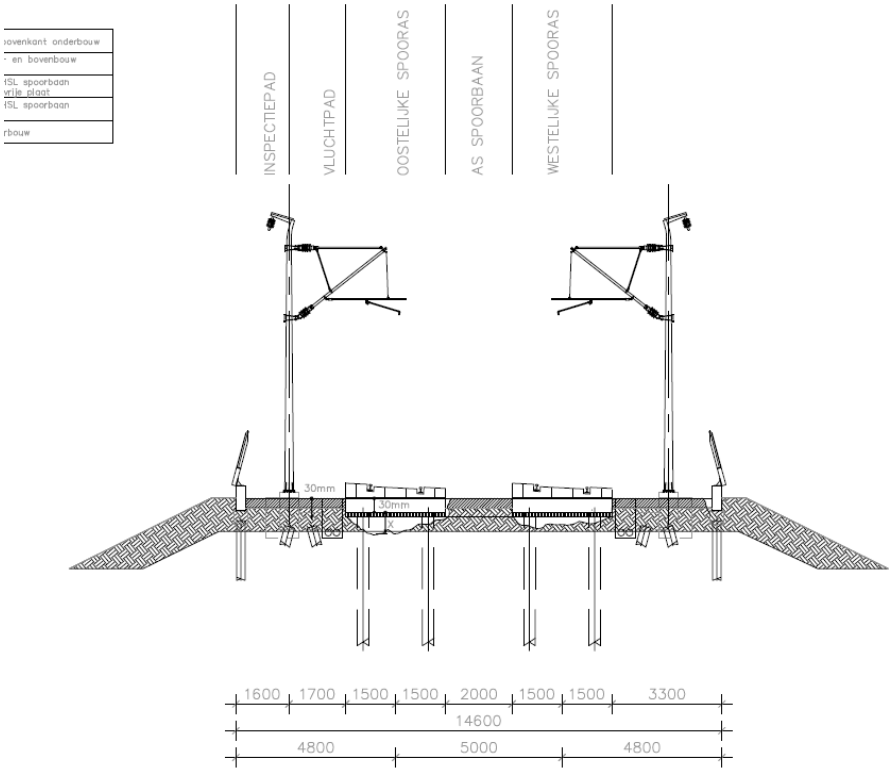

Figure 4 Rheda track structure and concrete foundation piles

The superstructure is a ballastless Rheda structure. This consists of concrete sleepers which are casted in concrete. The method is applied top-down to ensure a perfect track alignment. With the top-down construction first the rail and sleepers are placed in the correct alignment, and afterwards the sleepers are embedded in concrete to form the solid concrete Rheda slab. The Rheda slab is constructed on top of the settlement free plate and these are connected with dowels.

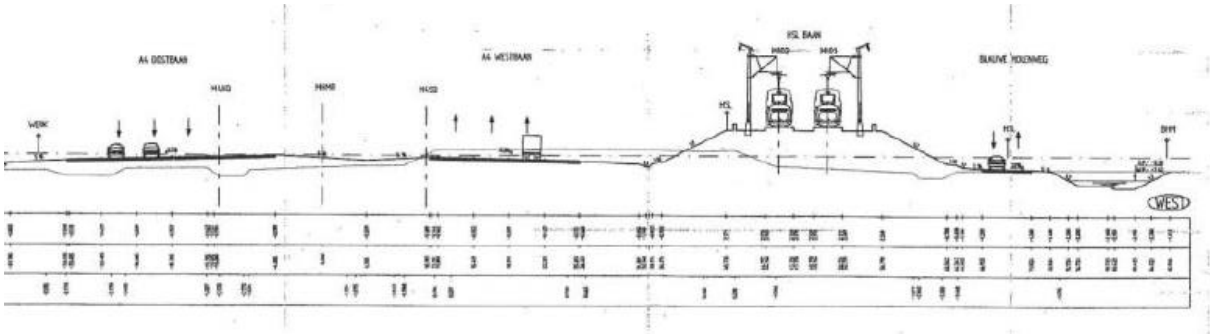

Figure 5 Section of the HSL structure in its surroundings (at KM 132.6)

The track structure is constructed on top of a soil body and is located against the east side of the soil body of the highway A4 which can be seen in Figure 5. The A4 consists of a large soil body which is constructed around 1960. For the construction of the A4 a canal (cunet) was dug and filled with sand, creating a large and heavy structure. The sand structure has settled through time to an 8-meter-deep structure with a very high stiffness. This high stiffness is reached after years of consolidation of the structure.

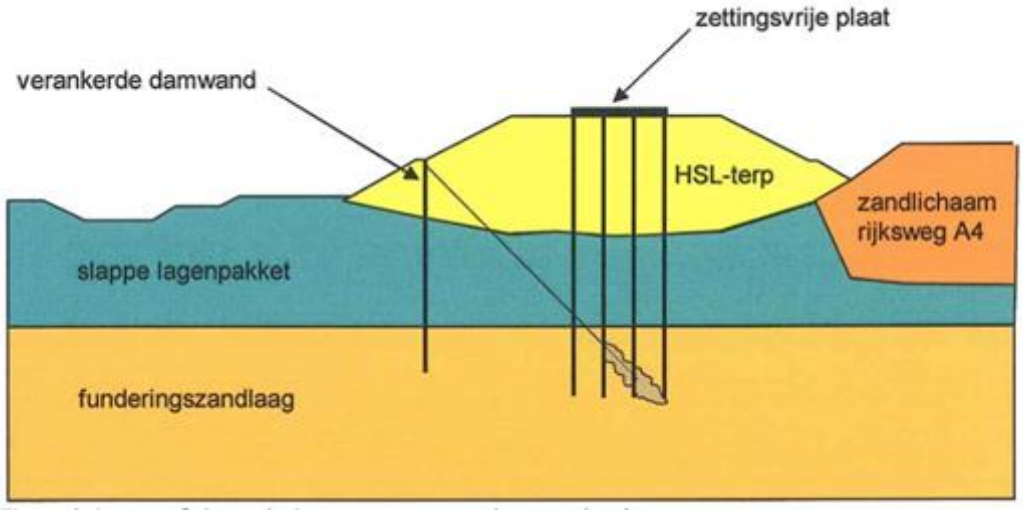

Figure 6 Schematic overview of soil, settlement free plate and sheet pile

For the case of Rijpwetering the problem consists of large horizontal (lateral) deformations of the superstructure of the rail. The biggest problems will occur when the lateral deformations will reach 100 mm deformation according to the research report by APcon [4]. This value is based on a study regarding the maximum bending moment resistance in the head of the foundation piles. This means that a deformation of 100 mm of the top of the foundation piles or the attached concrete slabs must be avoided because this will cause cracking of the piles and leads to a complete reconstruction of the structure.

The horizontal (lateral) deformations are expected to be correlated to the vertical settlements [5]. The expectance is that the soil and structure have a greater influence on the deformation than the (dynamic) loading.

5.1 Case study dimensions

The embankment of the high-speed rail structure near Rijpwetering differs in height over the area. The picture below shows the height of the rail structure from the highway crossing viaduct to the viaduct over the Rijpwetering canal. The embankment starts at around ground level and increases over the distance to a height of 4.7 meters.

Figure 7 Height profile of the embankment over the distance at the case study (AHN (Actueel Hoogtebestand Nederland))

The embankment consists of a flat top of 26 meters width. The slope is created with 2:1 width to height ratio. In Figure 8 the profile, the soil layers and average water level is shown.

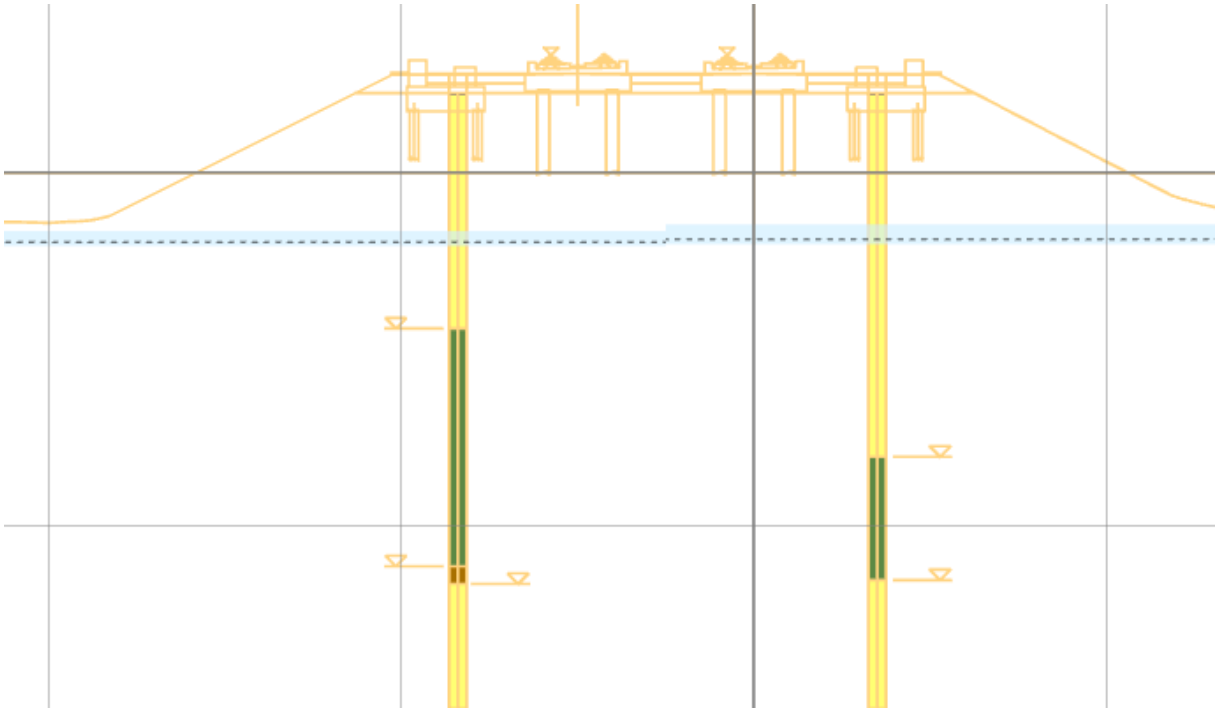

Figure 8 Section of the HSL embankment with soil profile and water level (Source: ARCGIS visualisering RHDHV– ProRail)

5.2 Soil structure

The high-speed rail embankment is constructed in the neighbourhood of the village and canal Rijpwetering. It is located in a field with very soft soils and lots of water content in the soil. Multiple soil investigations have taken place to compose the soil parameters for the calculations. Before construction a geotechnical length profile is composed which indicates the soil layers underneath the length of the track. The results of the soil composition are given in the appendix. For the modelling a representative average value is chosen in the most problematic location at km 132.7

Deel 3-1	km 32.58 - 32.71	
	bovenzijde [m NAP]	onderzijde [m NAP]
Veen, kleiig	-1,2	-5,6
Klei, humeus	-5,6	-7,4
Klei, siltig	-7,4	-10,6
Veen, Basisveen	-10,6	-11,6
Zand, pleistoceen	-11,6	-35,0

Table 1 Soil composition km 32.58-32.71

As shown in the table the soil can be considered to exist of 4 different layers. The top layer consists of a clay-like peat, followed by a clay layer. As third a regular peat layer of 1 meter

deep is found before the Pleistocene sand layer which goes as deep as the maximum measurements. In the table the clay layer is subdivided into two layers, with only slight variation in parameters. For this study the layer is considered to be homogeneous. As can be seen in the table the ground level is at -1.2 m NAP. The water level can vary because of weather conditions but is usually stable at around -4 m NAP.

From soil tests the following soil parameters are composed. This is a statistical interpretation of similar locations of the soil layers since no data is available at every specific location. Parameters used are shown in Table 2 and Table 3.

Grondsoort		γ	γ_{sat}	$c_{V\,gem}$	P_g	C_p	C'_p	C_s	C'_s
Omschrijving	code	[kN/m^3]	[kN/m^3]	[m^2/s]	[-]	[-]	[-]	[-]	[-]
				*10^{-8}					
Ophoogzand		17,0	19,0	Nvt	-	-	-	-	-
Klei	K	14,5	14,5	6,0		22,5	9	180	72
Zand siltig [3]	Zs	16,5	18,9	78		129	60	1032	482
Veen [1]	V	10,1	10,1	5,0	25	14,5	5,2	47,0	17,0
Klei zandig	Kz	17,3	17,3	7,7		36,2	16,4	289	131
klei siltig [1]	Ks	15,6	15,6	7,7	41,3	34,1	9,7	219	62,3
klei humeus [2]	Kh	14,0	14,0	5,0		14,5	5,2	47,0	17,0
veen kleiig [1]	Vk	11,1	11,1	5,0	25	14,5	5,2	47,0	17,0
zand kleiig [4]	Zk	17,5	17,5	147		150	80	1200	636
Basisveen [1]	V	10,6	10,6	7,7	24,5	33,1	51,2	152	24
Zand Pleist.	Z	17,0	20,0	-	-	-	-	-	-

1) i.t.t. de overige parameters zijn hier de resultaten van de statistische analyse gebruikt.
2) Door een gebrek aan voldoende samendrukkingsproeven op deze laag zijn, op basis van de sonderingen en de diepte, de zettingsparameters van veen aangehouden.
3) Parameters afkomstig van km 35.1 – 38.0.
4) Parameters afkomstig van km 38.0 – 45.9.

Table 2 Settlement parameters used in design (Bouwcombinatie Hollandse Meren [6])

Grondsoort	γ	γ_{sat}	c'	ϕ'
	[kN/m^3]	[kN/m^3]	[kPa]	[°]
Ophoogzand	17,0	19,0	0	32,5
Klei	14,5	14,5	4	23,0
zand siltig	16,5	18,9	0	27,5
Veen	10,1	10,1	3	20,0
Klei zandig	17,3	17,3	2	25,0
klei siltig	15,6	15,6	5	21,5
Klei venig	12,9	12,9	5	15,0
klei humeus	14,0	14,0	5	15,0
veen kleiig	11,1	11,1	5	17,5
zand kleiig	17,5	17,5	0	27,5
Basisveen	10,6	10,6	3	25,0
zand pleistoceen	17,0	20,0	0	32,5

Table 3 Stability parameters used in design (Bouwcombinatie Hollandse Meren [6])

In 2016 a report with new geotechnical investigations have taken place. This time 8 cone penetration test as well as 2 mechanical drill states were taken at KM 134.1. These tests [7] show the soil composition after consolidation.

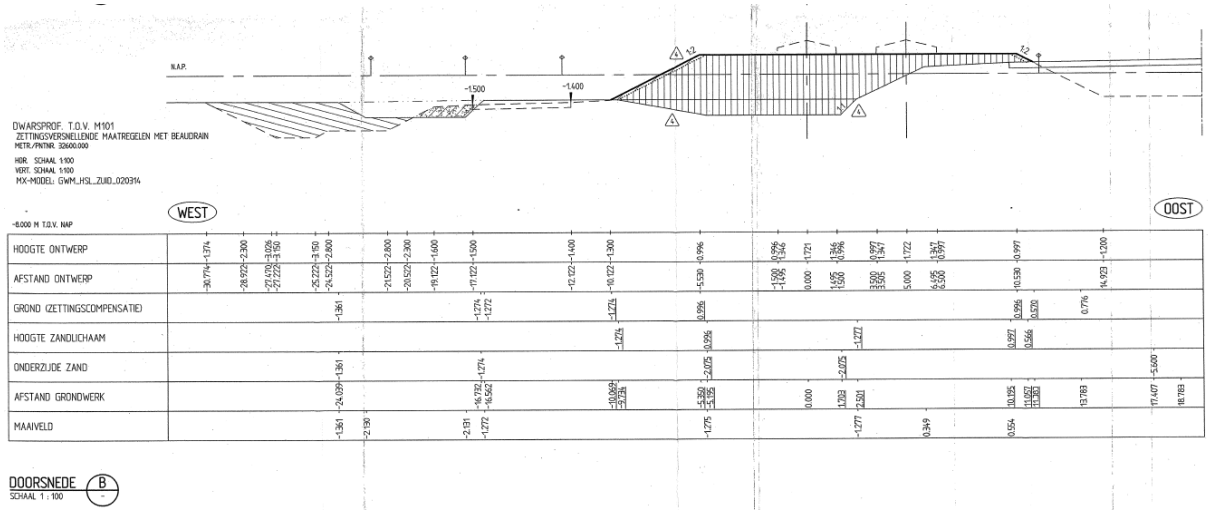

Figure 9 lateral cross section, Embankment constructed half on the highway cunet (as built drawing HSL Grondwerk km 31.800-km 32.7)

As can be seen in Figure 9, the embankment is constructed partly on the existing cunet of the highway A4, which results in an asymmetrical layer in the soil composition. The rail embankment is drawn in stripes the original soil is white. The exact shape and size of the highway cunet is unknown because it's hidden underground and differs per location but reaches at least a few meters under the toe of the embankment to halfway under the embankment and the track structure.

5.3 Rail structure

As explained in II.5 the track is built on a Rheda structure. The Rheda system consists of a three-layer system. Which is a bi-block lattice-truss sleeper, casted in a slab of infill concrete and a reinforced trough slab to provide a homogeneous concrete track-supporting layer. Together with the concrete bed that encloses them, the concrete sleepers, featuring non-prestressed-reinforcement, form a solid structure. A superstructure that can be uniformly implemented with a minimum of structural height on all track substructure suited for non-ballasted tracks. The structure is especially frequently used on high speed rail projects around the world.

Figure 10 Ties of a Rheda 2000 slab track system before they are casted in the concrete (left) and after casting (right)

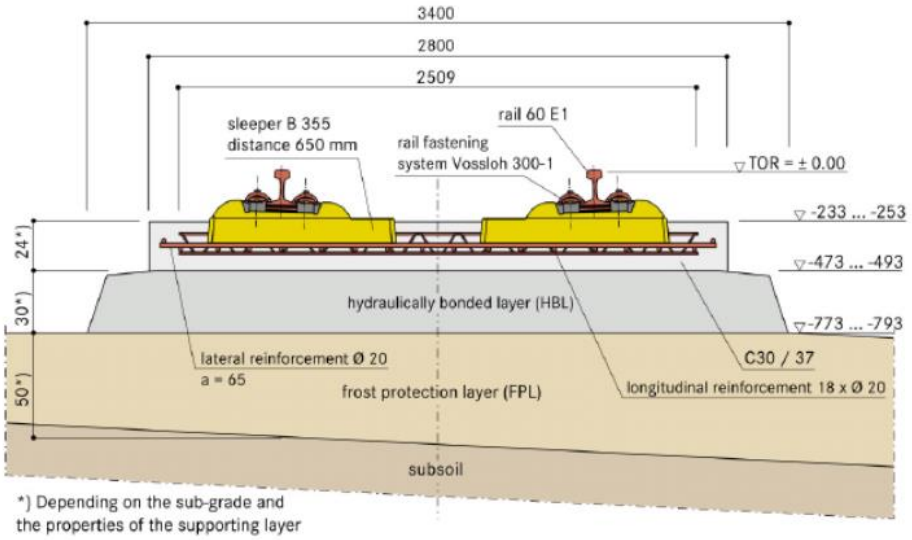

Figure 11 Rheda 2000 slab track system

The main advantages of slab track systems are:

- Reduction of the structural height
- Straight alignment
- Low maintenance
- High service life
- High lateral track resistance
- No ballast movements due to suction at high speed

5.4 Main risks of the problem situation

In 2016 a risk dossier has been made by Infraspeed [8]. From the risk dossier the following main risks are established.

- Cracking of the foundation piles under the settlement free plate

Due to the lateral deformations the bending moment in the foundation piles increases. Together with vehicle loading forces the bending moments could exceed the maximum bending moment capacity.

- Vertical deformations (irregularities) of the inspection path aside the track

Due to the vertical deformations of the soil, holes have formed underneath the structure and on the inspection path. The holes lead to loss of lateral stability of the piles and dangerous working conditions surrounding the track.

- Adjustability of the rail fastening system at maximum (no adjustability left)

The rail is fastening with a fastening system. The fastening system has a certain adjustability to compensate for slight deformations and corrections. The adjustability has a maximum of 28mm in either direction, which is almost completely reached.

- Damage to the rail system assets (cables)

Because of both vertical and horizontal deformations, the rail assets will deform as well. That means that cable ducts, and railway systems can break due to the ongoing deformations.

- Rail geometry changes due to substructure deformation

Since the Rails are directly coupled to the foundation piles and the concrete plate every deformation of the substructure will lead to deformations of the substructure. With the ongoing displacement the longitudinal rail geometry is changed. Small deviations can be compensated by the fastening system but as deformations increase the problem will cause issues.

6. Construction process

The track structure around Rijpwetering is constructed by the contractor Bouwcombinatie Hollandse Meren. The construction design has been approved in February 2002. Construction of the embankment has started in July 2002.

In the beginning of the construction, the consolidation process has been tried to be accelerated with the use of drains. The construction site was first heightened with a sand layer of 1.5 m. After that a "Beaudrain" system is applied, in which vertical drains are driven in the soil and connected to a vacuum pump to remove excess water. Drain are proven to be a very efficient measure to accelerate consolidation and control deformations both on long term and on short term [9]. But this only holds if drains are functioning properly and consistently. The local water authority demanded that the drains could not be driven deeper than 2m above the Pleistocene sand layer to prevent saltwater from the sand to enter the layers above. This means the consolidation process of the deepest 2 meters could not be accelerated. When the vacuum pumps where in place the sand body was steadily increased over time to slowly increase pressures.

The embankment is constructed with sand and is heightened in multiple steps to ensure a controlled consolidation over time. The total increment time of the embankment is 265 days. The increment is shown in Figure 12 for multiple locations on the case study. The total height of the increment is about 1.5 meter higher than the desired final height to compensate for the settlement. The over-height is removed before construction of the concrete substructure.

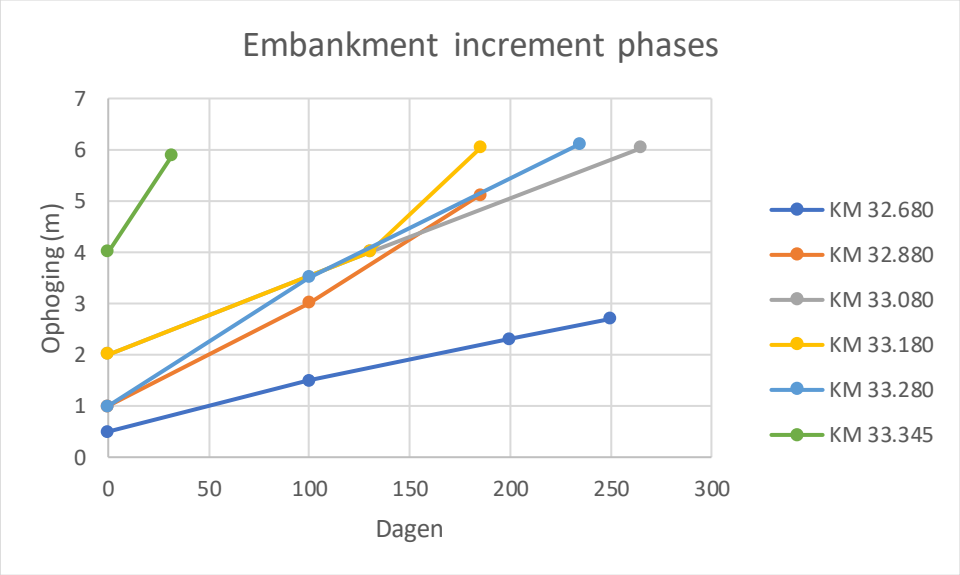

Figure 12 Embankment increment phases

During construction of the soil body large horizontal shear collapses occurred. This led to a redesign of the structure with the implementation of an unsupported sheetpile wall near the bottom of the soil body (toe of the embankment) on the western side, to prevent further horizontal deformations or collapses during construction.

Because analysis by GeoDelft showed that due to creep the horizontal deformation of the settlement free plate would become more than the allowed 10 mm it was decided to change the structure again. A part of the soil body on the eastern slope of the embankment is removed and in its place EPS blocks are placed to reduce the structure weight and with it the settlement [4].

After construction was finished, tachymetric measurements of the concrete structure have started since horizontal deformations were expected [10].

The measurements showed that horizontal deformation was larger than expected. This led to the implementation of a post-tension sheet pile wall with an anchor [4]. This is to limit the horizontal displacement by adding horizontal pressure to the soil body.

Figure 13 Post tensioned sheetpile wall

Due to the larger expected deformation, the track structure is also changed to a track structure with a larger adjustability [4]. This means the rail can be adjusted with respect to the sleeper to a maximum of 28 mm in the lateral direction (instead of 8 mm for the regular Rheda system) to compensate for the structure to move horizontally. Next to that, the adjustability has been positioned eccentrically to be prepared for compensation in one direction.

For the timeline of the construction and problem occurrence see appendix K.

7. Measurements

At the area of the HSL near Rijpwetering multiple monitoring measurements are taken to investigate the problems at the area. The monitoring consists of the following measurements:

Monitoring Measurements	*Company*	*Since date*
Location surveying		
Tachymetric surveying measurement	Arcadis	2005
Global Navigation Satellite System (GNSS)	Arcadis	2009
Vertical deformation measurements		
Settlement beacon (Zakbaken)	Deltares	18-5-2011
Extensometer	Fugro	30-3-2005
Horizontal deformation measurements		
Inclinometer (top of the embankment)	Deltares	26-4-2005
Inclinometer (near the sheet pile wall)	Deltares	2-8-2006
Waterlevel measurements		
monitoring wells (peilbuizen)	Deltares	24-4-2017

Table 4 Monitoring measurements

7.1 Vertical deformation measurements

Settlement Beacons

In the section near the Viaduct Zuidweg 10 settlement beacons have been installed.

A settlement beacon is a measuring pole with large footplate used to determine changes in the level of deeper soil layers when subject to forces caused by filling. A settlement beacon consists of a square or round steel footplate of 0.5 to 2 m in diameter. In the centre of this plate a metal pipe is welded on to it vertically. The height of the top of the measuring pole has been accurately measured beforehand. By repeating this height measurement in the course of time, it is possible to determine the rate and amount of setting of the soil [11].

The settlement beacons are placed divide over the area of the case study as shown in Figure 14

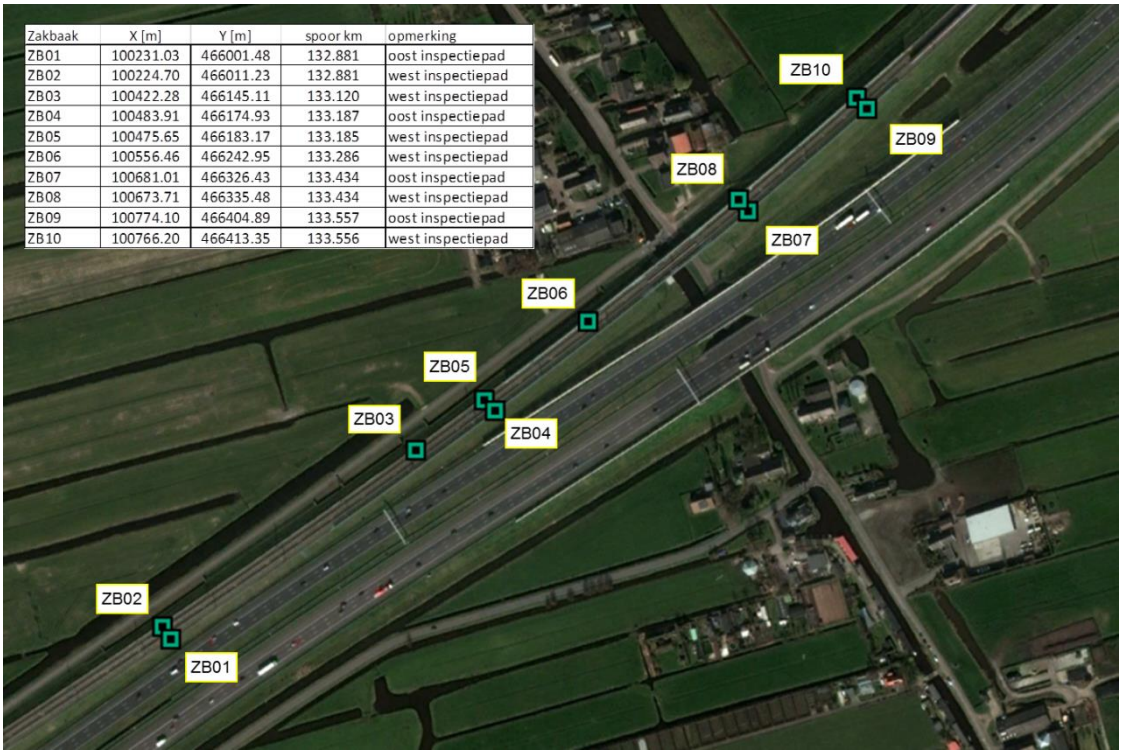

Zakbaak	X [m]	Y [m]	spoor km	opmerking
ZB01	100231.03	466001.48	132.881	oost inspectiepad
ZB02	100224.70	466011.23	132.881	west inspectiepad
ZB03	100422.28	466145.11	133.120	west inspectiepad
ZB04	100483.91	466174.93	133.187	oost inspectiepad
ZB05	100475.65	466183.17	133.185	west inspectiepad
ZB06	100556.46	466242.95	133.286	west inspectiepad
ZB07	100681.01	466326.43	133.434	oost inspectiepad
ZB08	100673.71	466335.48	133.434	west inspectiepad
ZB09	100774.10	466404.89	133.557	oost inspectiepad
ZB10	100766.20	466413.35	133.556	west inspectiepad

Figure 14 Settlement beacon locations (Deltares)

The first 6 settlement beacons are shown in Figure 15. These are all located on the Southern side of the viaduct. The Beacons show a very linear settlement behaviour over time since installation in 2011. All the beacons have a similar settlement rate which does not show a decrease in rate. Therefore, we can conclude that the settlement has not finished yet.

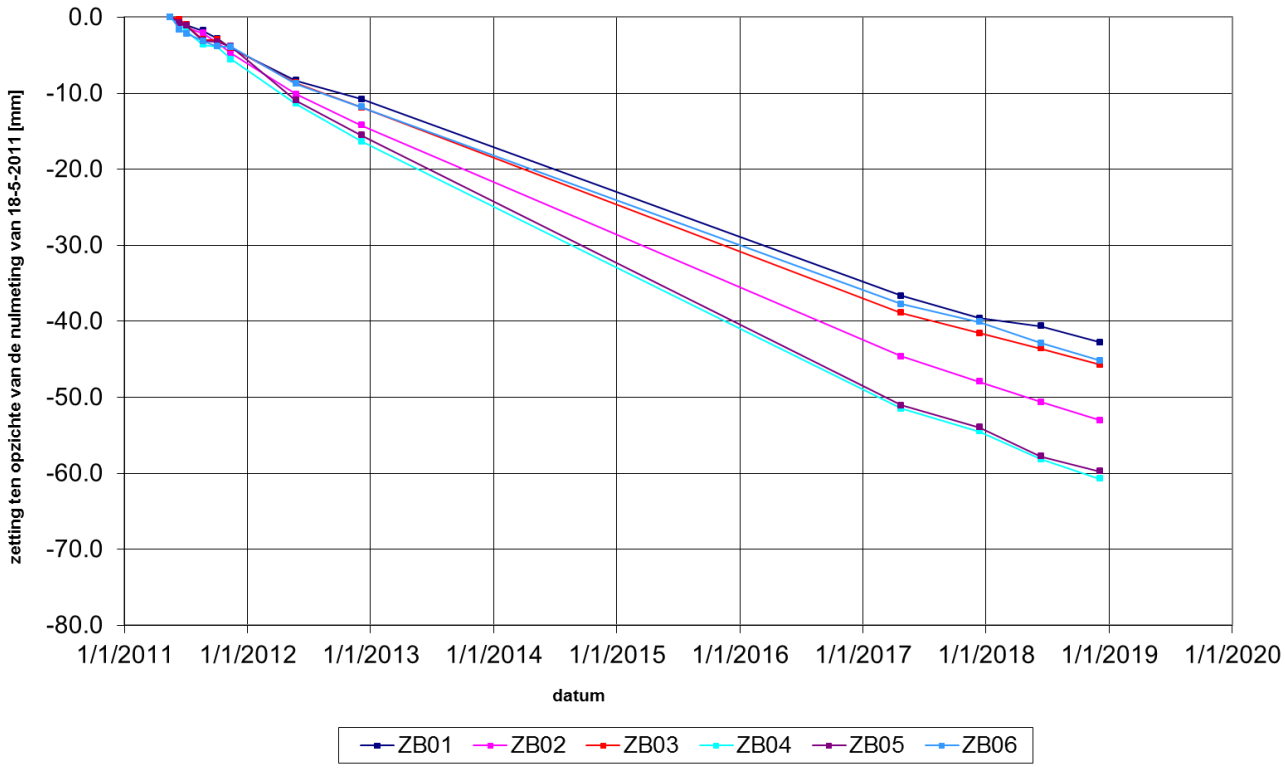

Figure 15 Settlement beacon data for beacons 1-6 (Deltares)

The latter 4 settlement beacons are plotted in Figure 16. These beacons are all located on the northern side of the viaduct. This shows 2 different scenarios, a fast and high settlement rate for beacons 7 and 8 and a much slower rate for beacons 9 and 10. It seems that further north of the viaduct the settlements reduce.

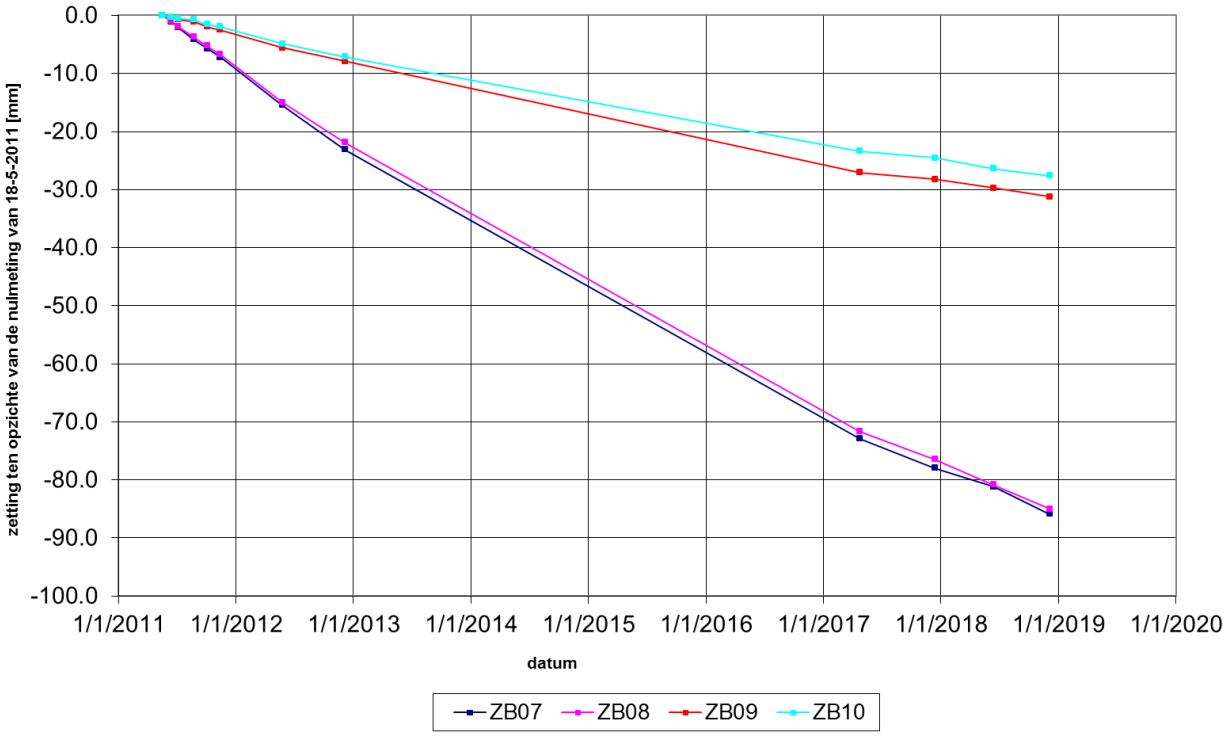

Figure 16 Settlement beacon data for beacons 7-10 (Deltares)

Extensometers

Since 2005 2 extensometers have been installed in the HSL embankment.

The extensometers have 5 anchors which can be installed in different soil layers to investigate the deformation per layer. The anchors are located at km 133.180 and km 133.300 which is on the southern side close to the viaduct Zuidweg. The anchors have been installed according to the following depths.

Name	Location (km)	Ground level	Depth anchor 1	Depth anchor 2	Depth anchor 3	Depth anchor 4	Depth anchor 5
03A- EX	133.180	4.16	-14.34	-9.83	-7.84	-5.84	-0.83
03D- EX	133.300	4.17	-14.33	-9.83	-7.33	-4.83	-0.84

Table 5 Extensometer anchor depths

The extensometers show the displacements for 4 different soil layers with regard to the deepest anchor. For that reason anchor 1 is constantly zero. The extensometers show a gradual settlement over time. In the location of extensometer 03A the sheet pile is installed at the end of 2009. This has a very clear influence on the settlement behaviour.

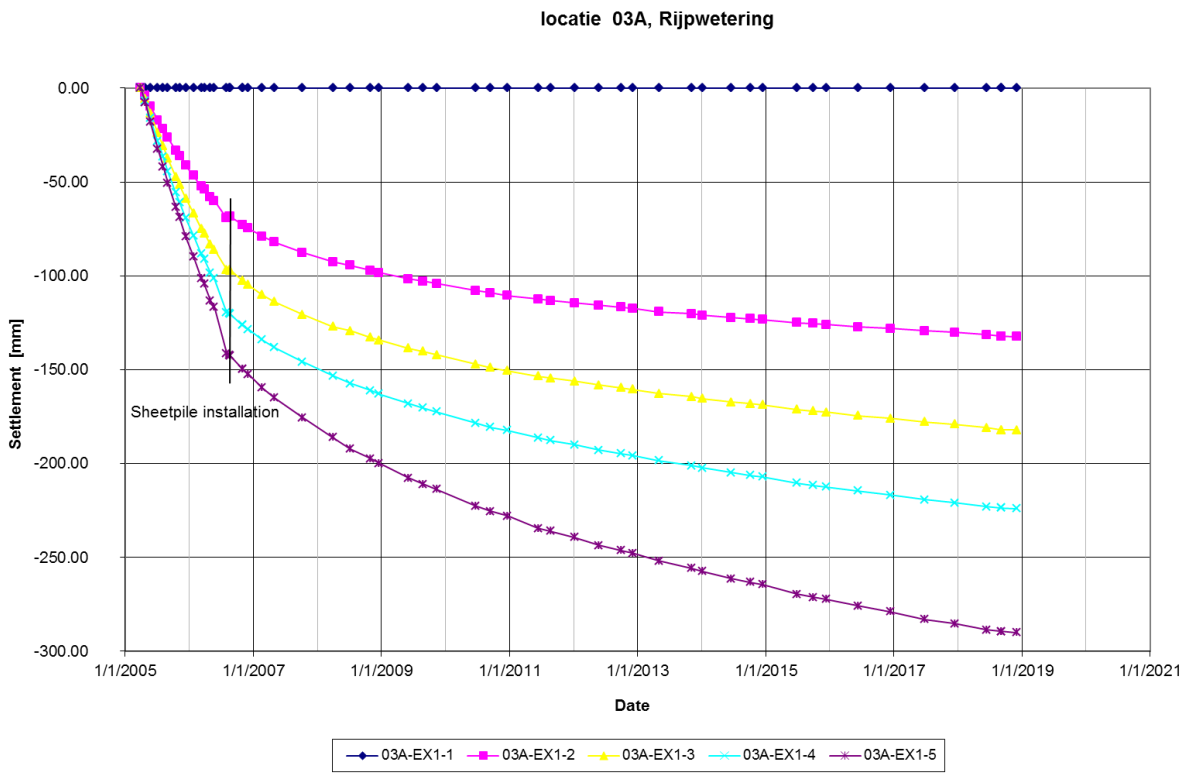

Figure 17 Extensometer 03A data

At the location of extensometer 03D a sheetpile wall was already installed before the installation of the extensometer.

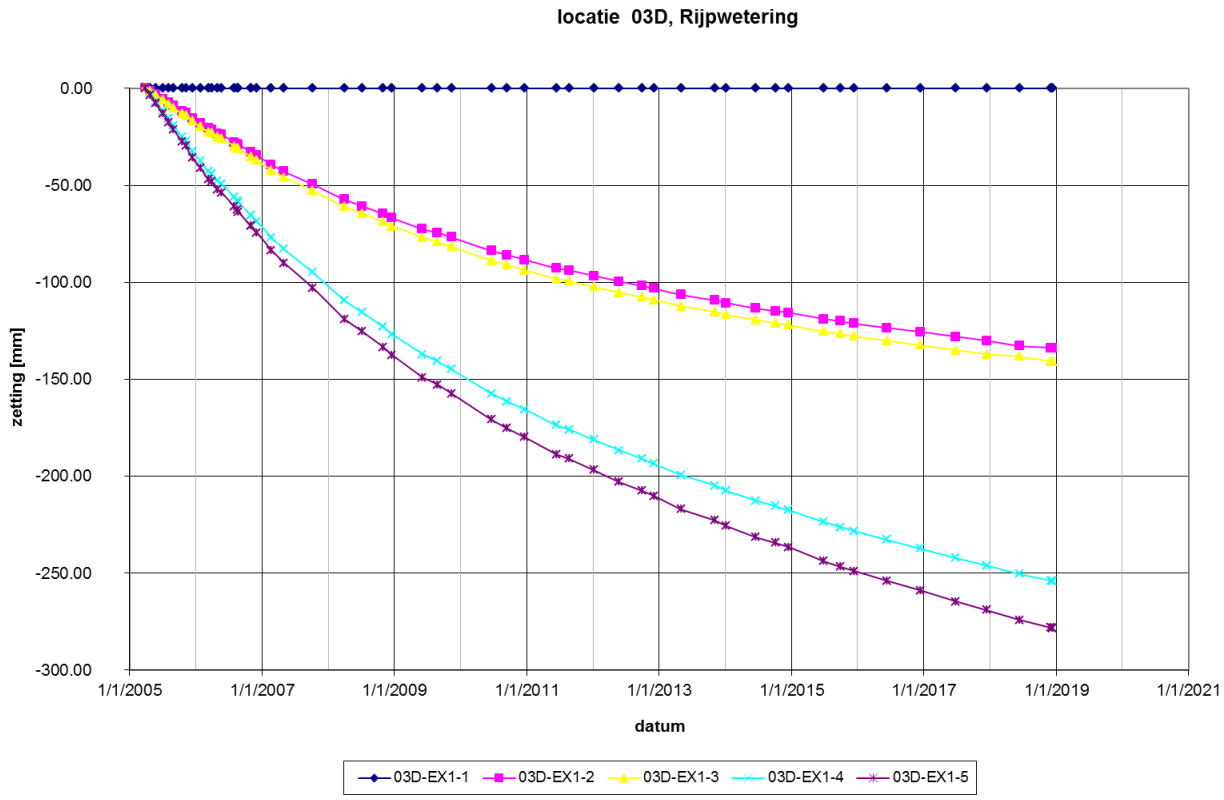

Figure 18 Extensometer 03D data

For both the extensometers the sections are supported by sheet pile walls in the toe of the embankment. The total displacement in 2019 is of the similar order. The rate of settlement is largely influenced by the sheetpile.

7.2 Horizontal deformations

GNSS measurements

Since 2005 the company Arcadis started surveying measurements to analyse the location of the substructure of the HSL over time, with the goal to detect horizontal displacements with a high accuracy and reliability. The analysis consists of 10 points in the area from km 132.6 till km 133.7 which is around the viaduct near Rijpwetering.

Figure 19 GNSS measurement locations (Visualisering RHDHV[12]*)*

Since 2008 the measurements have changed from tachymetric surveying to Global Navigation Satellite System (GNSS) measurements to increase the accuracy and reliability. Since 2008, 18 different GNSS measurements have been taken which shows the deformation over time. From 2013 3 extra points have been added to improve the results. The last available measurement (GNSS – 18) is taken in July 2019.

puntnummer	0 (2009) - pilot	1 - 0 [mm]	2 - 0 [mm]	3 - 0 [mm]	4 - 0 [mm]	5 - 0 [mm]	6 - 0 [mm]	puntnummer	7 [mm]	8 [mm]	9 [mm]	10 [mm]	11 [mm]	12 [mm]	13 [mm]	14 [mm]	15 [mm]	16 [mm]	17 [mm]	18 [mm]
GNSS-01	+0.7	+0.6	+1.5	+1.2	+8.2		+8.9	GNSS-01	+12.4	+11.4	+13.4	+13.1	+11.6	+16.0	+13.5	+13.4	+12.8	+14.8	+12.1	+14.3
GNSS-02		+1.2	+1.5	+4.1		+10.6	+19.8	GNSS-02	+22.7	+23.0	+24.6	+21.8	+23.6	+25.8	+23.9	+27.3	+26.2	+26.8	+26.9	+30.0
GNSS-03	-3.1	+1.4	+3.9	+5.9	+9.2	+6.7	+19.7	GNSS-03	+18.4	+19.8	+24.3	+23.2	+24.9	+29.0	+28.0	+30.1	+30.4	+33.0	+31.7	+33.6
GNSS-04		+0.3	-0.4	+0.9	+3.9	+6.5	+10.3	GNSS-04	+17.8	+18.8	+19.7	+17.8	+19.2	+20.7	+18.2	+21.6	+19.4	+21.2	+21.0	+22.1
GNSS-05	-2.7	+1.7	+3.0	+4.4	+6.1	+8.0	+15.4	GNSS-05	+19.4	+21.4	+20.3	+18.7	+20.0	+24.3	+22.2	+25.2	+24.2	+28.6	+27.0	+29.8
GNSS-06		+2.6	+3.6	+5.7	+6.6	+8.4	+15.5	GNSS-06	+17.3	+19.3	+20.5	+20.4	+20.2	+24.5	+22.1	+22.9	+23.0	+25.3	+24.1	+27.3
GNSS-07	+1.2	+1.6	+1.5	+2.6	+4.2	+5.0	+9.0	GNSS-07	+13.2	+14.4	+15.5	+12.7	+12.7	+14.2	+12.2	+13.8	+13.9	+15.3	+14.5	+15.0
GNSS-08		+1.3	-2.0	+7.3	+7.8	+8.0	+7.8	GNSS-08	+8.0	+6.6	+8.7	+7.0	+5.1	+9.0	+6.5	+7.6	+7.6	+9.1	+7.5	+9.3
GNSS-09	+2.6	+0.1	+0.5	+1.0	+4.6	+3.0	+2.5	GNSS-09	+4.2	+2.6	+6.1	+0.2	+6.0	+7.5	+5.2	+7.4	+5.3	+6.2	+4.5	+7.7
GNSS-10								GNSS-10	-0.8	-8.8	-10.9	-10.9	-5.7	-4.0	-4.9	-5.7	-8.6	-7.7	-6.6	-3.0
GNSS-11		-1.1	-1.8	-7.0	-6.4	-6.4	-13.0	GNSS-11	-12.7	-18.2	-21.1	-24.4	-20.5	-17.9	-20.3	-23.6	-30.1	-37.7	-29.7	-25.0
GNSS-12								GNSS-12	+1.5	-0.9	-0.4	-1.0	-0.7	-0.2	-2.3	-0.8	-3.0		-2.2	-0.3
GNSS-13								GNSS-13	+2.8	+1.5	+3.6	+1.2	-1.3	+1.1	+0.2	-0.9	-1.2	-1.7	-1.3	+1.2
								+ = verschuiving in noordw estelijke richting (naar links) - = verschuiving in zuidoostelijke richting (naar rechts)												

Table 6 Horizontal displacements of the substructure perpendicular to the rail with regard to the zero measurement 2008

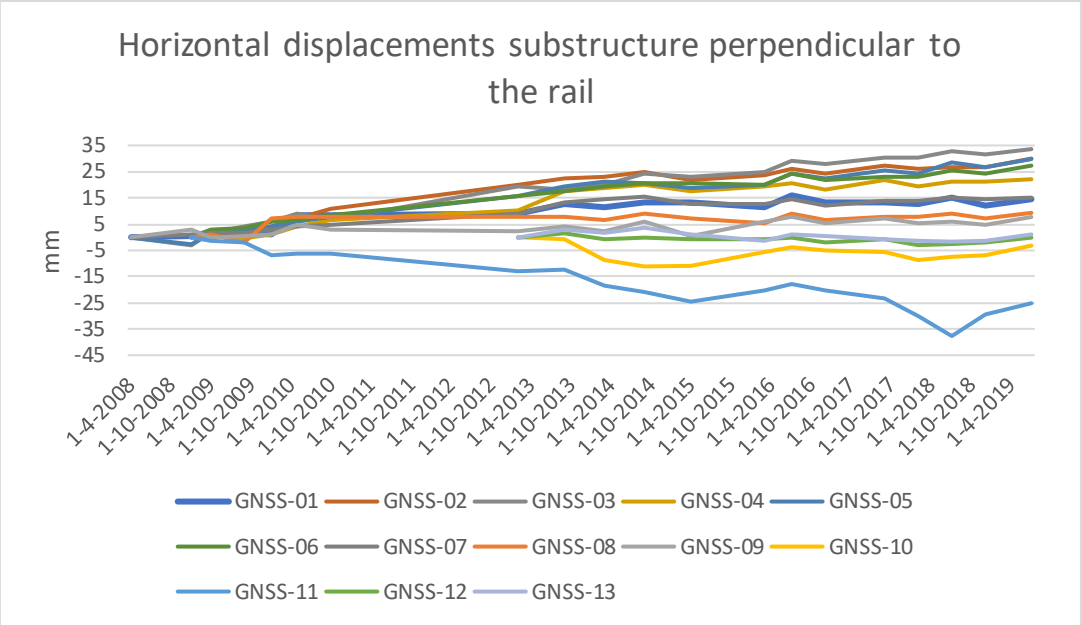

Figure 20 Horizontal displacements of the substructure perpendicular to the rail with regard to the zero measurement 2008

In Table 6 and Figure 20 you can see all the GNSS measurements for the substructure in lateral direction perpendicular to the rail. The 13 measurement points show quite a variation in the rate and total displacement of the substructure. Therefore, the data is specified in to 3 different groups with similar behaviour.

The first group are the points 2, 3, 5 and 6 and those displacements are shown below with a “zero line” in black in Figure 21.

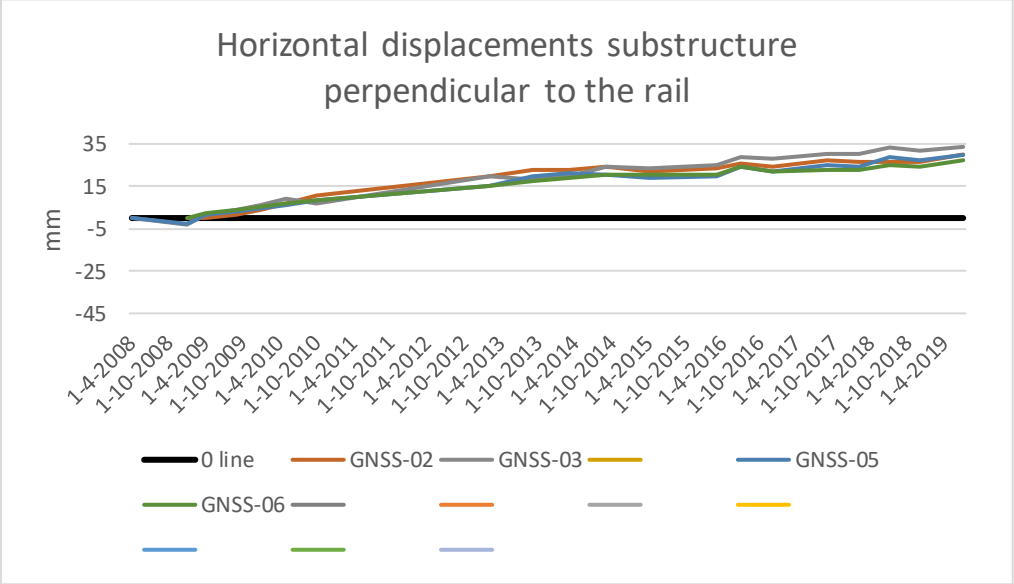

Figure 21 GNSS measurements horizontal displacements locations 2,3,5,6

These points have both the highest maximum displacement and the highest rate of displacement which is almost linear in time. The maximum value is reached by point 3 with a value of 33.6 mm. The rate is between 2.7 and 3.3 mm per year.

This group consists of all locations where the embankment is not supported by means of a tensioned sheet pile or EPS is used to control the displacements. Only location 6 is just on the edge area of a sheet pile section.

The next group are the points 1, 4, 7, 8 and 9. Those displacements are shown below.

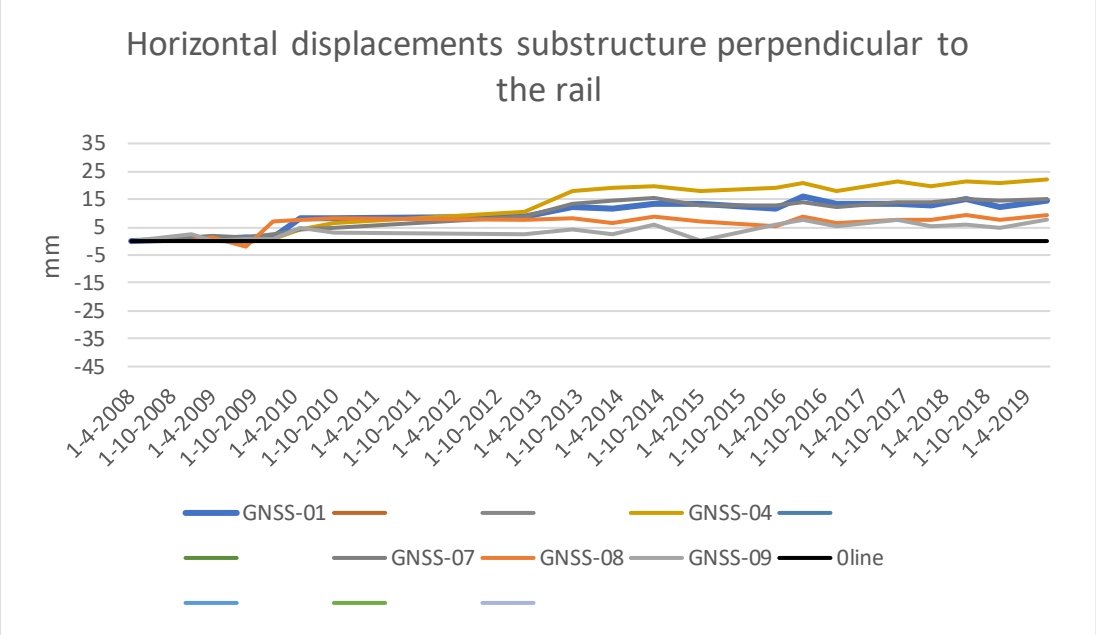

Figure 22 GNSS measurements horizontal displacements locations 1, 4, 7, 8, 9

These points have a lower displacement rate and a much lower maximum displacement. The rate also significantly decreases after approximately 2013 after which the displacement does not increase at a very significant rate. The total displacement after 2013 has only increased between 0 (for point 7) to 2.4 mm (for point 4) in 5 years' time, which leads to a rate of 0 to 0.5 mm per year.

Point 1 the embankment is the lowest of the whole section and thus has a lower displacement. Points 4, 7, 8 and 9 are all within the range of a supported area with prestressed sheet pile walls. Points 7, 8 and 9 are also supported and have a part in which EPS is used in the structure. These 3 points show the lowest deformations

The next group is the points 10, 11, 12 and 13. Those displacements are shown below.

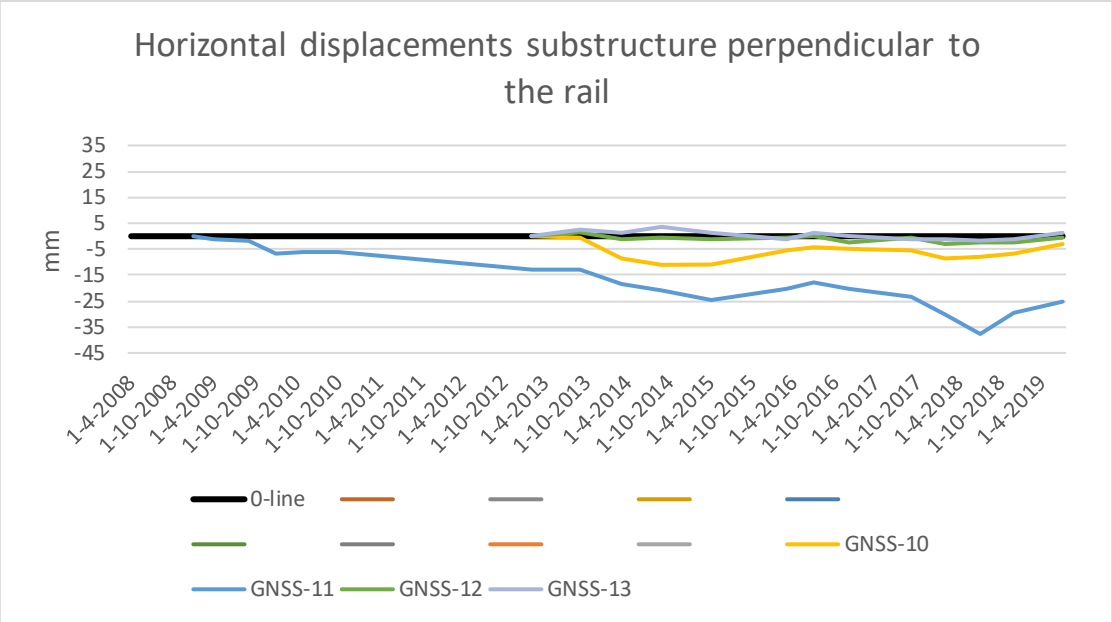

Figure 23 GNSS measurements horizontal displacements locations 10,11,12,13

These points are all on the northern side of the Rijpwetering viaduct Zuidweg. And they show a negative displacement which means a displacement in the east direction towards the A4 highway.

From the graph we see the points 10, 12 and 13 have a very little maximum displacement and a non-significant linear rate. Only point 11 shows a large displacement with a maximum measured value of 37.7 mm. The points in this group are all on the north side of the viaduct and are not supported by sheet pile or EPS.

The GNSS measurements are also represented in a top view of the location. These pictures are shown in appendix J. From the measurements shown in the picture in the appendix it's clear that supported locations have shown are lot more displacement then the unsupported sections.

8. Hypotheses

From the results of the GNSS measurements related to the structure we can draw some hypotheses for the simulation.

- For points 1 to 6 the subsoil consists of a nonsymmetric soil structure. On the west side of the embankment the peat layer is much thicker than it is on the east side. On the east side the peat is replaced with a sand layer. This is most probably due to the presence of the cunet from the old A4 highway which is constructed in 1957. A cunet is an excavation of weak soil which is filled up with sand to create a stiff subsoil for the construction of infrastructural structures. This old sand structure is completely consolidated and therefore assumed to be rather stiff compared to the surrounding peat and clay layers.

- For the entire section the embankment is located right next to a ditch parallel to the rail. The ditch exists to control the water level in the surrounding area and is approximately 3 meters below the ground level at a depth of -4,2 m NAP. This results in a significant height difference between the top of the embankment and the bottom of the ditch of 8 m within 25 m of distance. This could lead to some instability problems.

- On the east side of the embankment the A4 highway is located parallel to the rail embankment. Together with the construction of the rail embankment the road embankment has been enlarged. The construction works took place at the same time which means additional sand was brought to the east side of the rail embankment which could lead to extra forces from the side.

- For the points 4, 7, 8 and 9 a sheet pile wall is constructed on the west side of the embankment which is pre-tensioned by a grout anchor. This is done after construction of the concrete substructure since large displacements already occurred early during and after construction. The sheet pile wall should obstruct lateral displacement of the embankment.

The expectation is that all the 4 different mentioned cases will have an influence of the horizontal deformation behaviour of the structure. We see from the GNSS measurements that the part without the pretensioned sheet pile and the asymmetrical soil structure causes the largest deformation and the largest deformation rate. The rate is also quite constant over time, even after 10 years of measurements. We expect that the asymmetrical soil has a large influence on this long-term deformation behaviour.

III. Simulation and validation

9. Method

To analyse the problem and model the impact of the variants the situation will be modelled using the Finite Element Method. Finite element method (FEM) is a method in which many engineering and mathematical problems can be solved in a numerical way. In FEM the problem is modelled, and this model is subdivided into elements (meshing). Elements are components of a certain geometry which do not overlap. The elements reaction to each other is calculated with a number of algebraic equations for each node of the elements. Combining the results for all nodes gives a solution to the global problem.

9.1 Plaxis Finite Element Modelling

The directorate-general for public works and water management of the Netherlands (Rijkswaterstaat) gave the task to the TUDelft in 1987 to create a simple 2D Finite Element Method program to make quick analyses of soft soil river beddings. This led to the program Plaxis, which is nowadays a well-known FEM product in the geotechnical field. The program works with models which are divided into several small elements which all have a certain behaviour. Models can vary which lots of different parameters to create a useful model for the problem at hand.

Plaxis consists of a 2D and a 3D package. For problems with a uniform cross section in one of the dimensions a 2D model can be used to simulate the case. 2D models have much less elements which seriously decreases the calculation time of the problem.

In the soil models a relation is given between the changes in effective stress (σ) and the changes in strain (ε) of the material. Both 2D and 3D simulations can be performed. This leads to a matrix $\underline{\underline{M}}$ which gives the stress-strain relation in the Cartesian directions.

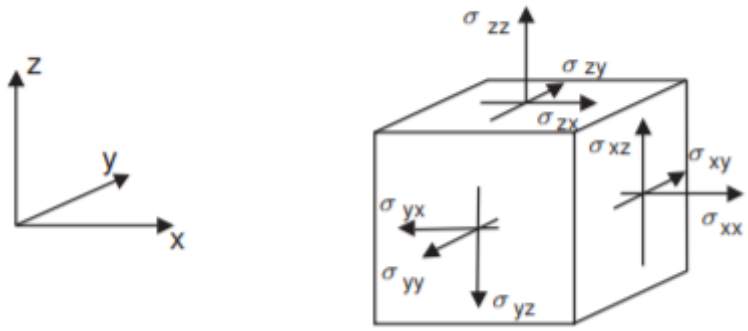

Figure 24 Cartesian directions (Plaxis manual [13]*)*

The general definition of a soil model in Plaxis is:

$$\sigma = M * \varepsilon$$

For this research it is chosen to use only a 2D finite element modelling. Different studies have shown that results from 2D models in similar simulations give sufficient results.

According to [14] the use of two-dimensional plane strain model in the analysis of embankments on soft soils could be justified by converting three-dimensional structures such as drains, piles and plates to an equivalent system. In [15] a study has been done to test embankments on soft soils, to compare the finite element modelling to the real case. In this study it showed that 2D analysis could lead to better results compared to 3D models, if updated mesh and water pressure functions are applied.

9.2 Geometry

The model dimensions are chosen to represent the case study as much as possible. Some components are left out or simplified to create a schematic overview for research purposes. The model consists of 5 soil layers which are a representation of the average soil condition in the area.

The subsoil of the finite element modelling is most accurately based on the available data at the location of the case study. That means that the soil layers, depths and the water level are taken from the report [6] and [16] "Zettingen en stabiliteit HSL baan Rijnstreek Zuid tussen de boortunnel (km 30.400) en de Rijpwetering (km 33.400)" by Bouwcombinatie Hollandse Meren.

The model consists of 5 soil layers representing the soil composition. The water level is located at -2 NAP.

Soil		**Clay**	**Peat**	**Clay**	**Peat**	**Sand**
Specific		Silty	Clayey	Silty	Basis	Pleistocene
Top	(m)	-1.2	-1.7	-5.6	-10.6	-11.6
Bottom	(m)	-1.7	-5.6	-10.6	-11.6	-35
Thickness	(m)	0.5	3.9	5	1	23.4
Soil Model		Mohr-Coulomb	Soft soil Creep	Soft Soil Creep	Soft Soil creep	Hardening Soil

Table 7 Plaxis model soil layers

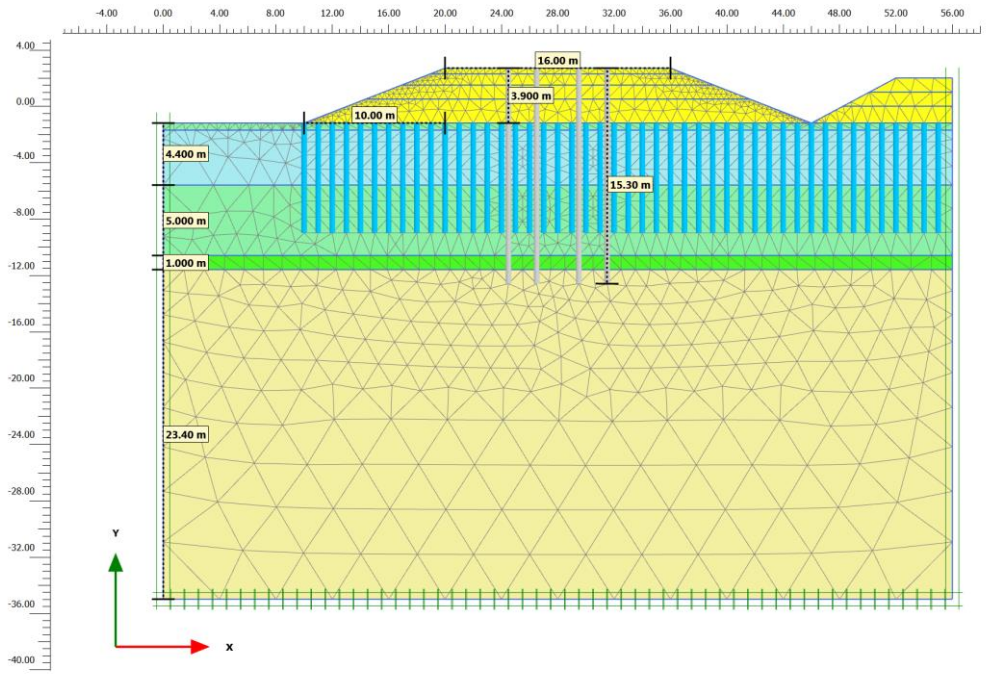

Figure 25 Plaxis model geometry dimensions

The embankment is then constructed on top of the soil model. The model is shown in Figure 25. The embankment construction is done in multiple phases of a sand layer over time. The phases of construction are shown in Table 8.

Embankment construction phases

Phases	Height	top level (m) NAP	top level (m) ground level	days before construction	total days
Phase 1	1.95	0.75	1.95	2	2
Phase 2	0.75	1.5	2.7	100	102
Phase 3	0.8	2.3	3.5	100	204
Phase 4	0.4	2.7	3.9	50	257

Table 8 Embankment construction phases

The foundation piles are constructed after completion of the final sand layer (i.e. after phase 4). First the total structure will have a consolidation period of 150 days before construction of the piles. The piles are 15.3 m long and embedded in the Pleistocene sand layer. The foundation is modelled as a hinged structure in the bottom and can freely deform over the height. The top of the piles have a rotational fixity which means the tops cannot rotate. This represents the fixity of the piles to the concrete slab.

9.3 Boundary conditions

The modelling will rely on certain boundary conditions to start the calculation of the elements. The model is 2D which leads to 4 boundaries 2 in the X-direction and 2 in the Y-direction. On the x=0, x=56 and y=-35 plane, u_x=0 and u_y=0. The upper value of y has no boundary condition. The soil elements are normally fixed at the boundaries, therefore sufficient space has to be in between the embankment and the boundaries such that they do not influence the results. The X boundaries and positive Y boundary are open for groundwater flow, the negative Y boundary is closed for groundwater flow.

9.4 Material models

Plaxis contains a number of different soil models to model the layers of soil. Each model has different benefits but also its cons. Here the models used in this study are briefly described.

Mohr-Coulomb

The Mohr-Coulomb model is a simple linear elastic perfectly plastic model. It can be used as a first approximation of the soil behaviour. The elastoplastic model is decomposed into an elastic and a plastic part.

$$\underline{\varepsilon} = \underline{\varepsilon^e} + \underline{\varepsilon^p}$$

Hooke's law of isotropic elasticity is the basis of the linear elastic part of the model. The plastic part of the model is based the Mohr-Coulomb failure criterion.

Mohr Coulomb model

Symbol	Parameter	Unit
E	Young's modulus	kN/m²
ν	Poisson's ratio	-
c	Cohesion	kN/m²
φ	Friction angle	°
ψ	Dilatancy angle	°
σ_t	Tension cut-off and tensile strength	kN/m²
G	Shear Modulus	kN/m²
E_{oed}	Oedometer modulus	kN/m2

Table 9 Mohr-Coulomb model parameters

Hardening soil

In the hardening soil model, the plastic part is different in comparison to the elastic perfectly plastic model. The yield surface of a hardening plasticity model can expand due to plastic straining. The soil stiffness in the model is stress dependent. There are two different forms of hardening, namely shear hardening and compression hardening. Both types are included in the hardening soil model.

The model is an advanced model for simulating both soft and stiff soils. Some characteristics of the model are:

- Stress dependent stiffness according to a power law
- Plastic straining due to primary deviatoric loading
- Plastic straining due to primary compression
- Elastic unloading /reloading
- Failure according to the Mohr-Coulomb failure criterion

Hardening Soil model

Symbol	Parameter	Unit
Mohr-Coulomb parameters		
c	Cohesion	kN/m²
φ	Friction angle	°
ψ	Dilatancy angle	°
σ_t	Tension cut-off and tensile strength	kN/m²
Stiffness parameters		
E^{ref}_{50}	Secant stiffness in standard drained triaxial test	kN/m²
E^{ref}_{oed}	Tangent stiffness for primary oedometer loading	kN/m²
E^{ref}_{ur}	Unloading/reloading stiffness	kN/m²
m	Power for stress-level dependency of stiffness	-
Advanced parameters		
υ_{ur}	Poisson's ratio for unloading-reloading	-
K_0	σ'xx / σ'yy stress ratio (horizontal/vertical stress)	-
p^{ref}	Reference stress for stiffnesses	kN/m²

Table 10 Hardening soil model parameters

Soft Soil Creep

The soft soil creep model (SSC) is based on the Hardening Soil (HS) model and uses also the Cam Clay model. SSC has the benefit that it's the only model which also takes creep (secondary compression) in to addition [17]. This is very important for the simulation in this thesis because creep can have a large effect on the long-term behaviour (settlement) of soils. According to [17] secondary compressions can become substantial in later years if large primary settlements have occurred for instance in the construction of dams and embankments of soft soils.

According to the Plaxis 2D manual [13] and [17], some characteristics of the SSC model are:

- Stress dependent stiffness (logarithmic compression behaviour)
- Distinction between primary loading and unloading-reloading
- Secondary (time-dependent) compression
- Failure mechanism according to Mohr-Coulomb criteria
- Permanent strain in visco-elastic behaviour (creep) instead of plastic behaviour

Modelling of compression and creep behaviour in SSC is based on the 1D theories and uses isotropic behaviour. Compression in SSC is modelled by the following equation in which the strain is considered of multiple vectors for 2D or 3D, elastic strain (ε^e), plastic strain (ε^p) and creep (ε^c).

$$d\underline{\varepsilon} = d\underline{\varepsilon^e} + d\underline{\varepsilon^p} + d\underline{\varepsilon^c}$$

In the first stage elastic strain will occur. Elastic strain is a form of strain in which the distorted body returns to its original shape and size when the deforming force is removed. The elastic strain is calculated by the following equation.

$$-d\varepsilon^e = \kappa^* \frac{dp'}{p'} = \frac{1+v_{ur}}{1-v_{ur}} \frac{\kappa^*}{1+2K_0} \frac{d\sigma'}{\sigma'}$$

Permanent strains are subdivided in two forms of strain. Plastic strain (ε^p) results from consolidation and creep (ε^c) as a secondary (time dependent) strain depending on the material characteristics. Plastic strain is modelled by the Mohr-Coulomb model. Creep is modelled with the following equation.

$$-d\varepsilon^c = \frac{\mu^*}{\tau}\left(\frac{p^{eq}}{p_c^{eq}}\right)^{\frac{\lambda^*-\kappa^*}{\mu^*}} = \frac{\mu^*}{\tau}\left(\frac{1}{OCR}\right)^{\frac{\lambda^*-\kappa^*}{\mu^*}}$$

The parameters used in the soft soil creep model are shown in the table below.

Symbol	Parameter	Unit
Mohr-Coulomb parameters		
c	Cohesion	kN/m2
ϕ	Friction angle	◦
ψ	Dilatancy angle	◦
Stiffness parameters		
κ*	Modified swelling index	-
λ*	Modified compression index	-
μ*	Modified creep index	-
Advanced parameters		
υ_{ur}	Poisson's ratio for unloading-reloading	-
K_0	σ'xx / σ'yy stress ratio (horizontal/vertical stress)	-
p'	Effective isotropic stress	-
σ'	Effective mean stress	kN/m2

Table 11 Soft soil creep model parameters

The soil parameter M is the slope of the critical state line. The critical state line represents the failure criterium of the soil. In the figure the Mohr-Coulomb ellipses are given. Within the ellipses under the Mohr-coulomb line the soil will behave elastically. If the isotropic stress increases, the deviator stress can increase because the ellipse grows.

For settlements in soft soils the soft soil creep model predictions are the most accurate on the long term according to the study in [18]. In which different models are used to compare to actual settlements of an embankment founded on soft soils.

Embedded beam

Since it's impossible to model a beam element in a 2D model, the embedded beam is a simplified approach to deal with a row of piles in a 2D plane strain model. The embedded beam is modelled as a Mindlin beam element which is not located in the 2D mesh but imposed on the mesh. The soil mesh is therefore not influenced by the presence of the pile. The underlying soil mesh is continuous, and the pile element interacts with the surrounding elements. As can be seen in Figure 26. The pile is surrounded by an elastic area around the pile. The interaction of the soil and the pile is defined by (K). Friction between the soil and pile is determined by the relative displacement of the elements, therefore both negative as positive shaft friction is considered.

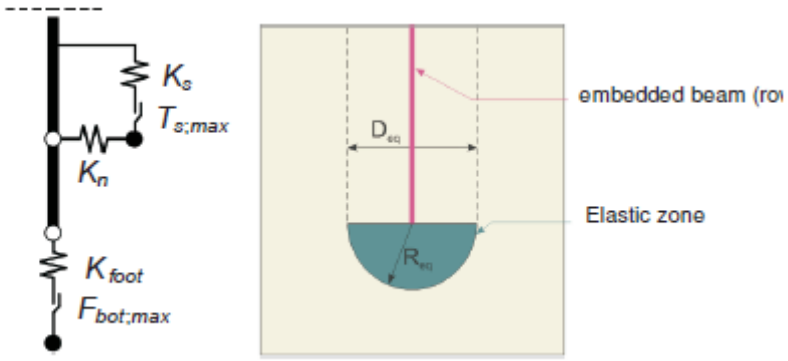

Figure 26 Stiffness of the embedded interface elements and the elastic zone around the pile (Plaxis Manual)

Embedded piles can be defined by their Elastic modulus (E), specific weight (γ), friction resistance (T_{max}) and the bearing capacity (F_{max}). The shape and size of the piles can be chosen and with that the moment of inertia.

Since a pile is modelled as a plate element the pile stiffness is changed into a stiffness of an plate element, such that soil-pile interaction is included in the model. The resulting moments in the pile element are shown per meter length as in case of a plate element. The actual working stress on the pile is depending on the soil area influencing the pile. This can be seen in Figure 27.

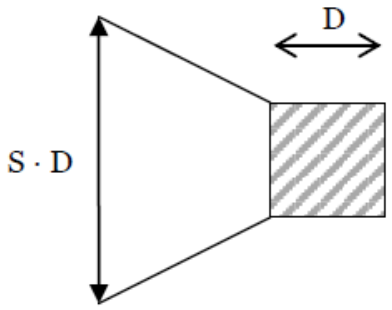

Figure 27 Shell factor for pile stiffness

To calculate the moments in a single pile of the row a shellfactor (S) and the pile diameter (D) has to be used. The following equation shows the calculation of the stiffness and moments. This will give a bending moment expressed in kNm/m.

$$EI_{plate} = \frac{EI_{pile}}{S * D}$$

$$M_{pile} = M_{plate} * S * D$$

The shell factor is usually between 2 and 8 and it's advised to not use larger values then 10. For situations with plastic behaviour a value between 3 and 5 is suitable [19].

In case multiple piles are used close to each other the affected area will overlap. In this case the bending moment needs to be multiplied by the distance between the piles to achieve the bending moment per pile, expressed in kNm [20].

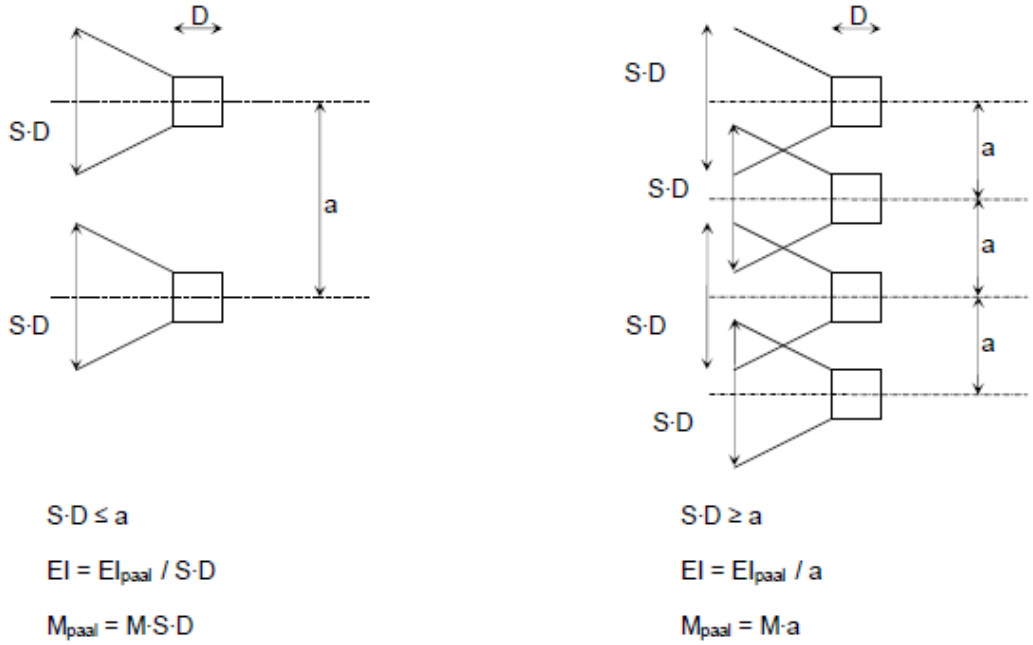

Figure 28 Schematisation of horizontally loaded piles [20]

Updated mesh and water pressure analysis

Small displacements have only limited influence on the mesh geometry and therefore the further calculations. Plaxis will neglect the small displacements and the changing geometry in normal calculations. If larger displacements occur, as in this case, the influence on the calculation results will increase. Therefore, it is advised to use the updated mesh function in the program. The updated mesh will renew the coordinates of the nodes during the calculation, which therefore forms an updated mesh. The function is especially advised in situations with reinforced soil structures, elements which will collapse due to rotation and situations in which very soft soil layers will cause large displacements [21]. This is the case at the rail embankment near Rijpwetering.

9.5 Parameters

For the different soil layers different soil models will be used. This depends on the soil properties and the results we want to achieve. The different soil models will also require different input parameters. The parameters are shown in the table below.

Material	Unit	Zand, Pleistoceen	Zand, ophoog	Veen, basisveen	Veen Kleiig	Klei, siltig
Material model		Hardening soil	Mohr-Coulomb	Soft soil creep	Soft soil creep	Mohr-Coulomb
Drainage type		Drained	Drained	Undrained (A)	Drained	Undrained (A)
General						
γ_{unsat}	kN/m³	17	18	10,4	11,1	15,7
γ_{sat}	kN/m³	20	20	10,4	11,1	15,7
e_{init}		0,5	0,5	15	15	0,5
Parameters						
E'	kN/m²		1,50E+04			4000
ν' (nu)			0,3			0,3
G	kN/m²		5769			1538
λ* (lambda*)				0,407	0,407	
κ* (kappa*)				0,08	0,08	
μ*				0,014	0,014	
c'_{ref}	kN/m²	0	0,01	5	4	2
ϕ (phi)	°	32,5	32,5	25	25	25
ψ (psi)	°	0	2,5	0	0	0
ν_{ur}				0,22	0,22	
K_0^{nc}				0,3	0,3	
M				2,37	2,37	
Flow parameters						
k_x	m/day	7,128	3,499	0,02	4,32E-03	0,04752
k_y	m/day	7,128	3,499	0,02	4,32E-03	0,04752
c_k		1,00E+15	1,00E+15	1	1	1,00E+04
Initial parameters						
OCR		1	1	1	1	1
POP	kN/m²	0	0	5	5	5
Data set		USDA	USDA	USDA	USDA	USDA
Model		Van Genuchten	Van Genuchten	Van Genuchten	Van Genuchten	Van Genuchten
Type		Sand	Loamy sand	Clay	Clay	Clay
< 2 μm	%	4	6	70	70	70
2 μm - 50 μm	%	4	11	13	13	13
50 μm - 2 mm	%	92	83	17	17	17

Table 12 Soil material parameters used in simulation

The foundation piles used are precast concrete foundation piles with an area of 400 mm * 400 mm and a length of 15.6 m. For the interface stiffness no values are known and therefore Plaxis advices to use the default parameters for layer dependent interface conditions [13].

The following parameters are used and based on the report KW1304 km. 32.800 - 33.300 - KW1408 Paalfundering, afdracht belastingen by the contractor Bouwcombinatie Hollandse Meren [22].

Parameters	Concrete foundation pile	
Beam type	Massive square beam	
Width	0.4	m
A	0.16	m2
I	2.13E-03	m4
Lspacing	2	m
E	3.82E+07	kN/m2
γ	25	
Axial skin resistance	Layer dependent	
Tmax	30	kN/m

Table 13 Foundation pile parameters used in simulation

For the simulation of the supported structure the embankment is supported by a sheetpile. The sheetpile used in the supported sections of the case study is an AZ48 sheetpile.

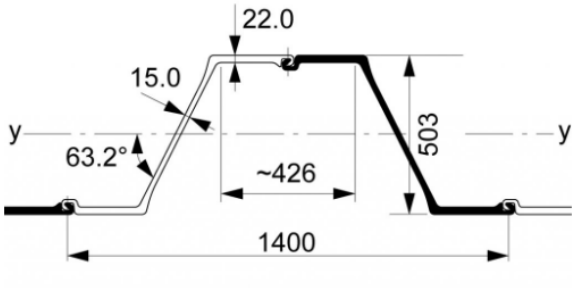

Figure 29 AZ-48 sheetpile dimensions

The parameters used in the simulation for the supported structure are shown in Table 14. The sheetpile is modelled as a plate structure.

Parameters	Sheet pile	
Name	AZ 48	
Material type	Elastoplastic	
EA	6,06E+06	kN/m/m
EI	2,43E+05	kNm2/m
d	0,673	m
v	0,2	
Mp	1333	kN/m/m

Table 14 AZ-48 sheetpile parameters used in simulation

10. Simulation

10.1 Variants of case study

In the modelling of the rail embankment we are trying to investigate the causes of the horizontal deformations that occur in the case study. We will investigate different cases in which an element of the case study is implemented to see the effects on the deformations and stresses in the soil body.

Case 0 – Symmetrical soil body

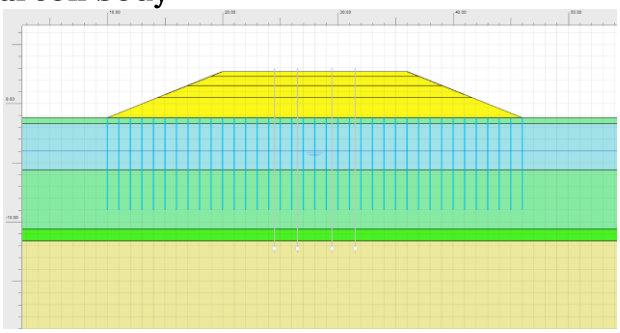

Figure 30 FEM model symmetrical case

For the reference case a symmetrical embankment is chosen with 4 foundation piles. This is the basic case from which the differences with the other cases can be compared.

Case 1 – Asymmetrical, soil body with a ditch on one side

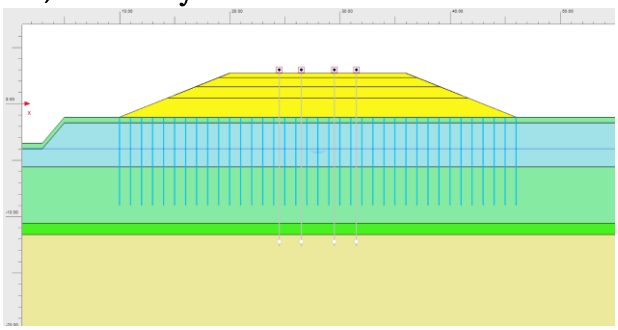

Figure 31 FEM model with a ditch on one side

In this case the influence of drainage ditch is analysed. In the case study a ditch is located parallel to and on the western side of the embankment.

Figure 32 Ditch located parallel to the rail embankment and highway broadening (beeldbank RWS)

This ditch has a width of approximately 11 m and a depth of 2 m. It is located 6 m from the toe of the embankment and has a slope of 2:1. The rest of the parameters are the same as for the symmetrical case to observe the differences. These differences give an idea of the influence of the ditch on the settlement behaviour.

Case 2 – Asymmetrical, soil body with extra embankment on one side

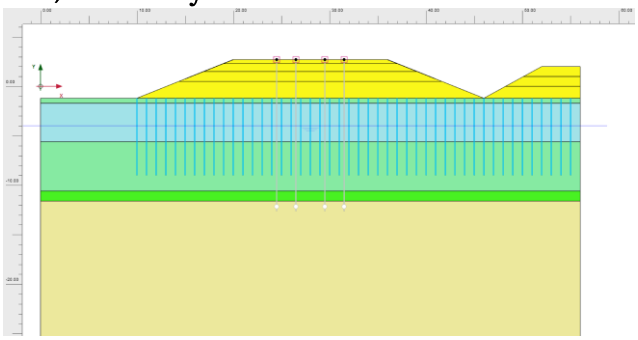

Figure 33 FEM model with extra embankment

In this case the influence of an extra embankment parallel to the structure is analysed. The extra embankment is located parallel on the eastern side of the rail embankment. It is constructed similarly in different phases simultaneously with the rail embankment. The height and size of the embankment reflect the A4 highway embankment which is constructed in the case study. This highway was already existing, but the embankment was enlarged simultaneously with the construction of the HSL. The expectance is that the extra embankment causes lateral forces to push the rail embankment to the western side (left side).

Case 3 – Asymmetrical soil layer from the middle

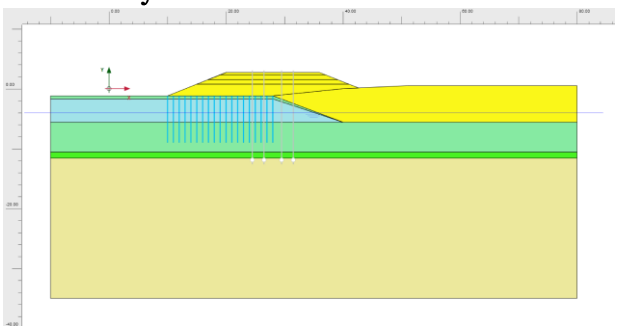

Figure 34 FEM model asymmetrical soil layer

In this case the influence of an asymmetrical soil structure is analysed. In the case study the soil investigation shows a difference in the soil structure underneath the embankment. Due to the cunet of the old A4 highway, the HSL embankment is constructed partly on sand and partly on the regular peat and clay layers. The sand layer reaches to halfway underneath the embankment. Therefore, half of the structure is founded on soft soils and half is founded on stronger soil.

Case 4 – Asymmetrical soil layer 5m from the middle

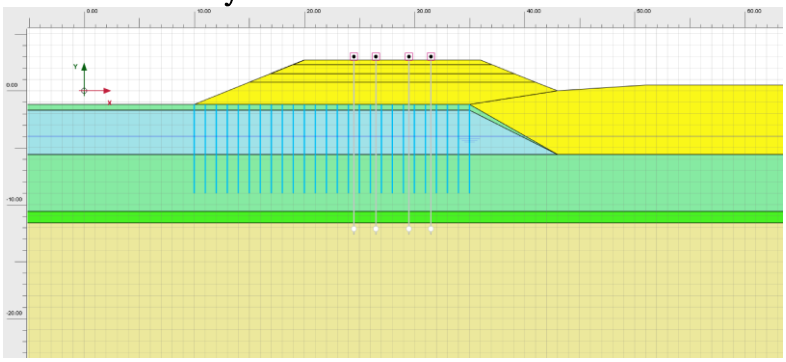

Figure 35 FEM model asymmetrical soil layer 5m from the middle

In this case the influence of the location of the asymmetrical soil layer is analysed. The same soil layer is used as in the previous case, but the location is shifted. The sand layer is shifted 7 meters to the right and reaches for 5 meters underneath the embankment.

Case 5 – Asymmetrical soil body with sheetpile wall

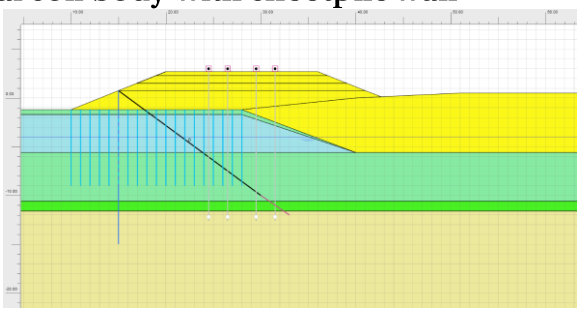

Figure 36 FEM model asymmetrical soil with anchored sheetpile

In this case the influence of a sheetpile wall is analysed. The soil structure is the same as for case 3. The sheetpile is modelled as a plate structure and is pretensioned by an anchor with

a prestressing of 50 kN. The sheetpile is located in the slope on the western side of the embankment and reaches to a depth of -15 NAP.

Case 6 – Combination of Case1, 2 and Case 3

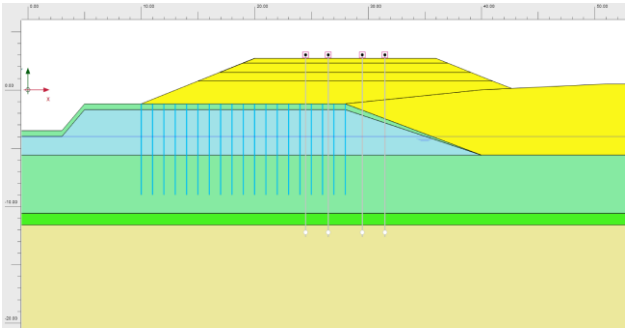

Figure 37 FEM model Combination of case 1, 2, 3

In this case the models of case 1, 2 and 3 are combined to see the influence of the variants together. The model consists of an unsupported structure with an asymmetrical soil layer, a ditch and the extra embankment on one side.

10.2 Results of the variants

Case 0 - Symmetrical soil body

For the symmetrical case study, the embankment settles symmetrically with maximum deformations around the slopes of the embankment. Maximum deformations are plotted 1 year after construction of the piles. The maximum vertical displacement is 52.9 mm and the maximum horizontal displacement is 13.3 mm.

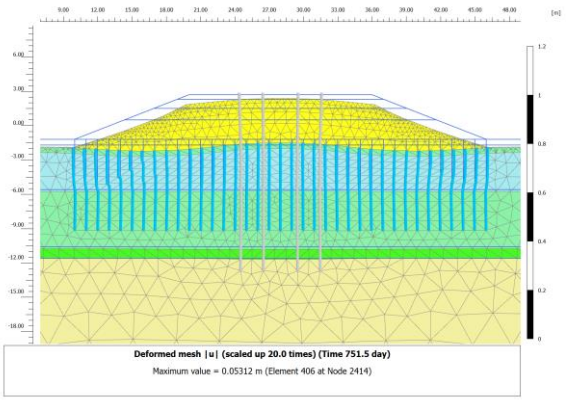

Figure 38 Deformed mesh for symmetrical case

The pile tops deform symmetrically to both sides towards the side of the embankments. The largest deformations occur on the slopes of the embankment both in vertical as in horizontal direction.

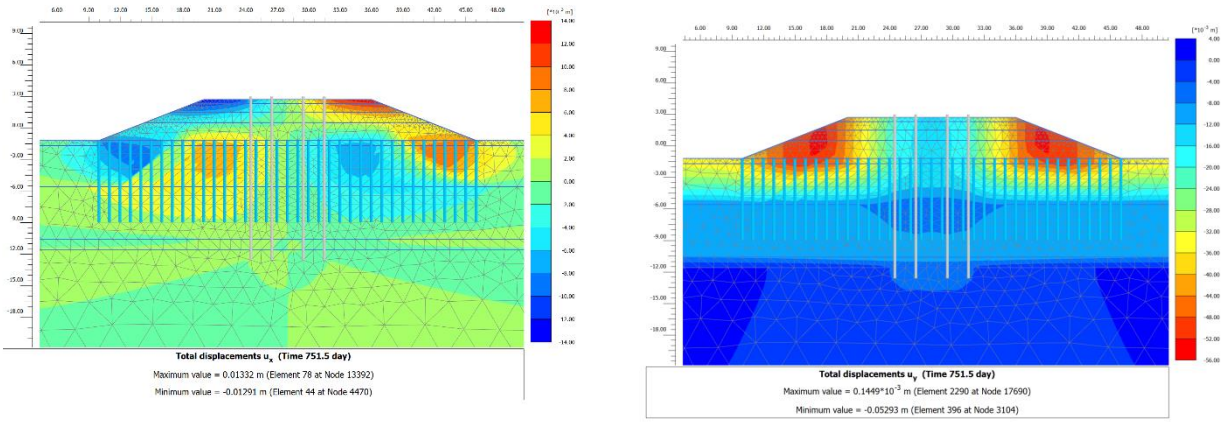

Figure 39 Contour plots (ux left, uy right) Case 0

The 4 foundation piles all move individually away from the centre of the embankment. The piles are numbered from left to right, 1 to 4. Pile 1 and 2 are the left piles which deforms in negative direction according to the XY-coordinate system. Pile 3 and 4 are the right piles which deform in positive direction according to the XY-coordinate system.

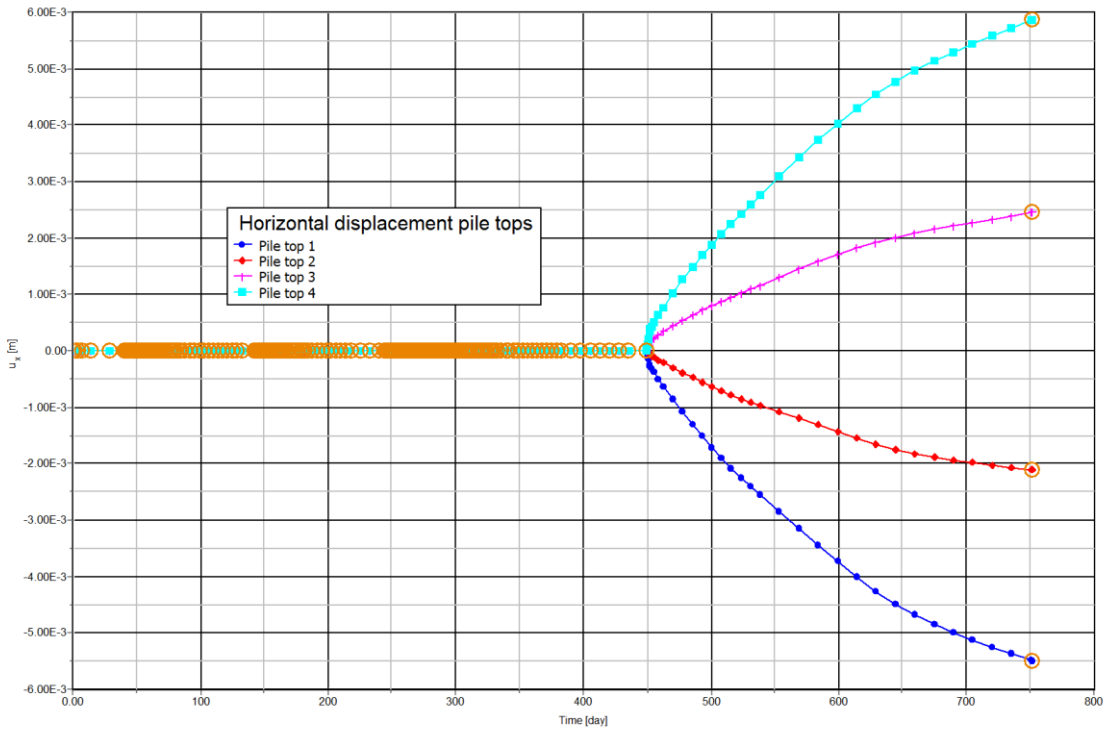

Figure 40 Horizontal displacement in time for top of the piles Case 0

Case 1 – Embankment with a ditch on one side

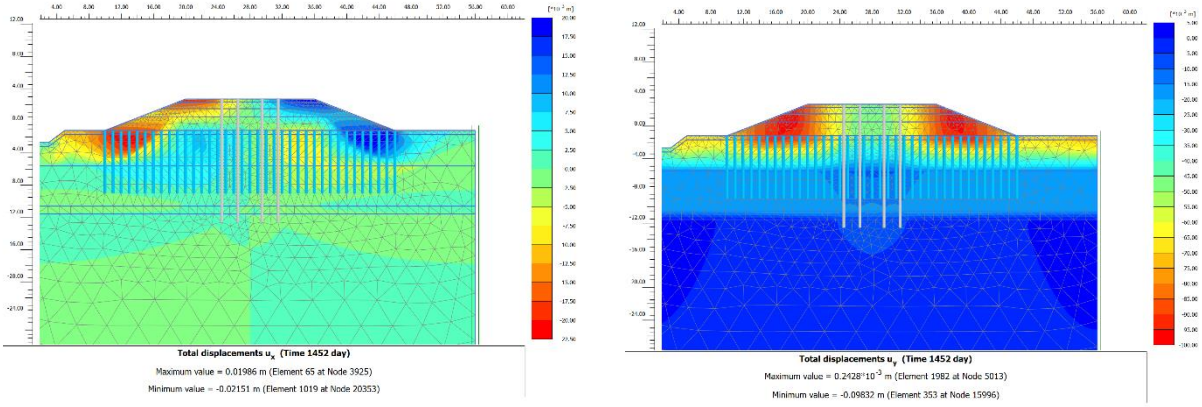

Figure 41 Contour plots (ux left, uy right) Case 1

The horizontal displacement of the pile tops show that the piles still deform to either sides of the embankment. But in this case the displacement of the piles 1 and 2 is larger than the displacement of piles 3 and 4. This shows that the overall movement of the embankment is influenced by the ditch to move slightly in this direction.

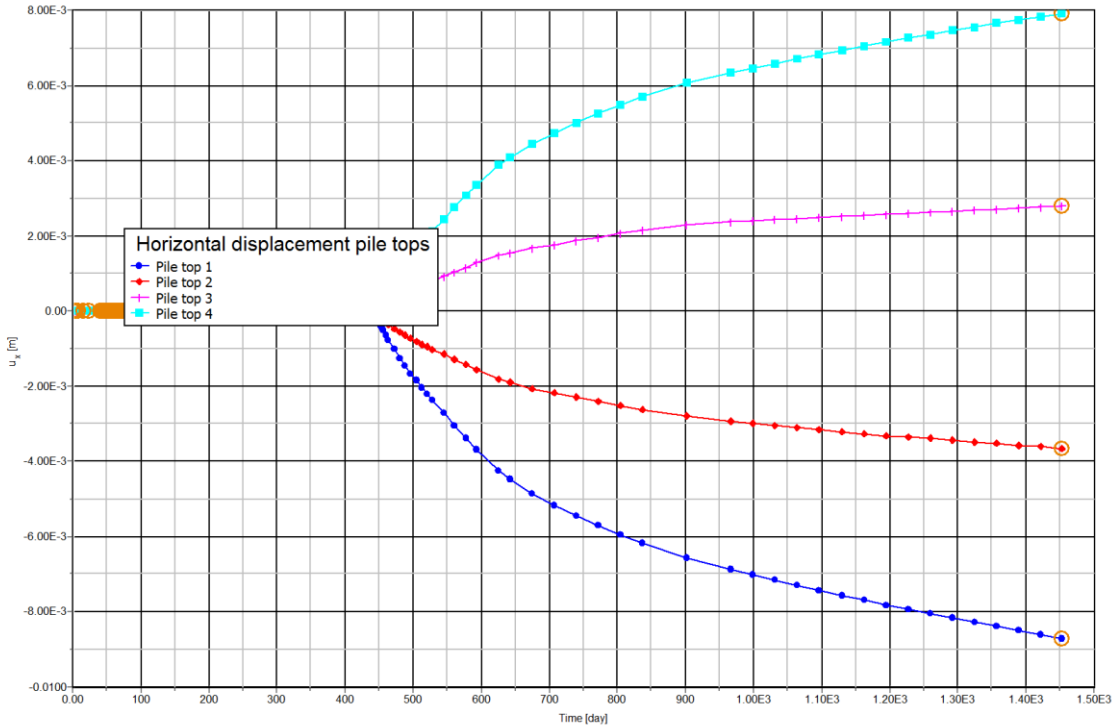

Figure 42 Horizontal displacement in time for top of the piles Case 1

Case 2 – Extra embankment constructed on one side

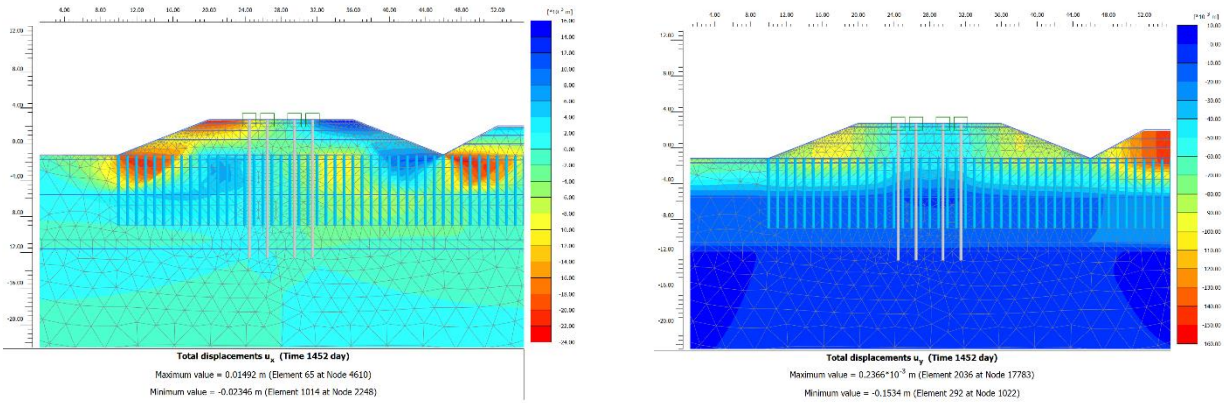

Figure 43 Contour plots (ux left, uy right) Case 2

In the figure the horizontal displacement of the pile tops is plotted. It's clear that the maximum displacement of piles 1 and 2 is much higher and the maximum displacement of piles 3 and 4 is much smaller. In other words, the average of the embankment is a significant deformation towards the left side (negative direction).

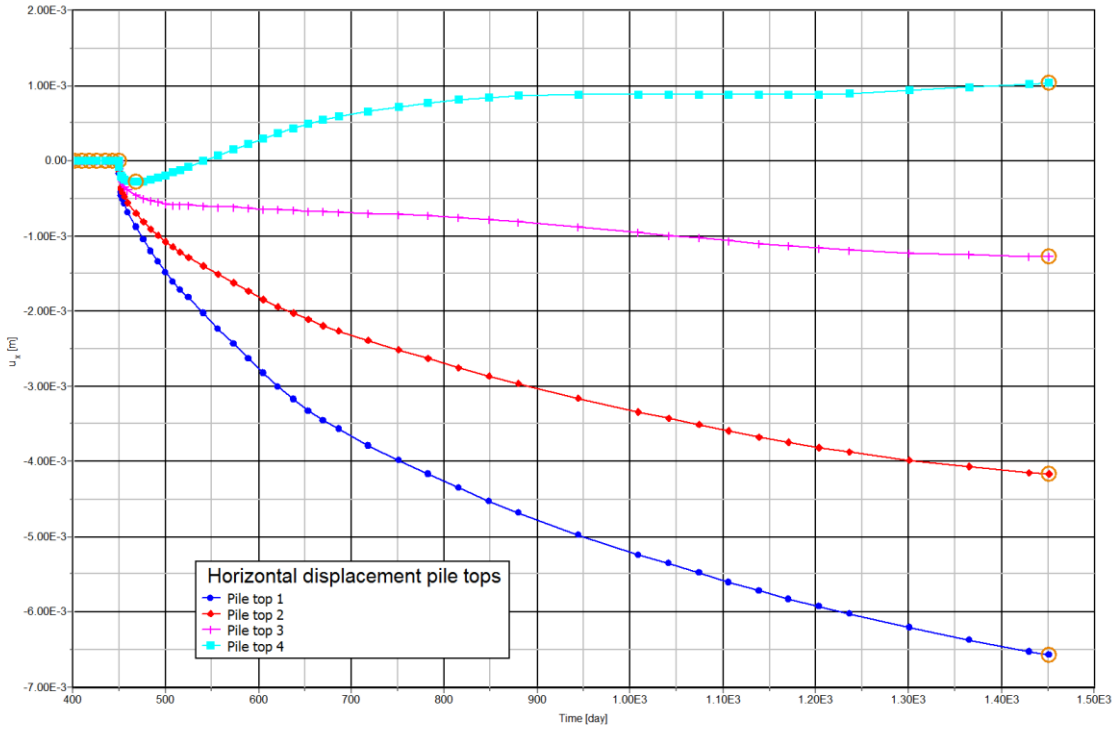

Figure 44 Horizontal displacement in time for top of the piles Case 3

Case 3 – Asymmetrical soil structure from the middle

The contour plots of the horizontal and vertical deformations show clearly a difference in the movement on eastern and western side of the embankment.

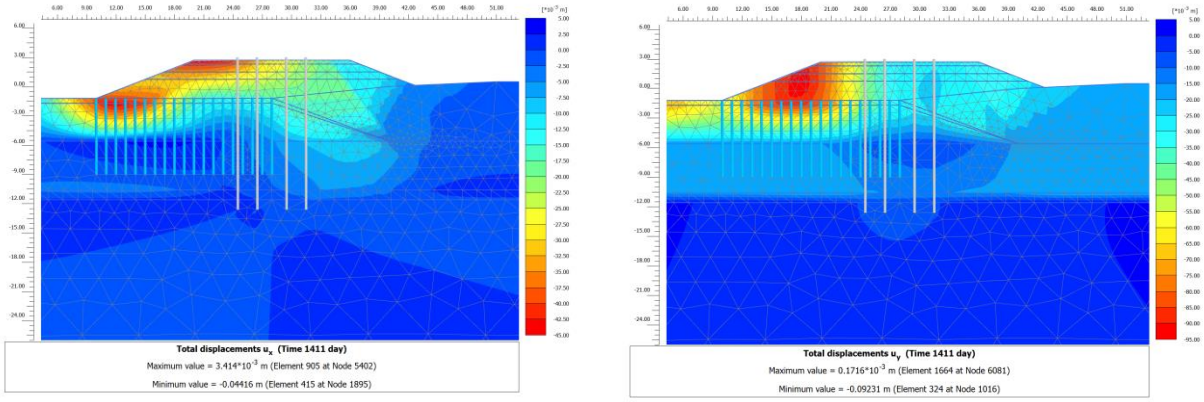

Figure 45 Contour plots (ux left, uy right) Case 3

By looking at the displacement of the pile tops it's clear that all 4 piles are now moving in the same direction. The piles move with a high rate in time and show a large displacement.

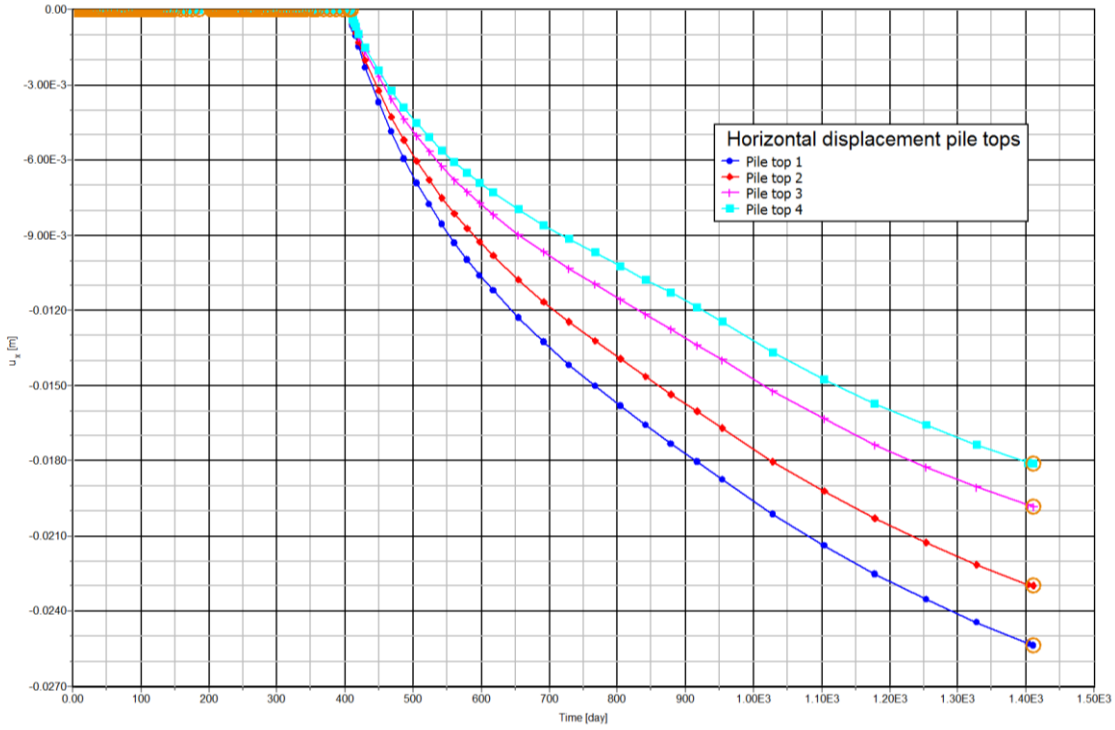

Figure 46 Horizontal displacement in time for top of the piles Case 4

Case 4 – Asymmetrical soil structure 5 m from the middle

From the contour plots it's clear to see the displacement of the embankment in negative x-direction. The vertical contour plot shows much larger displacements on the western side of the embankment compared to the eastern side. This results in a counterclockwise rotation of the embankment which leads to horizontal displacements at the top towards the western side.

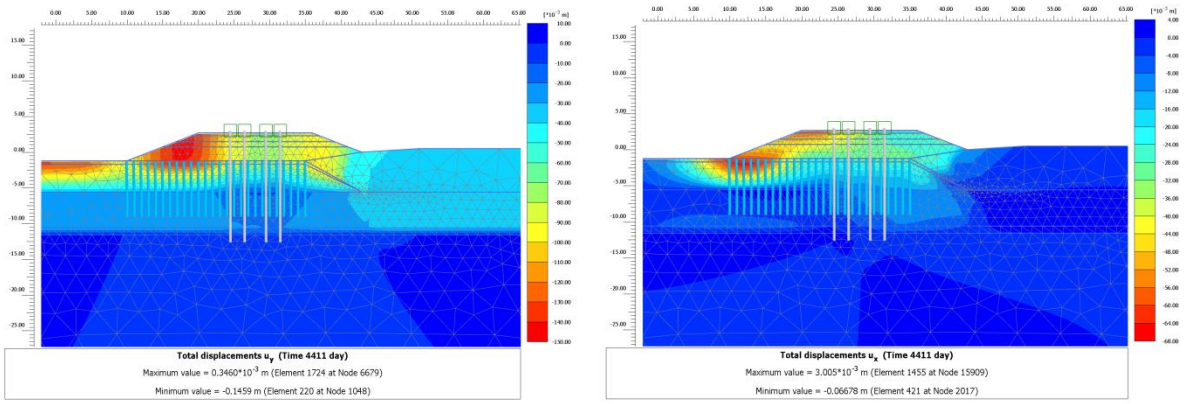

Figure 47 Contour plots (ux left, uy right) Case 4

In the graph with the horizontal displacement of the pile tops it's clear to see that large displacements towards the west occur. The west side deforms a bit more than the east side, similar to the previous case.

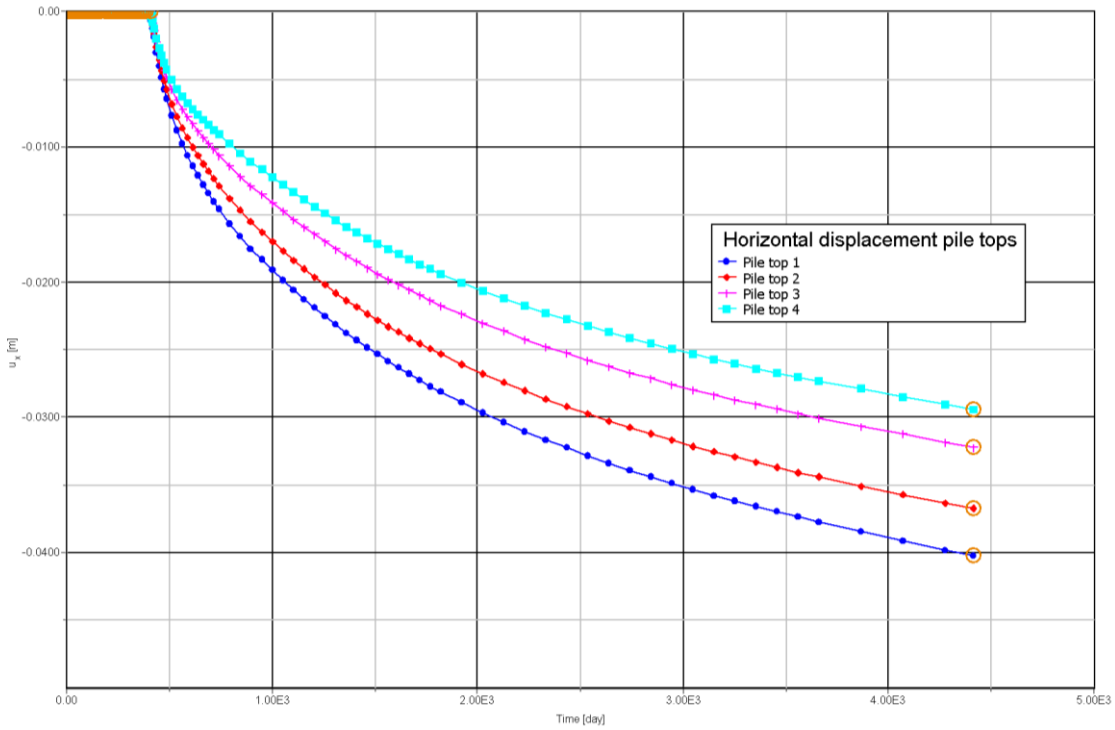

Figure 48 Horizontal displacement in time for top of the piles Case 5

Case 5 - Asymmetrical soil body with sheetpile wall

In the contour plots it's clear to see that both horizontal and vertical displacements are much smaller in the case of the sheetpile. The embankment is held together by the sheetpile which limits all the displacements.

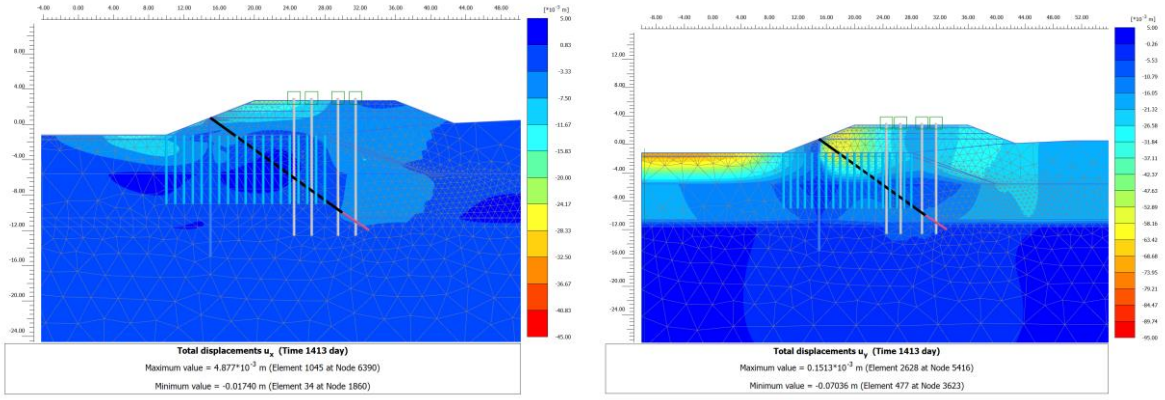

Figure 49 Contour plots (ux left, uy right) Case 5

The graph with the horizontal displacement of the pile tops shows an initial positive displacement because of the prestressing of the anchor. In time the displacements occur in a similar way as for the previous cases. The rate of displacement on the other hand is much smaller.

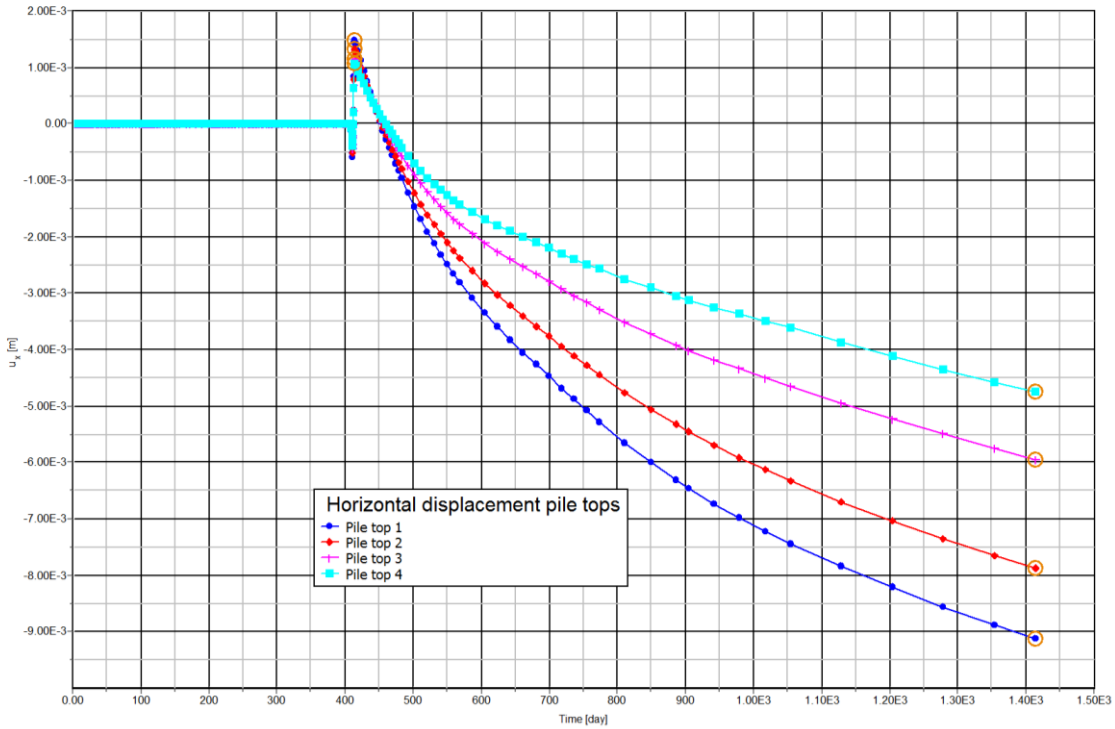

Figure 50 Horizontal displacement in time for top of the piles Case 6

Case 6 – Combination of Case 1, 2 and 3

In the contour plots it's clearly visible that both the horizontal as the vertical deformations are significantly larger on the western side of the embankment. The combination of different cases has contributed to each other leading to even larger displacements.

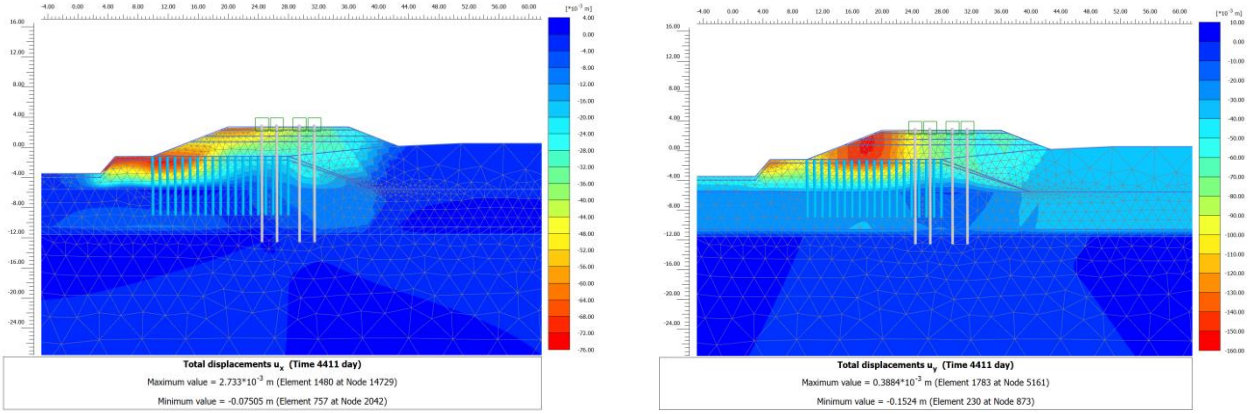

Figure 51 Contour plots (ux left, uy right) Case 6

The foundation piles are clearly deforming all in the same direction. The entire embankment is deforming towards the western side. The total displacement after 4000 days of consolidation is about 43 mm.

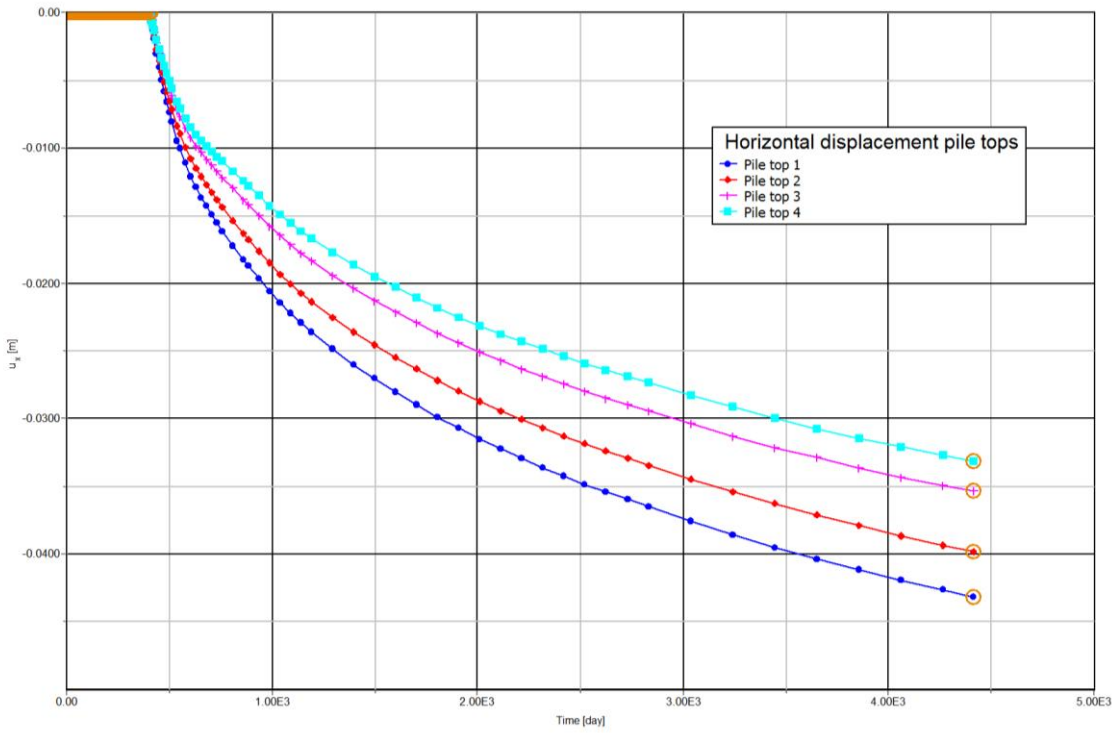

Figure 52 Horizontal displacement in time for top of the piles Case 7

10.3 Comparison of the variants

First the 4 cases results are compared to each other. At first the vertical displacement of the embankment soil is considered. The left top corner of the embankment displacement is plotted against time. This shows that the influence of the 4 different cases do not make a large difference. The vertical displacement is predominantly described by the soil configuration. The surrounding conditions only have a small influence. Case 1 and 2 increase the vertical displacement slightly while case 3 with the stiffer asymmetrical layer decreases the displacement slightly.

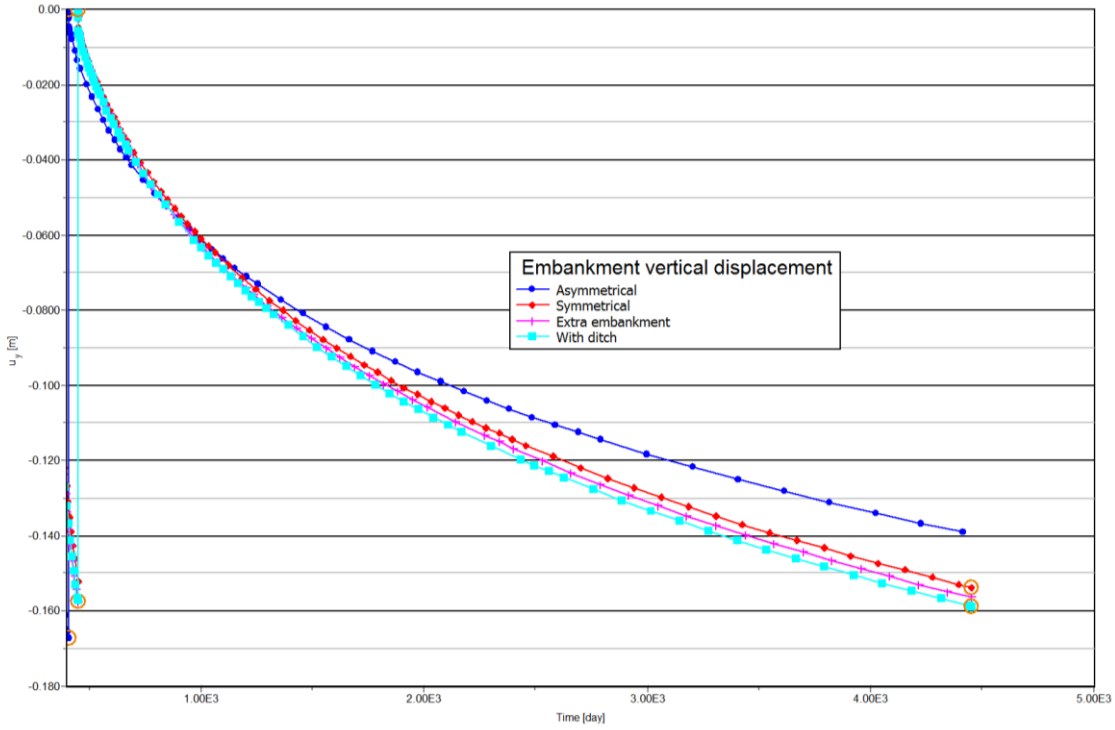

Figure 53 Vertical settlement of the embankment soil left top

In the following graph the horizontal displacement of the pile top of the most left foundation pile is platted against time. The total simulation consists of 4000 days after construction of the piles. From the graph it's clear that the ditch and the extra embankment have a small influence on the maximum displacement. The asymmetrical soil layer leads to a much higher maximum displacement and in a much higher rate. The rate of the asymmetrical soil simulation is also still high after 11 years of consolidation, whereas the other simulations show that the displacement rate has nearly disappeared.

The difference between the location of the asymmetrical soil layer have a small effect on the horizontal displacement. The sheetpile installed from the beginning results in a much lower displacement and the rate after 11 years is significantly reduced.

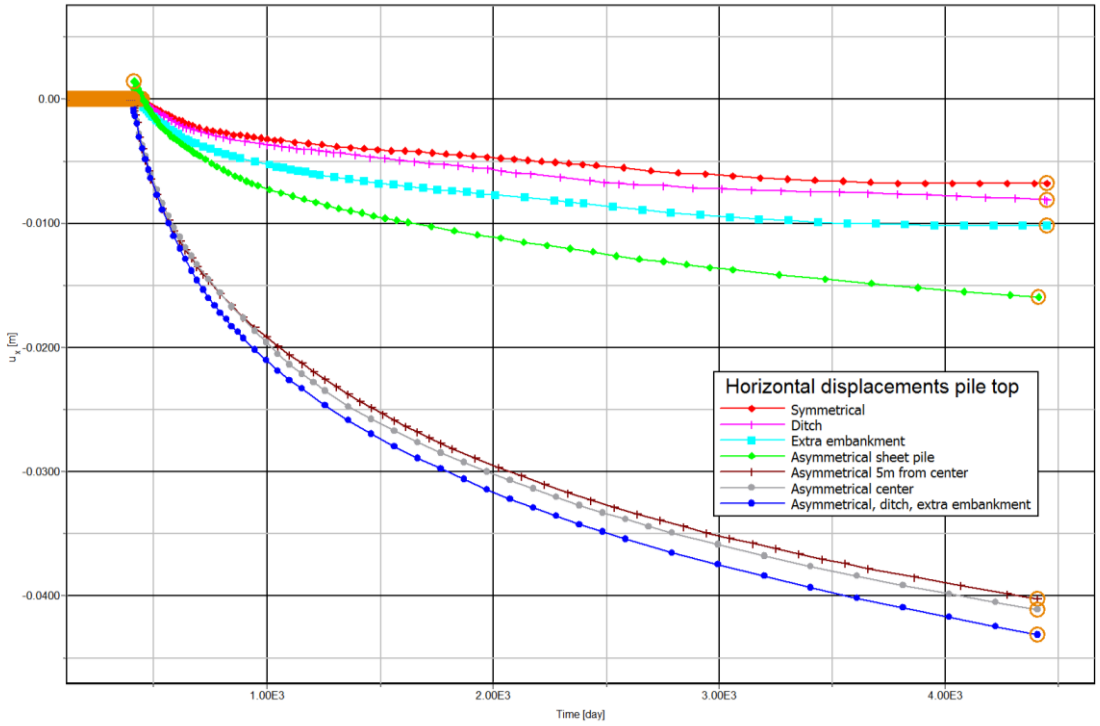

Figure 54 Horizontal displacement of the pile tops

In Figure 55 the pile displacements over the depth are shown. It's clear to see that the shape of the piles is not influenced by the variants. These are all mostly depending on the soil layers. But the amount of displacement has a large difference for all the cases. It's clear from the results that the Asymmetrical soil layer has the largest influence on the deformation.

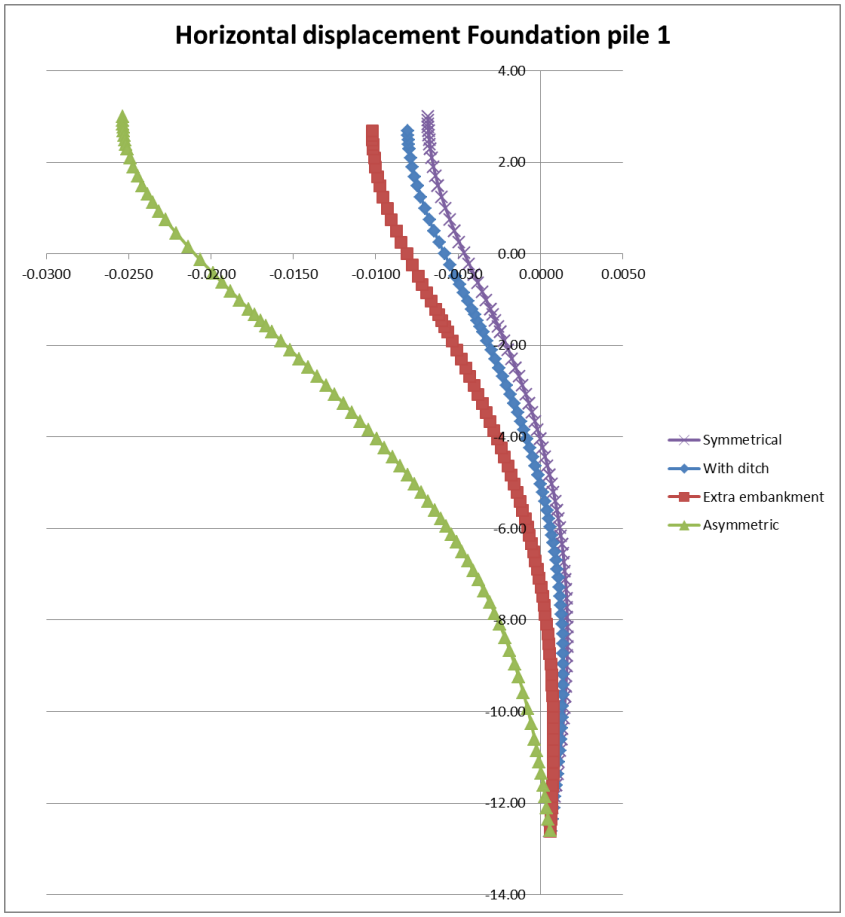

Figure 55 Horizontal displacement of the foundation pile over the depth

In Table 15 the variant results are compelled in a table. The table shows the maximum deformation of the pile top and the maximum moment reached in the foundation piles. From these results it's very clear again that the ditch and extra embankment have a very small influence on the deformation of the pile top compared to the asymmetrical soil layer. But it does also show that already quite some loading occurs to the foundation piles, since the maximum moment has more than doubled. Nevertheless, the main contribution comes from the asymmetrical soil layer.

Case	Description		Pile top	Foundation pile
		Time (days)	Max deformation X (mm)	Max. moment (kNm/m)
0	Symmetric	4451.5	6.81	10.49
1	With ditch	4451.5	8.09	22.6
2	extra embankment	4451.5	10.2	26.17
3	Asymmetric soil middle	4451.5	41.09	62.41
4	Asymmetric soil 5m from side	4451.5	40.02	54.96
5	Asymmetric soil middle + ditch + extra embankment	4451.5	43.09	63.66
6	Asymmetric sheet pile	4451.5	15.94	33.14

Table 15 Comparison of the simulation variants

10.4 Comparison to the measurements

To compare the simulation to the case study measurements the right model has to be selected. There are 2 parts of interest that we will compare with our results. First there is the part with the asymmetrical soil which is not supported by means of a sheetpile wall nor by EPS structure. These are the sections which are measured by GNSS measurements with numbers 2, 3, 5, 6 The second is the case in which the structure is supported by a sheetpile wall but without use of the EPS structure and on the southern side of the viaduct. These are the sections which are measured by GNSS measurements with number 1, 4, 7, 8, 9.

Unsupported embankment

For the unsupported case the measurements of GNSS 3 are used. This is the section in which the structure shows the largest displacements and is therefore the most important section to analyse.

GNSS measurements of the structure have started in 2008 so a total of 11 years of data is known. 2009 was 5 years after construction of the foundation piles and concrete slab. Therefore, the deformation data from the simulation has to be reset to zero after 5 years. From then the incremental displacements are plotted over time for 11 years. The results are shown in Figure 56.

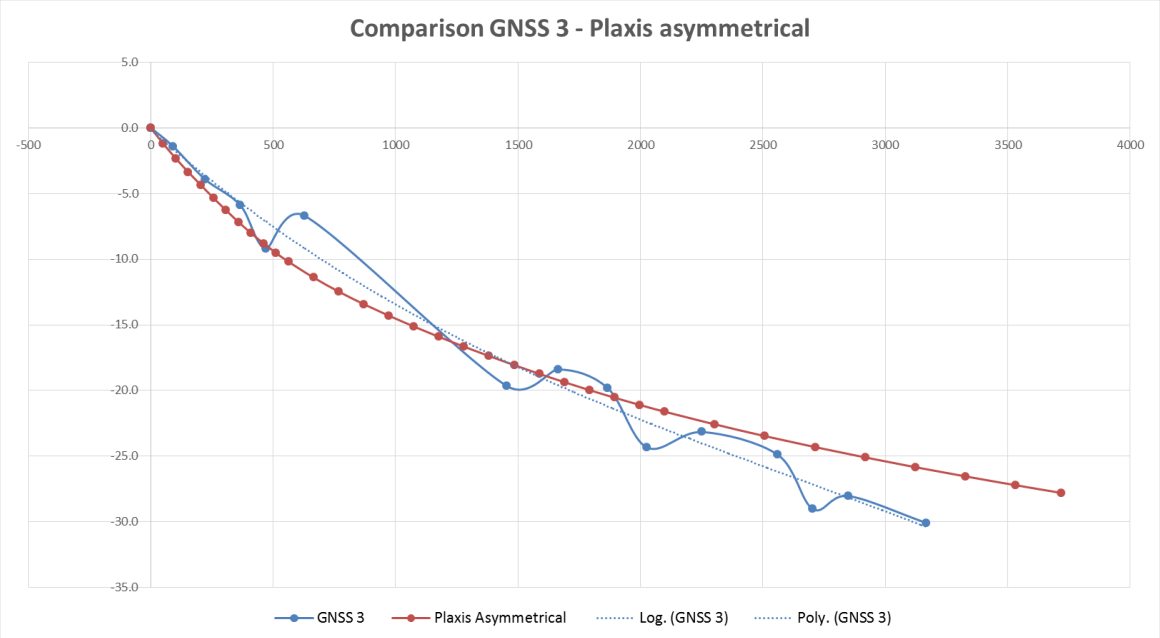

Figure 56 Comparison of the asymmetrical case to GNSS 3 measurements

The data from the GNSS measurements and the Plaxis simulation are already quite identical. The total amount of displacement is very close to the measured displacement. The rate on the other hand differs in both cases. The Plaxis simulation shows a high displacement rate at the beginning and it decreases over time. This also happens with the trendline of the measurements, but the rate does not change as fast. That means that the rate after 11 years is much higher than in the simulation. The expectance is that future displacements will turn out higher than the simulation will show.

But, in the case study we have a combination of multiple factors. In Figure 57 the influence of the combination of the asymmetrical soil and the ditch and the extra embankment is added. We see that the results get a bit closer to the field measurements. The rate of this displacement is 0.0043 mm/day which is 1.57 mm/year.

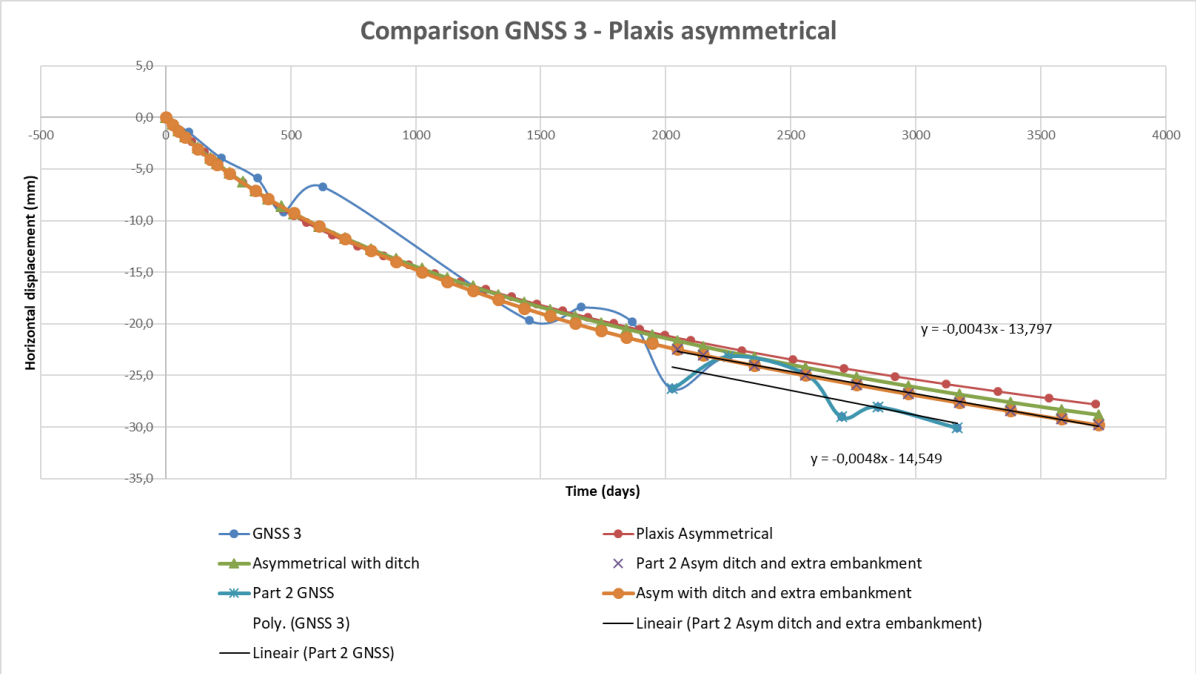

Figure 57 Comparison of the combined case with GNSS 3 measurements

Supported embankment

For the comparison of the embankment supported by the sheet pile wall we use the measurement data of GNSS 7.

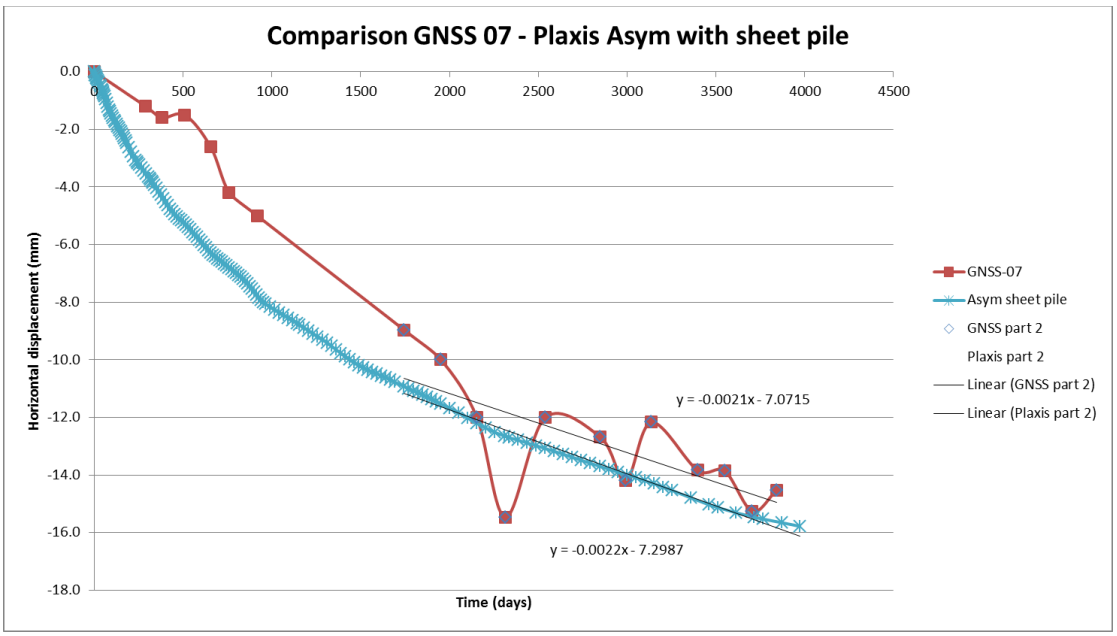

Figure 58 Comparison of the asymmetrical with sheet pile to the GNSS 7 measurements

In the figure the GNSS measurements form profile 07 are shown in comparison to the horizontal displacement of the pile top. The simulation case is case 4, the asymmetrical soil body with a prestressed sheet pile from the start of the simulation. The results show the displacement for the last 10 years.

The total displacement and the rate are quite similar for the simulation and the measurements. Especially the rate from 1744 days onwards is shows good comparability.

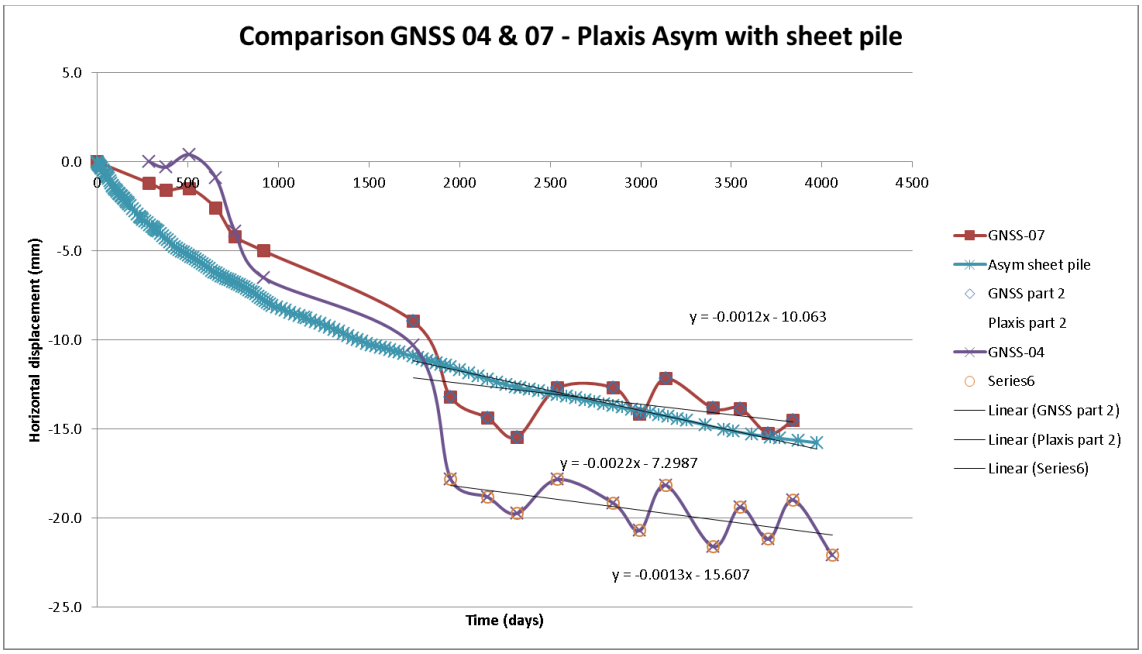

Figure 59 Comparison of the Asymmetrical case with sheetpile to the GNSS 4 and 7 measurements

In this figure the measurement data of GNSS 4 has been added to the graph. These results are very similar but show an instant increase between day 1744 and 1952. This can be referred to as result of an addition of extra sand to the structure. To fill up some of the vertical gaps extra sand has been added. This increases the weight and has caused extra deformations.

After that instant increase of displacement, the exact same rate is resulting again, but leading to a higher total displacement. Nevertheless, it shows that the model is a suitable simulation for the rate of displacement after approximately 5 years.

Conclusion

The results are quite close to the case study. It's clear what the influence of the different variants is on the horizontal and vertical deformations.

Horizontal displacement rate

Case	Measurements rate		Simulation rate	
	mm/day	mm/year	mm/day	mm/year
Unsupported	0.0048	1.752	0.0043	1.57
Supported	0.0013	0.438	0.0022	0.8

Table 16 Horizontal displacement rate comparison

Although the results are already insightful, they do not give a full representation of the influence on the future. For this the model parameters need to be improved and the results should line up closer with the case study. Therefore, in the next chapter the model will be optimized.

10.5 Train loading

To determine the impact of a train load on the horizontal deformations 2 loading scenarios are tested.

In the first scenario the train loading exists of only vertical load modelled by 2-point loads above the foundation piles of the western track. This can be seen in Figure 60. The loading simulates the Bombardier TRAXX locomotive used in the intercity direct. The locomotive weighs 84 tons and has a length of 18.9 m, the weight is spread over the two loads.

$$\frac{840\ kN}{18.9\ m * 2} = 22.2\ kN/m$$

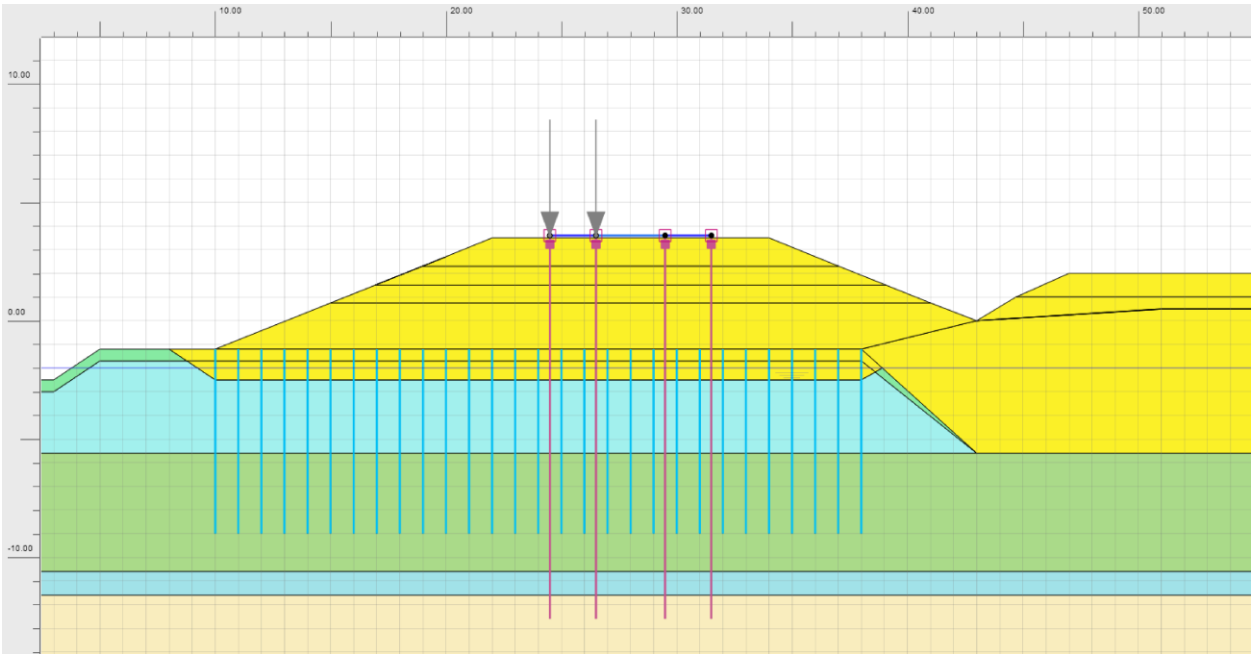

Figure 60 Train vertical loading model

The vertical loading consists of a semi-permanent loading of 0.01 day (14.4 minutes) 3000 days after construction of the track. After the loading phase another 3000 days are simulated.

The results of the horizontal displacement of the pile top is shown in figure.

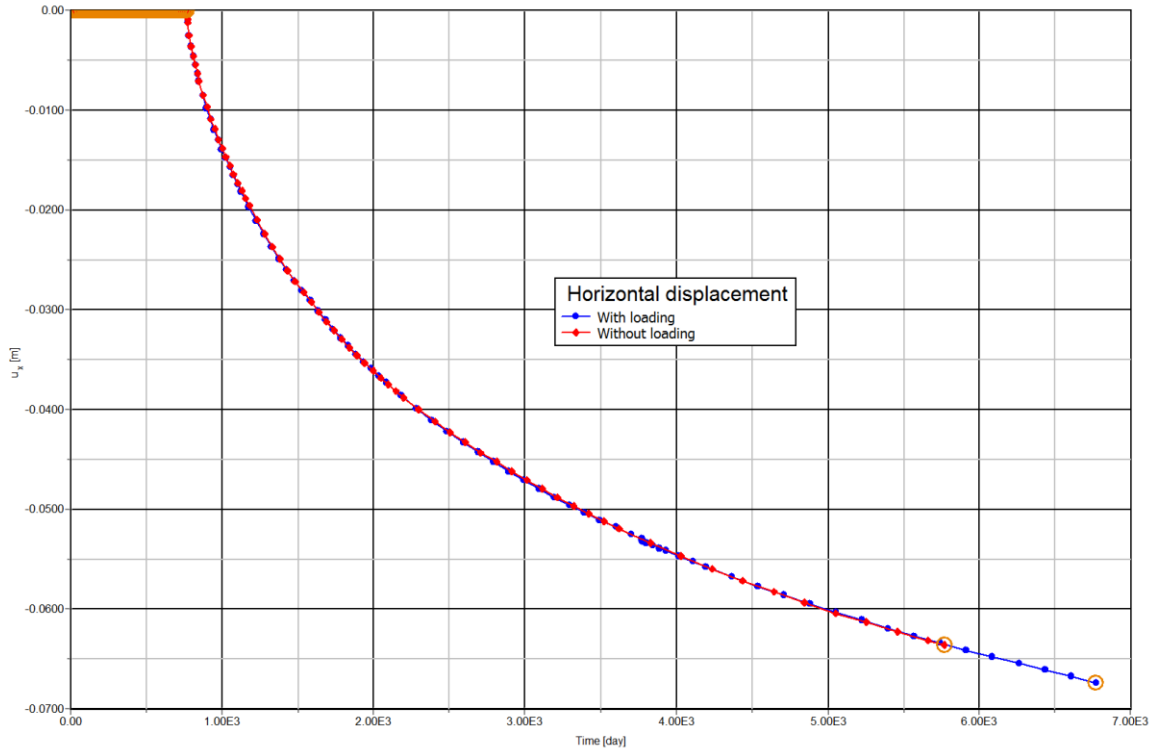

Figure 61 Train vertical loading results

The blue line represents the case with loading and the red line represents the case without loading. It's obvious that the vertical loading has no influence on the displacement.

In the next loading scenario, a lateral component is added to the simulation. This will represent the centrifugal force of the TRAXX locomotive through a curve. Although the section under investigation is just outside of the curve area some lateral forcing might be present. The curve radius is approximately 4500 m. The total weight of the whole train is approximately 410 ton and it has a length of 200 meter. The modelled speed is 160 km/h or 44,4 m/s.

$$F = \frac{m * v^2}{R * l} = \frac{410000 * 44{,}4^2}{4500 * 200} = 0.88\ kN/m$$

In the case of 2 train passing at the same time (in different direction) the force is doubled. Therefore, the point loads will get a lateral component of 1 kN/m per load, leading to diagonal point load with a vertical component of 22.2 kN/m and a lateral component of 1 kN/m.

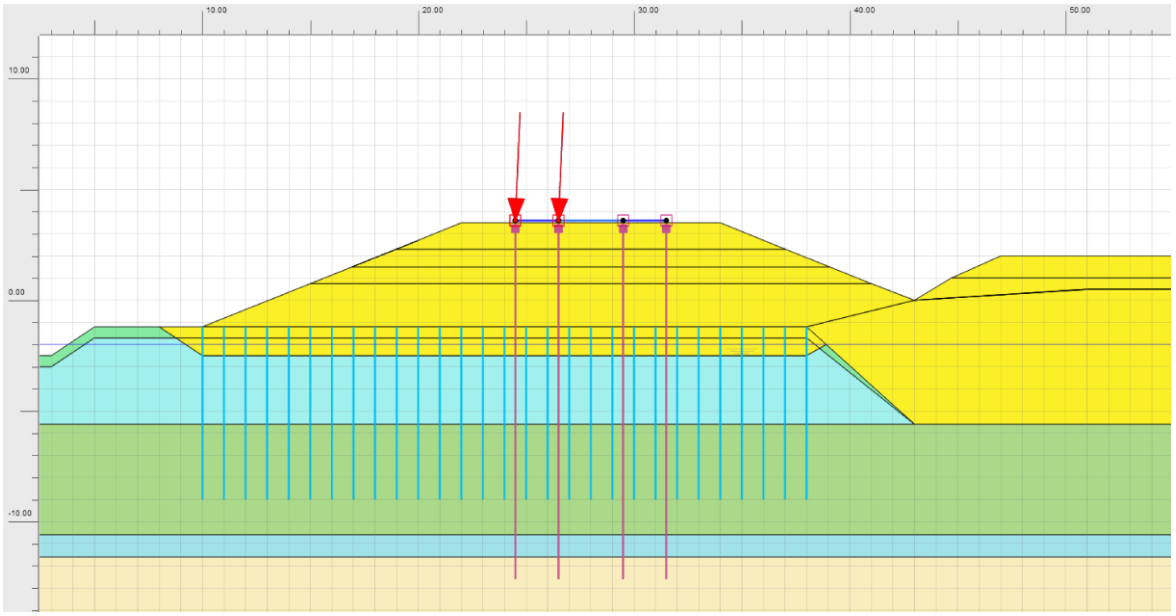

Figure 62 Train diagonal loading model

In this case we see the effect of the lateral train loading to the horizontal displacement. At the moment of loading a slight increase of the displacement occurs. This also leads to a small plastic deformation of approximately 0.5 mm. But in the stage after the loading the creep rate is lower. So, it does have an influence on the displacement but within a certain amount of time the structure will be back at the same displacement as for the case without loading. We will neglect the displacement caused by the loading because the effect is very small in comparison to the static loading by the soil weight.

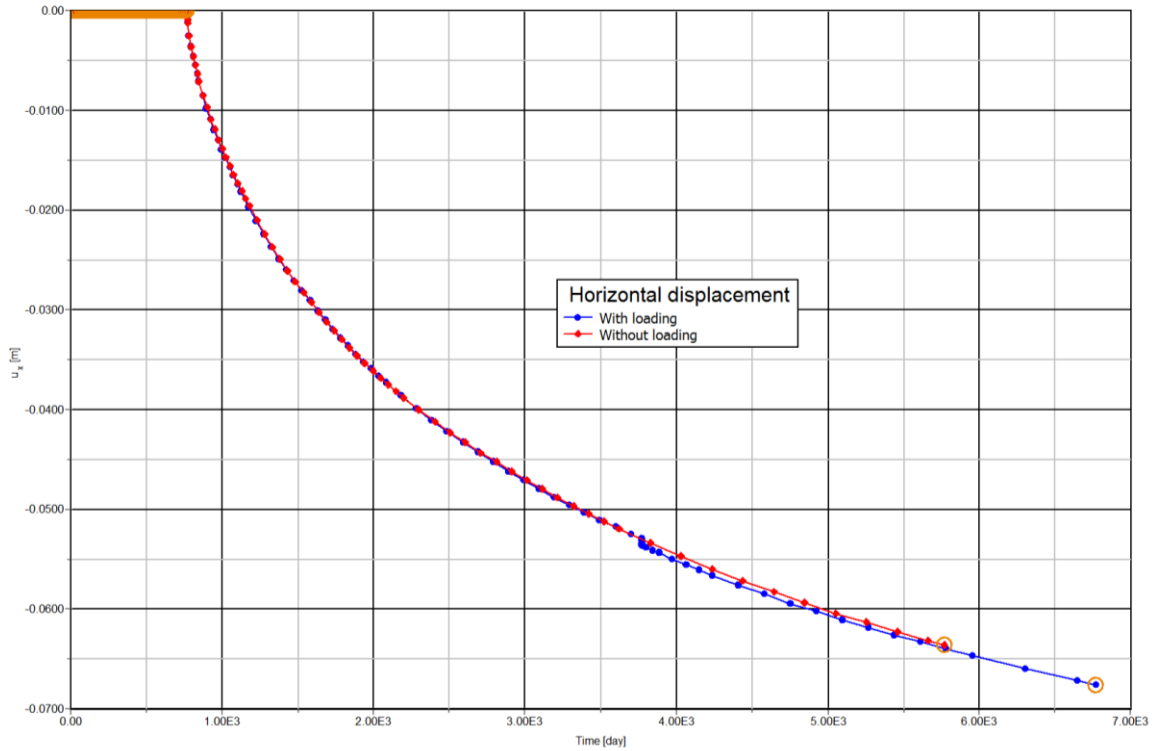

Figure 63 Train diagonal loading results

10.6 Optimization of the model

Now that the influence of the different variants has been analysed the model can be optimized to simulate the case study optimally. Therefore, a number of changes to the model have been done. Changes are made in the geometry, structure material properties, soil material properties and soil calculation models.

Geometry

The geometry of the soil structure has been changed to model the case study more realistic. The embankment has been heightened to a height of 4.7 m above the ground level.

The asymmetrical soil layer has been moved from the centre of the embankment to the eastern side and reaches 5 m under the toe of the embankment. This is the most comparable to the data that is known at this location. Before construction of the embankment a meter of the peat is excavated and filled with sand which represents the work floor for the installation of the drains. The foundation piles are all coupled at the top with a plate element which simulates the concrete slab. The connection between the piles and the slab is moment resisting connection.

Parameters

For the improvement of the case study the model parameters are changed. This way the results will be brought closer to the measurements to analyse the causes better.

First the clay layer model is changed from a simplified Mohr-Coulomb model to the advanced soft soil creep model which includes time dependent behaviour and creep (secondary compression), so it simulates the case more accurately.

Material		Sand, Pleistocene	Sand, Embankment	Peat (Basisveen)	Veen Kleiig	Clay, Silty
Material model		Hardening soil	Hardening Soil	Soft soil creep	Soft soil creep	Soft soil creep
Drainage type		Drained	Drained	Undrained (A)	Drained	Undrained (A)
General						
γ_{unsat}	kN/m³	17	17	11	11.1	15.6
γ_{sat}	kN/m³	20	19	11	11.1	15.6
e_{init}		1	1	1	15	1
Parameters						
E_50^ref	kN/m²	5.00E+04	1.80E+04			
E_oed^ref	kN/m²	6.49E+04	2.00E+04			
E_ur^ref	kN/m²	2.25E+05	8.00E+04			
λ* (lambda*)				0.3	0.407	0.131
κ* (kappa*)				0.03	0.08	0.013
μ*				0.013	0.014	8.00E-03
c'_{ref}	kN/m²	0.1	1	1	4	1
φ (phi)	°	32.5	32	30	25	25
ψ (psi)	°	5	2	0	0	0
ν_{ur}		0.2	0.2	0.15	0.22	0.15
K_0^{nc}		0.4627	0.4701	0.5	0.3	0.5
M				1.635	2.37	1.636
Flow parameters						
k_x	m/day	1	1	1.28E-04	4.32E-03	9.99E-05
k_y	m/day	1	1	6.41E-05	4.32E-03	4.99E-05
c_k		1.00E+15	1.00E+15	1.00E+15	1	1.00E+15
Initial parameters						
OCR		1.25	1	2.24	1	2.13
POP	kN/m²	0	0	0	5	0

The over consolidation ratio (OCR) and modified creep index (μ*) are highly important in the deformation rate of the creep stage. The creep stage determines the behaviour of the soft soils on the long term. Unfortunately, there is no accurate soil test data available in this location to determine the OCR and modified creep index. Therefore the OCR and μ* values have been updated to a more suitable value of the peat and clay layers because of the research in [9].

In the report horizontale verplaatsing zettingsvrije plaat te Rijpwetering by GeoDelft [3] the secondary compression modulus is calculated with the software program MSettle. With this program the settlement results have been analysed to supply suitable parameters. These parameters have been used in the updated version of this study.

In Figure 64 the optimized model for the unsupported situation is shown. It shows clearly the location of the asymmetrical soil layer. The sand starts not anymore from the middle of the structure but more form the eastern side.

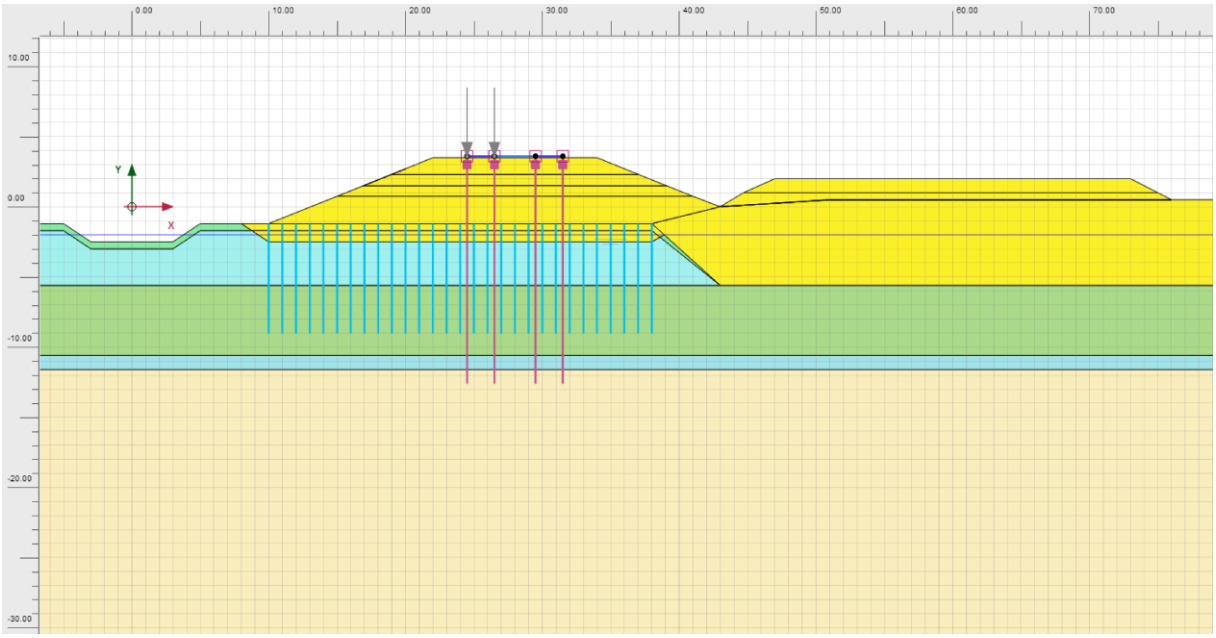

Figure 64 The optimized unsupported model for further calculations

In Figure 65 the optimized model for the sheetpile supported situation is shown. The sheetpile is located in the slope of the embankment at 5 m from the toe. The sheetpile reaches in the Pleistocene sand and the anchor is modelled at 45°. At the top of the anchor some sand is removed for the installation of the equipment.

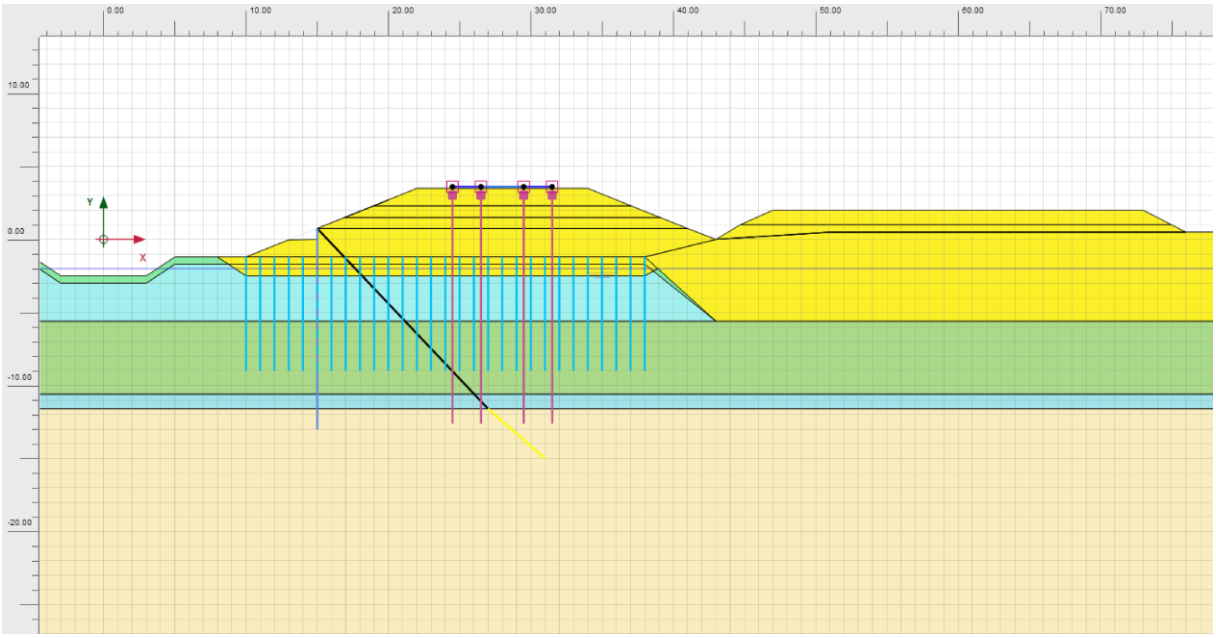

Figure 65 Optimized supported model for calculations

11. Results

The results are separated in the unsupported structure and the supported structure. The results are plotted against the data from the horizontal (GNSS) and vertical (extensometer and/or settlement beacons) measurements.

11.1 Unsupported embankment

Vertical settlement

The results of the unsupported model (blue) are plotted in Figure 66. The vertical settlement is measured from 4 meters aside of the superstructure in the inspection path of the embankment. The results show the settlement of the soil and not the settlement of the concrete structure. These are plotted against the measurement data of the extensometer located in the unsupported area. The results show a very similar pattern over a course of 4700 days or nearly 13 years.

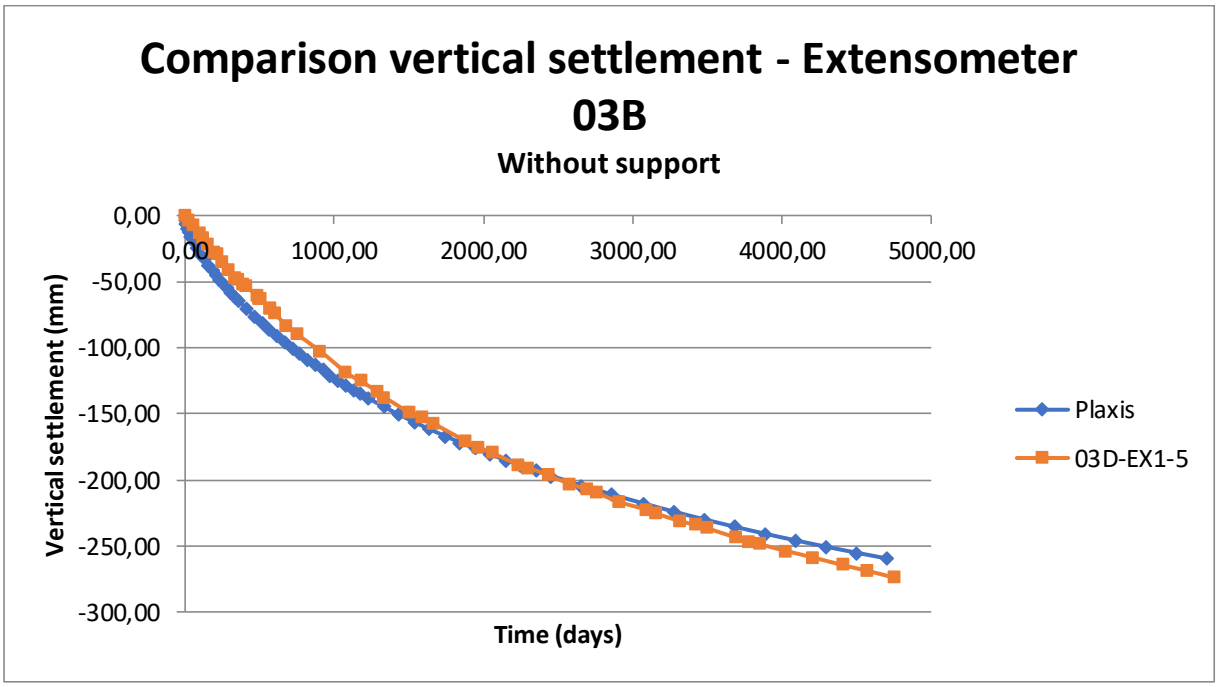

Figure 66 Comparison vertical settlement Plaxis unsupported model - Extensometer 03B

Horizontal displacement

The results of the horizontal displacements of the unsupported model (orange) are shown in Figure 67. The horizontal displacement is measured from the connection of the foundation piles to the concrete slab. These are plotted against the GNSS measurements of the points 2, 3, 5, 6 which are all located in an unsupported area and consist of measurements of the concrete structure. The results show a very similar pattern and achieve very good results to model the behaviour.

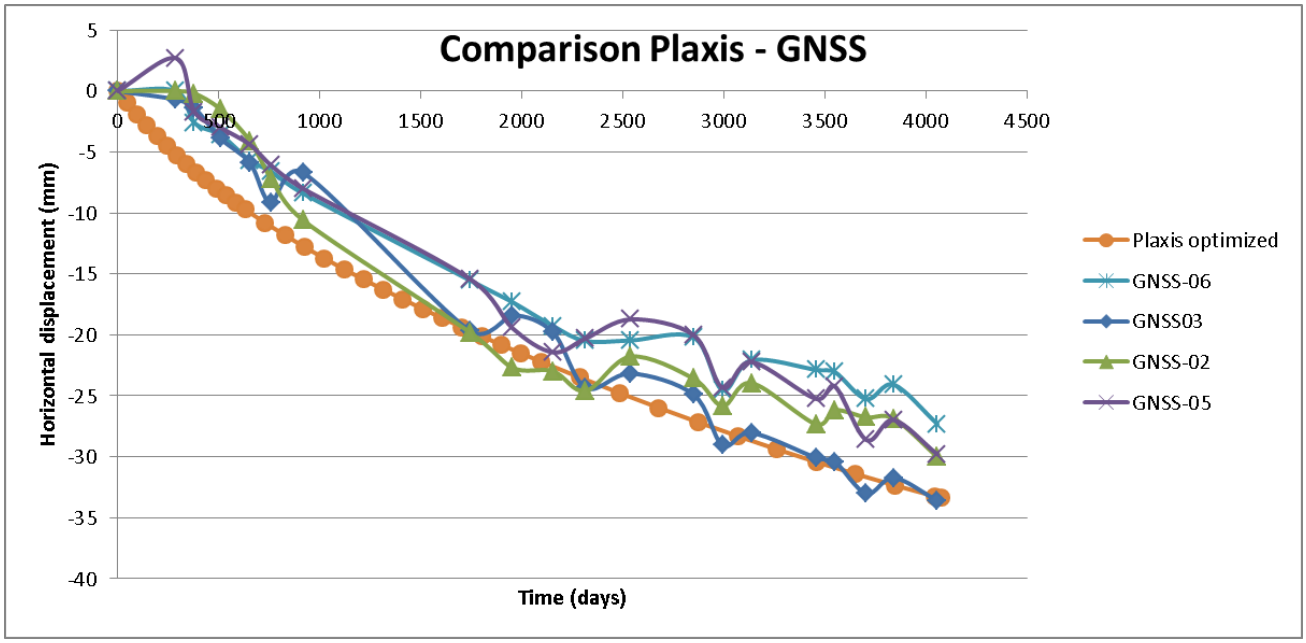

Figure 67 Comparison horizontal displacement Plaxis unsupported model - GNSS 2, 3, 5, 6

11.2 Supported embankment

Vertical settlement

The results of the vertical displacements of the supported model (orange) are plotted in Figure 68. The vertical settlements are measured from 4 meters aside on the western side of the track structure. They are plotted against the measurement data of the settlement beacons 1-6 which are all in the supported area and located aside of the track structure in the inspection path. The measurements show large differences over time between -42 and -60 mm. The model fits perfectly in between the measurements.

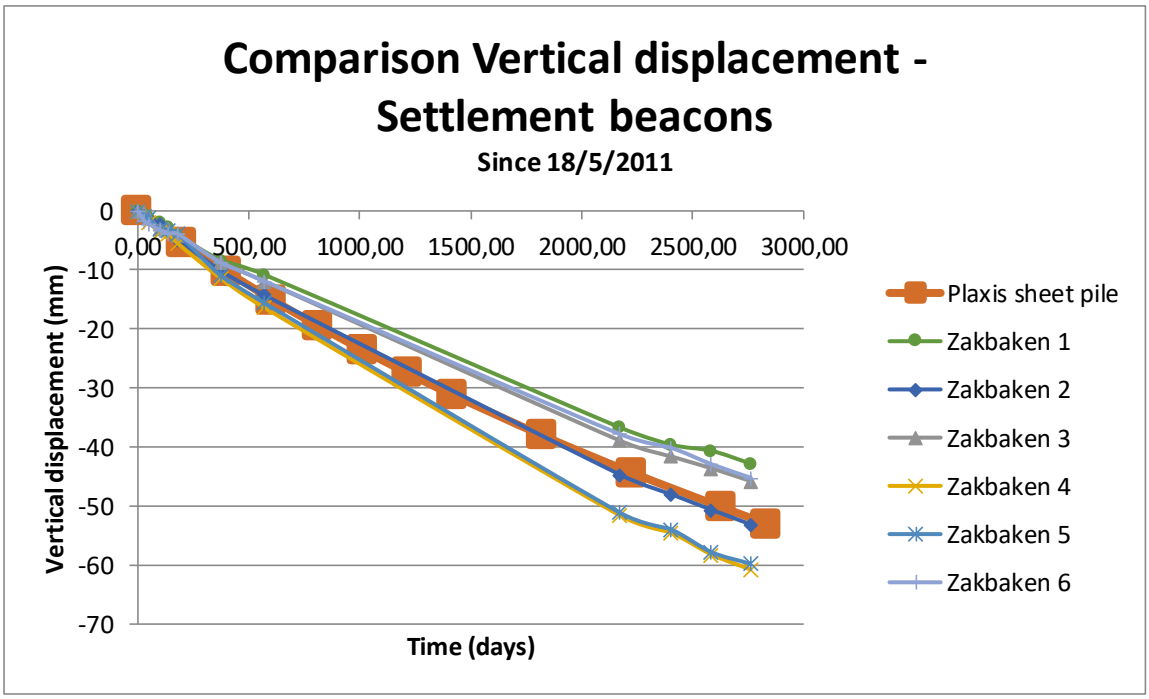

Figure 68 Comparison vertical settlement Plaxis supported model - Settlement beacons 1-6

The comparison with the extensometer is shown in Figure 69. For the vertical settlement in comparison with the extensometer the data starts from a settlement of 152.5 mm which was the settlement already existing at time of construction of the sheet pile. The incremental settlements after construction of the sheetpile are shown.

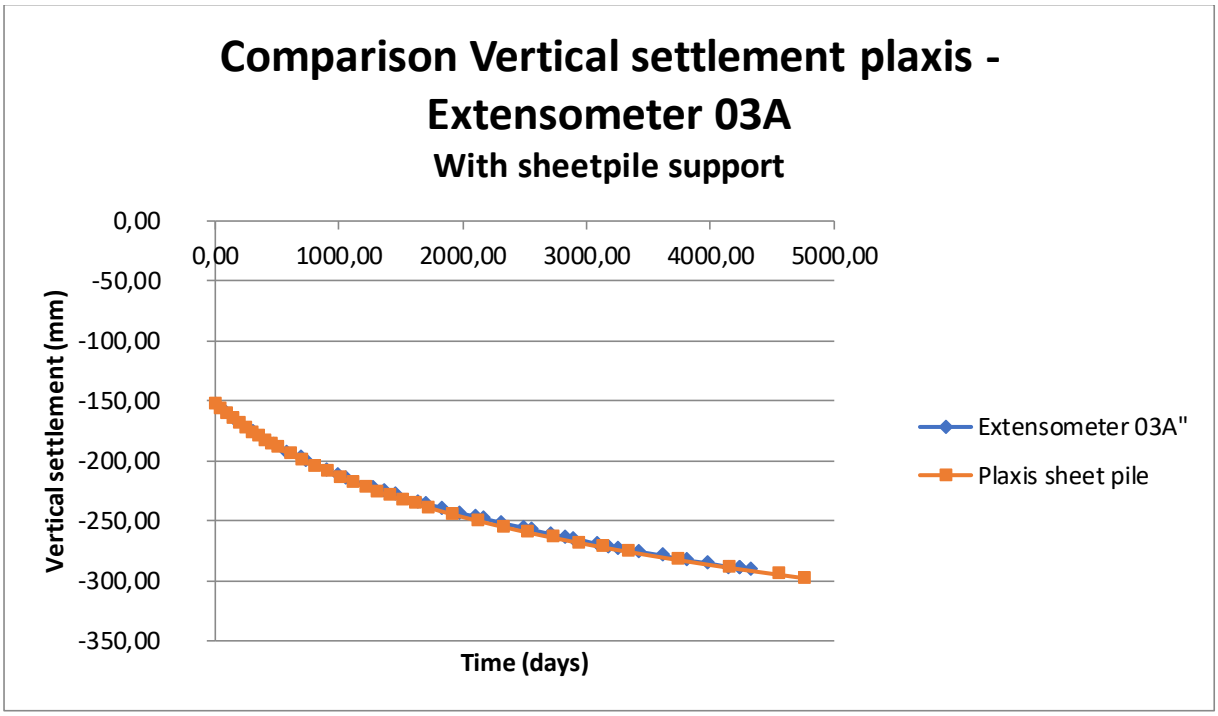

Figure 69 Comparison vertical settlement Plaxis supported model - Extensometer 03A

Horizontal displacement

The horizontal displacements of the supported model (blue) are shown in Figure 70. The horizontal displacement is measured from the connection of the foundation piles to the concrete slab. These are plotted against the GNSS measurements of the points 4 and 7 which are both located in a supported area and consist of measurements of the concrete structure. The results show the displacement for the 10 years of measurements. In this case the measurements show a up and down movement between measurements. To accommodate for the oscillations a trendline is made for the last 5 years.

The results of GNSS point 7 are first evaluated. The total displacement and the rate are very similar for the simulation and the measurements. the rate from 1744 days onwards is nearly identical with respectively 0.0012 mm/day for the measurements and 0.0015 mm/day for the simulation.

The results of GNSS point 4 are very similar but show an instant increase between day 1744 and 1952. This can be referred to as result of an addition of extra sand to the structure. To fill up some of the vertical gaps extra sand has been added. This increases the weight and has caused extra deformations.

After that instant increase of displacement, the exact same rate is resulting again, but leading to a higher total displacement. Nevertheless, it shows that the model is a suitable simulation for the rate of displacement after approximately 5 years.

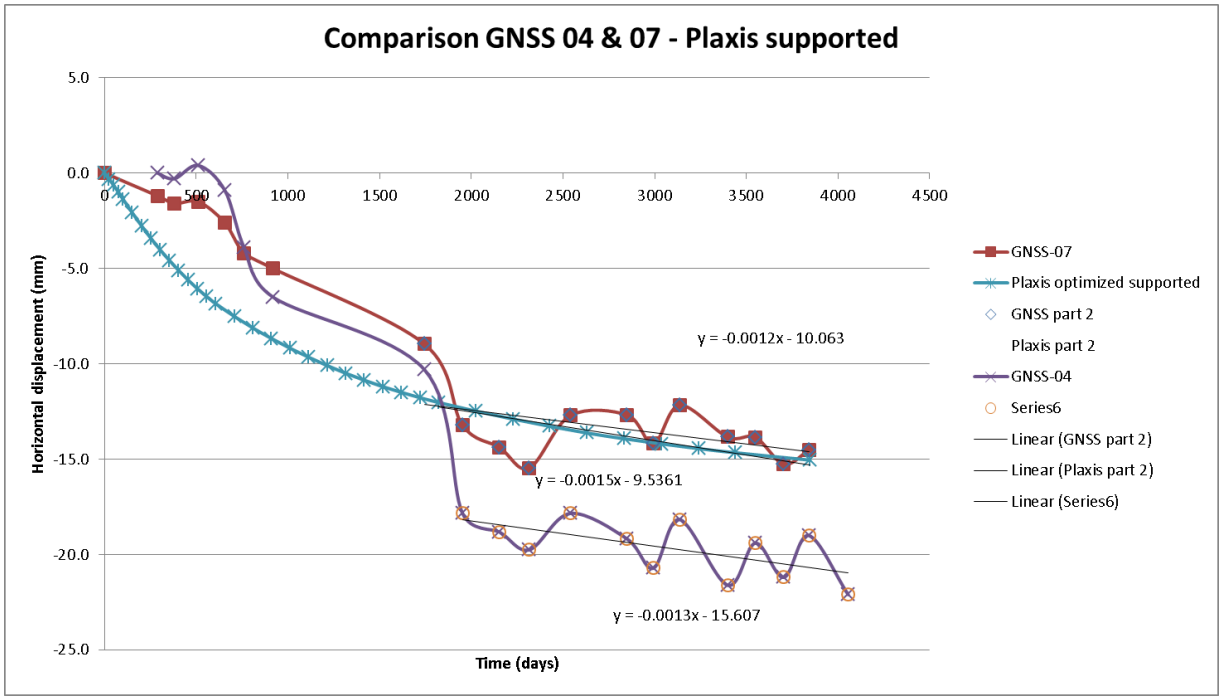

Figure 70 Comparison horizontal displacements Plaxis unsupported model - GNSS 4,7

12. Conclusion

This chapter has been divided in to two sections, the variant study and the optimized models. For each section a conclusion will be given.

Variant study

The variant study has showed a clear influence of different geometrical variants on the future displacement results. All the different cases have a certain effect in the lateral displacements of the embankment and structure. The asymmetrical layer in the subsoil has evidently the largest influence on the behaviour leading to lateral displacements. But the total displacement rate of the case study is a combination of all factors.

The train loading has a very minor influence on the lateral displacement results. From the simulation we can conclude that train loading is not the main factor leading to the continuing lateral displacements over time.

Optimized model

The lessons learned in the variant study are used to optimize the models to analyse the exact factors for the horizontal displacements occurring at the case study. The results of the optimized models for the supported and the unsupported case are shown in the table below. The displacement rates of each simulation are very close to the rate of the measurements at the case study.

Horizontal displacement rate

Case	**Measurements rate**		**Simulation rate**		**Incremental displacement after 10 years**
	mm/day	mm/year	mm/day	mm/year	
Unsupported	0,0048	1,752	0,0051	1,8615	14,68 mm
Supported	0,0012	0,438	0,0014	0,511	2,45 mm

Table 17 Horizontal displacement rate comparison

From this we can conclude that 2D finite element simulations can give a very good interpretation of the behaviour of settlements both in vertical as in horizontal direction. For the exact modelling solid input parameters are required, which means extensive soil tests in the field are necessary.

From Table 17 we can see the incremental displacement after 10 years. This is the additional displacement that would be realised if the simulation would continue for another 10 years from now on. From these results it's clear that the unsupported structure will continue to displace over time and have an extra displacing of 14.68 mm to be expected in the coming years. For the already supported sections the expected coming displacement is only 2.45 mm in the coming 10 years.

Maximum bending moment

The maximum observed bending moments in the foundation piles are shown in Table 18. The moment is multiplied by the shellfactor and the width of the pile to reach the actual bending moment.

From the evaluation it's clear that the supported structure has a much lower occurring bending moment. And the unsupported section gets very close towards the allowed maximum bending moment capacity.

Case	max moment		S	D	Max moment	
Unsupported	41,98	kNm/m	3	0,4 m	50,38	kNm
Supported	7,40	kNm/m	3	0,4 m	8,88	kNm

Table 18 Maximum bending moments in the foundation piles

Since this large displacement will add up to the already present deformations the total will come to an expected displacement of 75 mm. This is very close to the warning values where cracking of the concrete piles comes in to play. A solution needs to be applied to ensure the structural safety of the track.

IV. Design of solutions

In this chapter solutions are proposed to stop the horizontal deformation of the structure. The solutions will consist of 2 scenarios.

First the propositions will be tested to be implemented on the existing structure. That means the changes will be implemented after a simulation of 10 years with the current structure and will then be simulated to analyse the impact of the propositions. Secondly the propositions will be tested in a structure which will be newly constructed. The solutions will be tested if they can solve or reduce the problems for future similar structures.

13. Prestressed sheet pile

In this proposition the same anchored and pretensioned sheetpile as in chapter III.10.1 will be used. But in this case the sheetpile will be activated after a consolidation period of 5000 days. This will simulate the effect of installing the sheetpile support at the currently unsupported sections at this current time. With this we can evaluate if installing sheetpile walls at this time can stop the horizontal deformations.

Model

The sheet pile is located in the western slope of the embankment and has the same dimensions as in the variant studies. The anchor will get a pretension of 50 kN. The sheetpile is placed 4 meters from the toe of the embankment and reaches a depth of -13 NAP. The sheetpile consists of a plate structure modelled as AZ-48 sheetpile just as in the chapter 0.

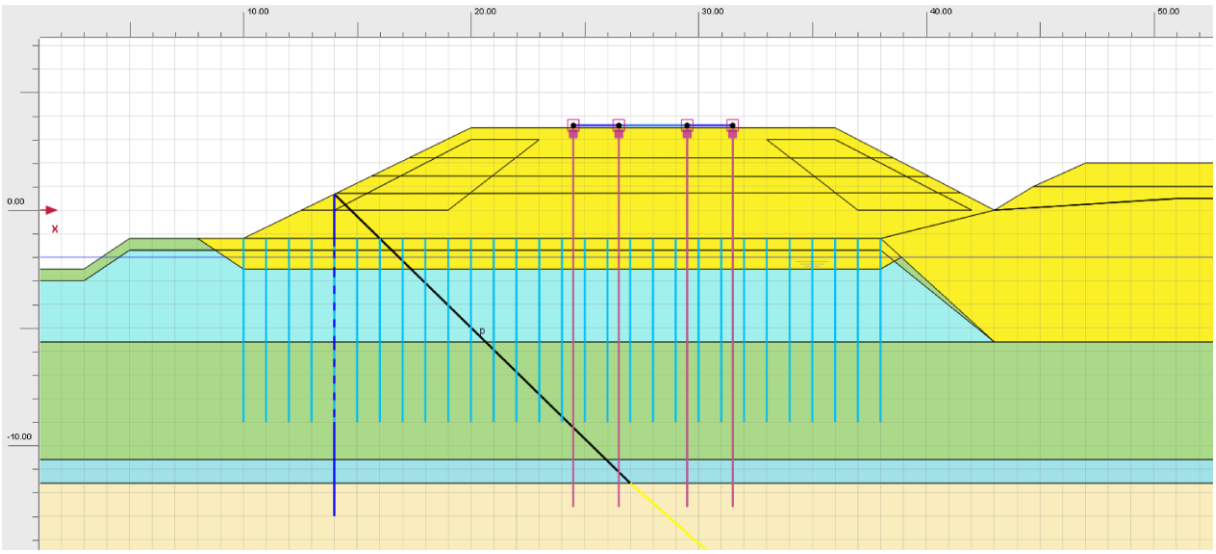

Figure 71 Pretensioned sheetpile in the embankment

Results

In Figure 72 the effect of applying the pretensioned sheetpile in the western slope of the embankment. The figure shows the horizontal displacement of the concrete structure against time. The figure is plotted over a total simulation time of 9000 days. The sheetpile is applied at the end of the measurements to see the effect of application for the future. The

results of the simulation are plotted together with the known measurements of the case study. This will show the effect the measure has to the real case.

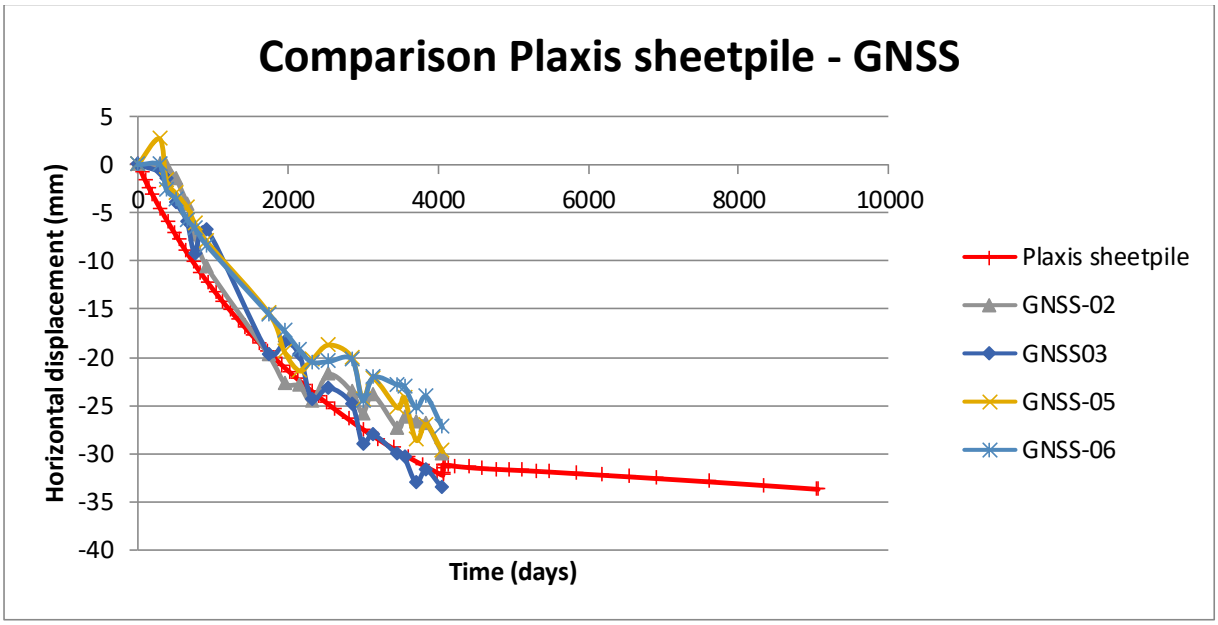

Figure 72 Comparison results case sheetpile -GNSS 2/3/5/6

From the figure we see a very positive result. The instant displacement back to the centre is small but shows the positive effect. The deformation rate has dropped significantly to a rate of less than 0.5 mm per year. By applying a higher prestressing force, we expect this rate to become 0. Therefore, in the next chapter the model is optimized to calculate the optimal prestressing force.

Optimization prestressing force

In Figure 73 the results for 4 different prestressing forces are shown. The different forces of prestressing are 50 kN, 60 kN, 100 kN and 150 kN. The impact of the prestressing force has 2 components. It changes the value of the instant displacement right after installing the prestressing. The higher the prestressing force the larger the displacement back to the original position of the structure is. Since these displacements could cause new problems and stresses to the structure it is advisable to keep these displacements minimal. Secondly the prestressing force results in a difference in the displacement rate for the years after installation. The aim is to have a resulting deformation rate of "0", which will have to show a perfectly horizontal line in the graph. From the results we see that the prestressing at 100KN results in a deformation rate of "0" for the first 3000 days (8 years) after installation but then starts to deform slightly. Prestressing at 150 kN results in a deformation rate back to the original position (undesired) for the first years and will eventually turn to a horizontal line.

From the results the advice is to install the sheetpile AZ-48 with a grout anchor and a prestressing force of 100 kN. In time this prestressing force could be enlarged to a value of 150 kN if small displacement over time will occur.

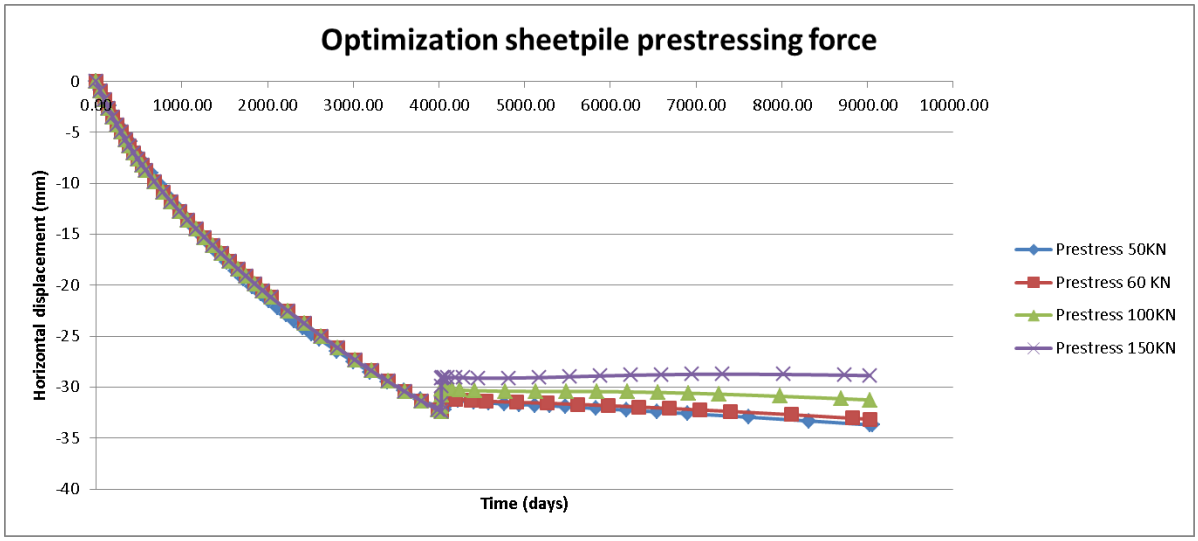

Figure 73 Optimization sheetpile prestressing force

14. Weight reduction

In this proposition a weight reduction will be tested. The idea is that by reducing the soil weight in the embankment the vertical and horizontal deformations will be reduced. To model this weight reduction a part of the sand embankment is replaced by material with a lower weight. In this model the properties of Expanded Polystyrene (EPS).

14.1 Weight reduction in the eastern slope

As in the current structure at some locations EPS has been implemented in the eastern slope of the embankment. In this simulation the results of the weight reduction on the eastern side are analysed.

Model

To model the weight reduction a polygon in the slope of the embankment is drawn. The soil in this polygon will change its properties.

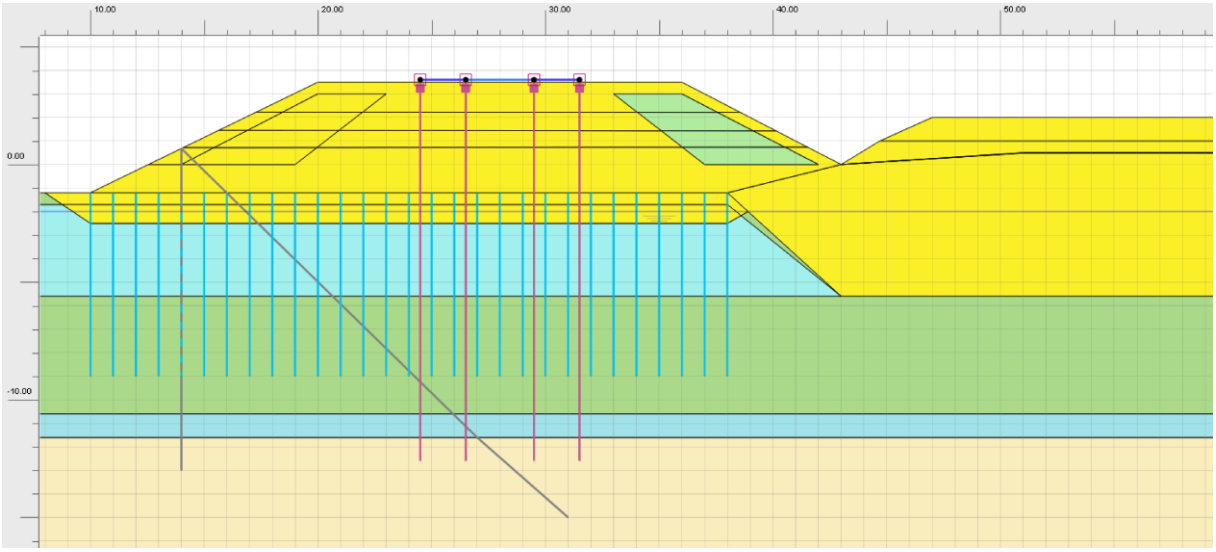

Figure 74 Weight reduction (green polygon) in the eastern slope of the embankment

As can be seen in Figure 74 the weight reduction polygon is located in the eastern slope of the embankment. The total area of the of the polygon is 12 m^2.

In the first phases of the modelling the embankment will remain the same as a full sand embankment. After consolidation of the soil the sand within the polygon is removed and the shape is filled with EPS material. The properties of the material are shown in Table 19.

EPS 60 Properties

Model	Linear Elastic	
γ	0.15	kN/m3
E'	60	kPa
v'	0.1	-

Table 19 EPS60 model properties

The area of the polygon is 19.24 m². By replacing the sand with EPS, a reduction of 202.2 kN/m can be achieved.

The weight reduction is shown in Table 20.

Area	12.00	m²
Weight Sand	17	kN/m³
Weight EPS	0.15	kN/m³
Difference	16.85	kN/m³
Reduction	202.2	kN/m

Table 20 Weight reduction properties

Result

In Figure 75 the effect of applying the weight reduction EPS material in the eastern slope of the embankment. The EPS is applied at the end of the measurements to see the effect of application for the future. The results of the simulation are plotted together with the known measurements of the case study. This will show the effect the measure has to the real case.

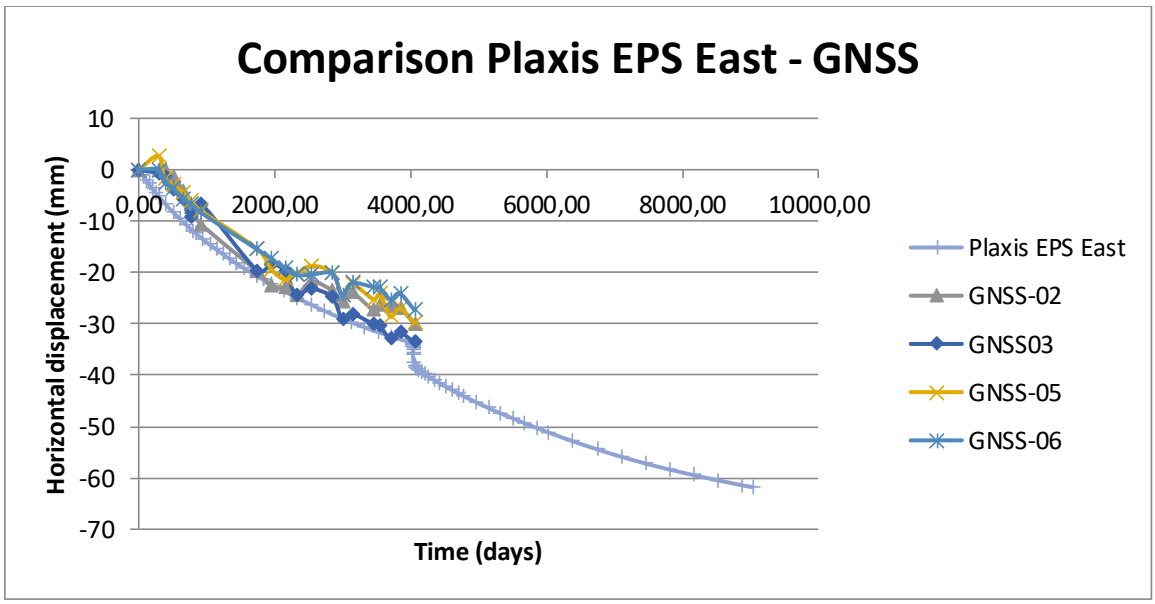

Figure 75 Comparison results case EPS East - GNSS 2, 3, 5, 6

The results show that the weight reduction in the eastern side of the embankment enlarges the displacement and the deformation rate. This means the measure has the opposite effect, the situation gets worse.

In Figure 76 the contour plot of the vertical displacement since installing the EPS is shown. The contour plot clearly shows the upward movement of the east side and downward movement of the west side of the embankment.

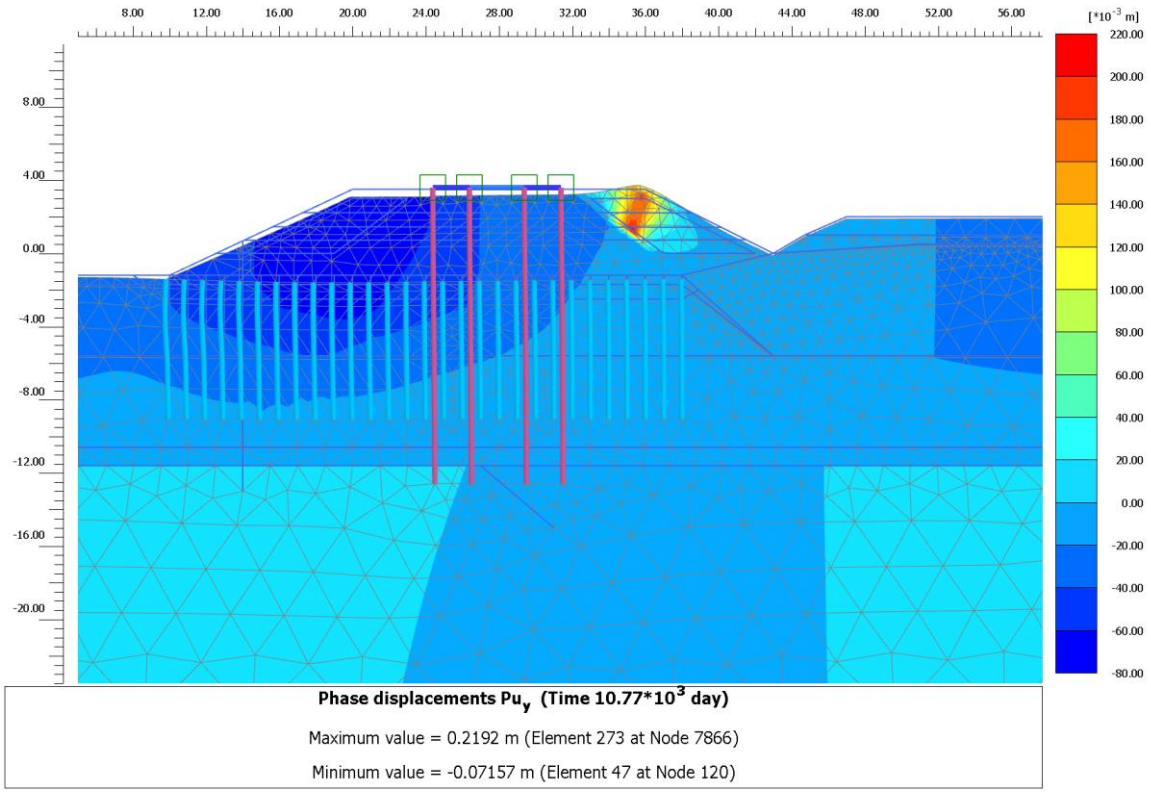

Figure 76 Vertical phase displacement contour plot EPS East

This difference in movement results in a rotation which is in counterclockwise orientation. The counterclockwise orientation will result in the top of the piles to deform towards the western side. This phenomenon is shown in Figure 77.

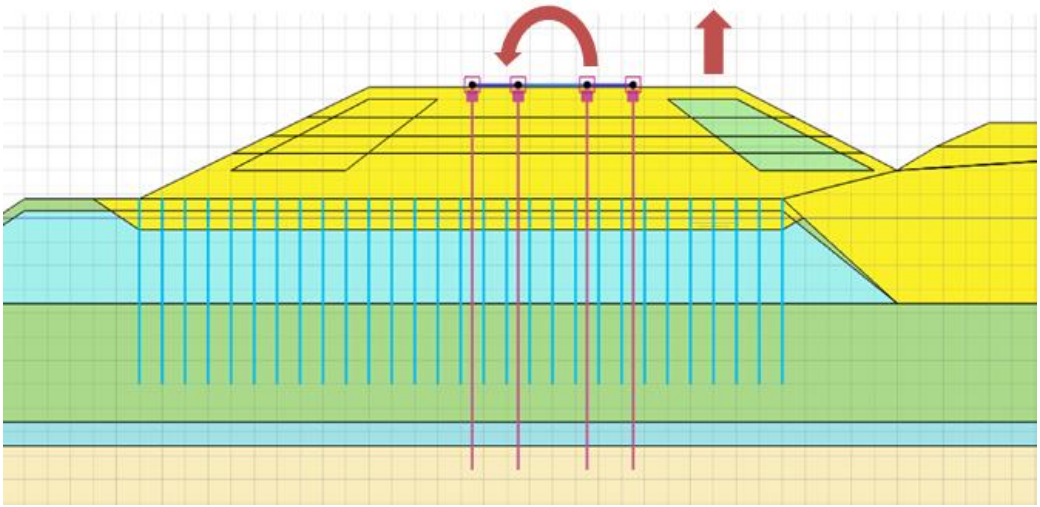

Figure 77 counterclockwise rotation due to weight reduction east

14.2 Weight reduction in the western slope

Since the east side imposes a rotation to the wrong side, the hypotheses is that applying weight reduction on the other side will give the opposite effect. The idea is that the soil on the eastern side of the embankment is much stiffer than on the western side. We expect to see a difference in the results of applying weight reduction of either side of the embankment. The hypothesis is that applying weight reduction on the western side of the embankment has a more positive influence on the horizontal deformation.

Model

In the model the weight reduction area is mirrored to the other side. The surrounding parameters do not change. Therefore, exact same shape and weight has been removed on the western side in the following simulation. The model can be seen in Figure 78.

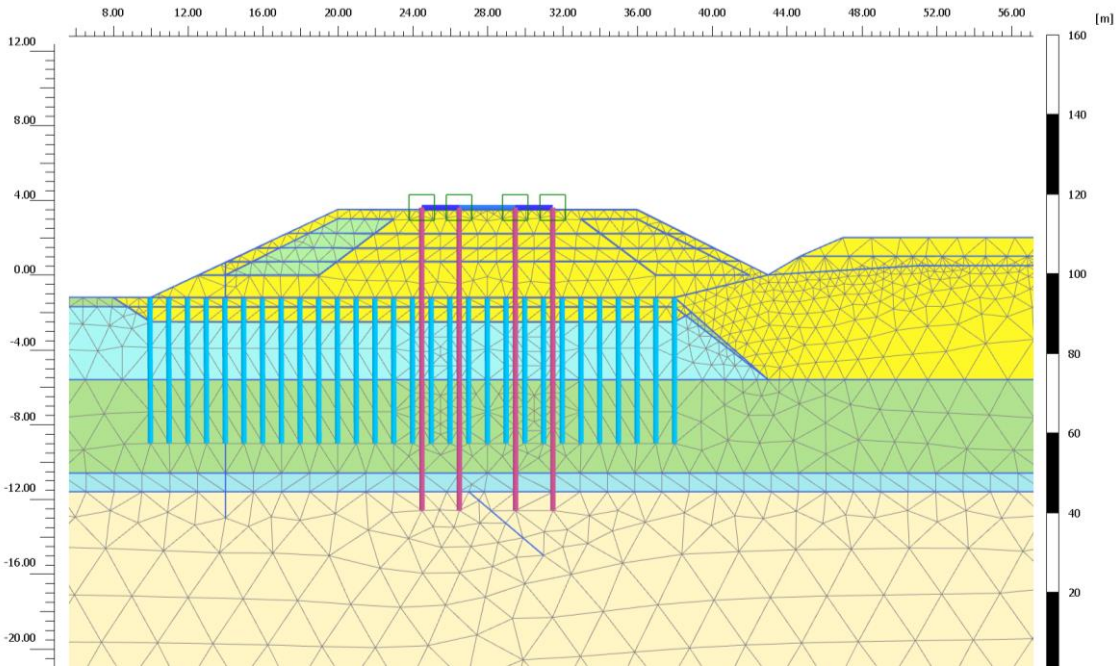

Figure 78 Weight reduction (green polygon) in the western slope of the embankment

Result

In Figure 79 the effect of applying the weight reduction EPS material in the eastern slope of the embankment. The figure shows the horizontal displacement of the concrete structure against time. The figure is plotted over a total simulation time of 9000 days. The EPS is applied at the end of the measurements to see the effect of application for the future. The results of the simulation are plotted together with the known measurements of the case study. This will show the effect the measure has to the real case.

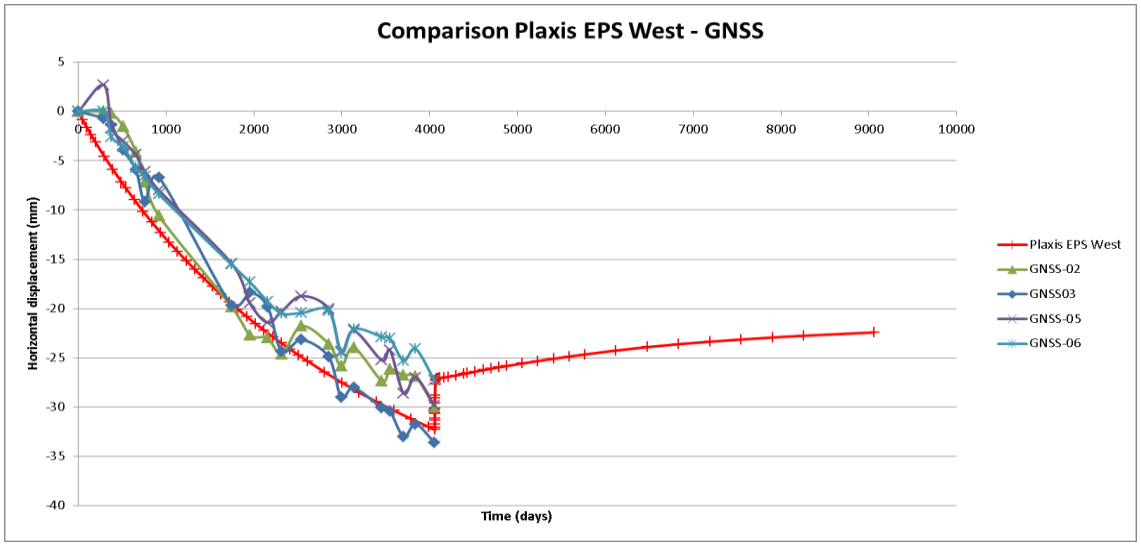

Figure 79 Comparison results case EPS West - GNSS 2/3/5/6

It's clear from the graph that applying the weight on the western side of the embankment has a positive influence on the horizontal displacement of the structure. Immediately after construction the structure moves back to the positive direction with 5mm and will keep moving back gradually over time.

In Figure 80 the contour plot of the vertical displacement since installing the EPS is shown. The contour plot clearly shows the upward movement of the west side and downward movement of the east side of the embankment.

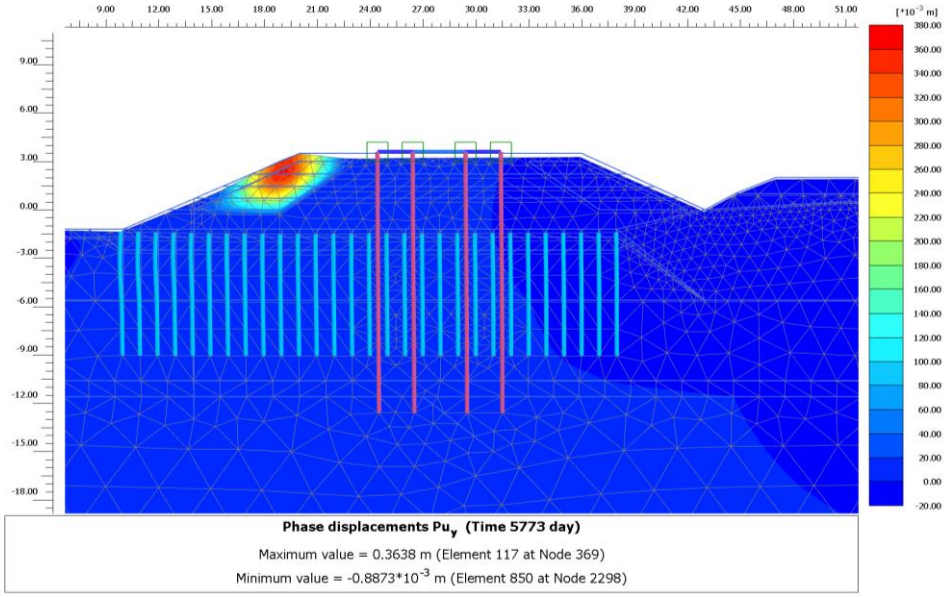

Figure 80 Vertical phase displacement contour plot EPS West

This results in the rotation mechanism occurring in the clockwise direction as is schematically shown in Figure 81.

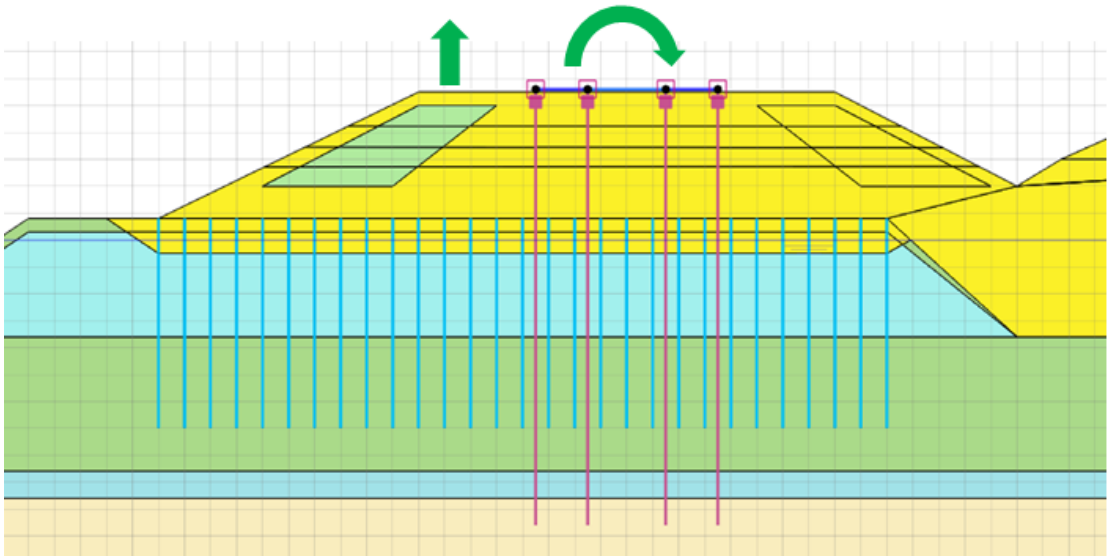

Figure 81 Clockwise rotation due to weight reduction west

This rotation mechanism is the effect which was aimed for. It will result in positive horizontal and vertical force on respectively the soil and concrete structure. The forcing will result in positive displacement over time.

The positive displacement will lead to new movements which could lead to new problems in the future. It implies that the weight reduction simulated was too much. In the ideal situation the displacements would reach a standstill in which the structure does not move in any direction. To find the correct weight reduction value, an optimization for the weight reduction value on the western side will be done in the following paragraph.

Optimization weight reduction western slope

To optimize the weight reduction the aim is to reach a horizontal displacement line after applying the EPS. To simulated multiple weight reduction parameters the unit weight of the EPS material is varied. 5 different unit weights are simulated to see the effect on the horizontal displacement. The results are plotted in Figure 82.

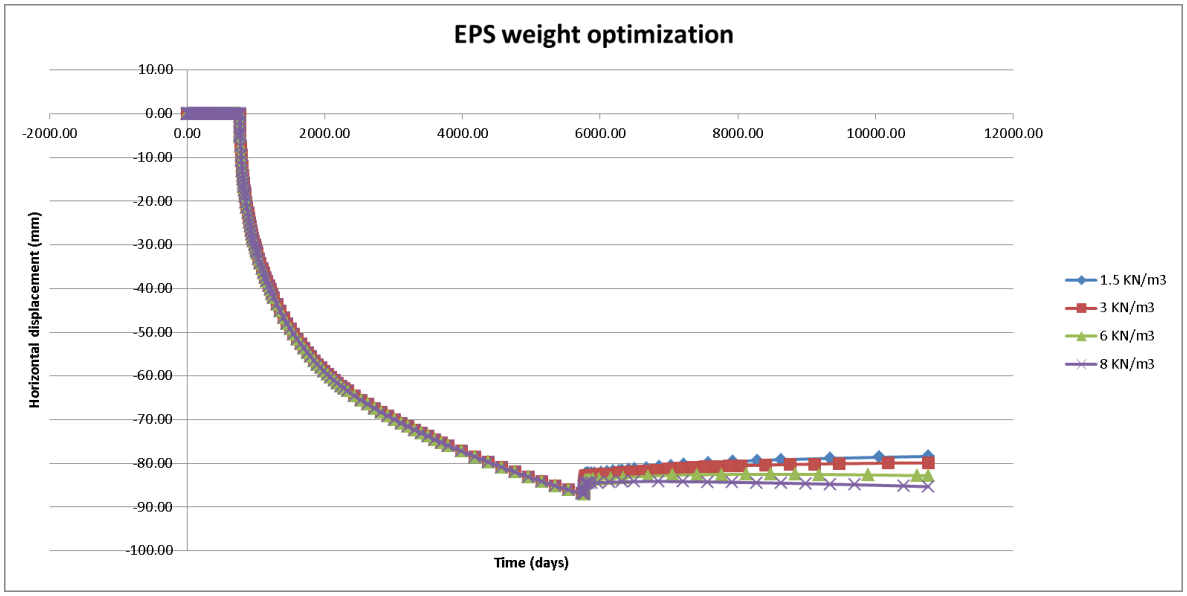

Figure 82 EPS weight optimization after 5000 days

The 5 variants for the unit weight all reduce the displacement instantly. The higher the weight of the EPS material and thus lower weight reduction will result in a lower positive displacement. To investigate the results closer the same simulation is plotted to start at "0" displacement and time at the moment of EPS application. This is shown in Figure 83.

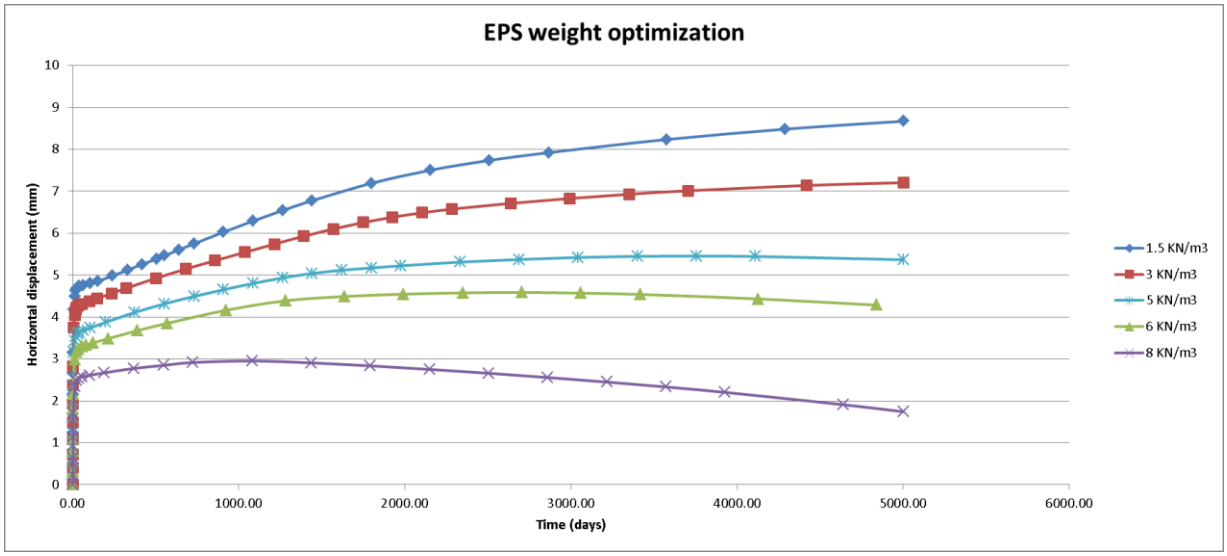

Figure 83 EPS weight optimization results, horizontal displacement since installing EPS

From the figure it shows that the weight of 1.5 and 3 kN/m3 lead to positive displacement rate over time. Simulations with a unit weight of 6 and 8 kN/m3 lead to a negative displacement over time. By applying a weight of 5 kN/m3 the displacement will almost stop deforming over time. In the first 2000 days the structure will deform about 1 mm back in positive direction. After the instant displacement of 3.5mm. To gain these results the total required weight reduction is back calculated. This requires a weight reduction of 144 kN/m in the western slope of the embankment as can be seen in Table 21.

Area	12,00	m^2
Weight Sand	17	kN/m^3
Weight EPS	5	kN/m^3
Difference	12	kN/m^3
Reduction	144	kN/m

Table 21 Weight reduction parameters for optimized model

This weight reduction can be achieved at a smaller area then used in the first calculation if the EPS material weight is reduced to the lowest available weight of 0.15 kN/m^3. This is the typically used EPS-60. The required area of the sand replacement in this case will be 8.55 m^2.

14.3 Weight reduction on both sides

Since the goal of these possible engineering solutions is to reduce the effect of asymmetry it's interesting to see what the influence of placing weight reduction on both sides. In this case on the west side the original amount of weight reduction is applied and on the east side a quarter of this amount is used to see the effect.

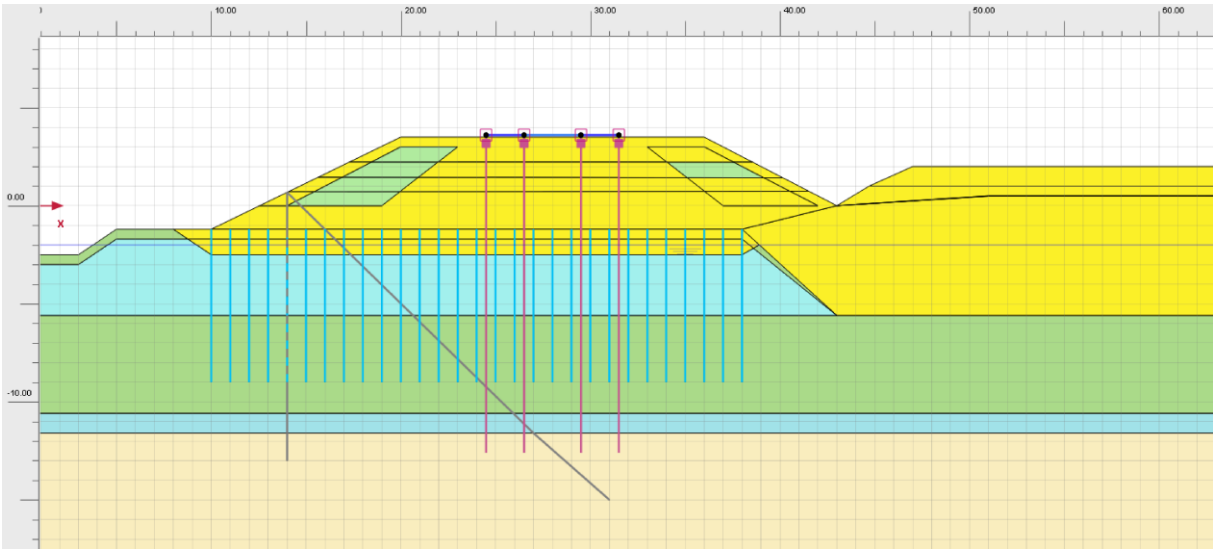

Figure 84 Weight reduction model on both sides

Result

In Figure 85 the result is plotted for the EPS on both sides in comparison to the weight reduction on one side. The figure shows that applying the weight reduction on both sides in which the weight reduction in the west slope is the same to the 5 kN/m3 case, but a quarter of that area is also reduced in the east slope. The horizontal displacement shows a lower shift back towards the east. Also the deformation takes place much more gradual and shows to reach a stability much faster.

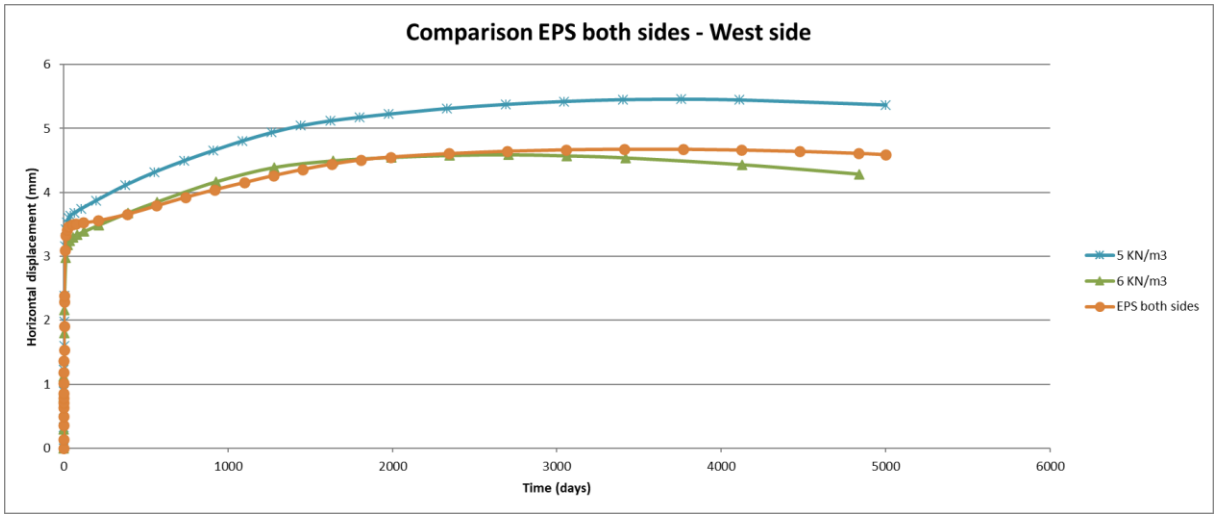

Figure 85 Comparison EPS both sides - West side

The results shows that applying a significant weight reduction in the west slope combined with a small weight reduction in the eastern slope leads to a similar immediate deformation of 3.5 mm but a lower total deformation over time. This long term behaviour shows very promising results with only a 1.2 mm displacement over the coming 6 years and stability afterwards.

14.4 Safety factor

The structure is considered according to the safety of the structure by using the Plaxis safety calculation. This calculation is a phi/c reduction procedure. The safety factor is approached by reducing the shear strength parameters tan φ and c of the soil as well as the tensile strength until failure of the structure occurs.

The total multiplier of the calculation is as follows:

$$\sum Msf = \frac{tan\varphi_{input}}{tan\varphi_{reduced}} = \frac{c_{input}}{c_{reduced}} = \frac{Tensile\ strength_{input}}{Tensile\ strength_{reduced}}$$

The structure will show deformation in time and until the structure deforms without reducing the parameters. The reduced parameters show the failure state of the structure. The value for the safety factor is a factor composed of the input values and the reduced value. A value of 1 has a meaning that the input parameters and reduced parameters are equal and thus the limit state of the stability of the structure. A safety factor higher than 1 means the structure is safe.

$$Safety\ Factor = \frac{available\ strength}{strength\ at\ failure} = value\ of\ Msf\ at\ failure$$

In Figure 86 the safety calculation is plotted. If the structure reaches a horizontal line it means the structure deforms without reducing the parameters, so failure has occurred. In blue the safety factor of the general embankment without measures is shown. It reaches a stability at a factor of 1.17. The red line shows the safety calculation of the EPS on the west side. The safety of the structure with EPS is 1.34 which is higher than the case without the measure. This means the stability of the structure is better.

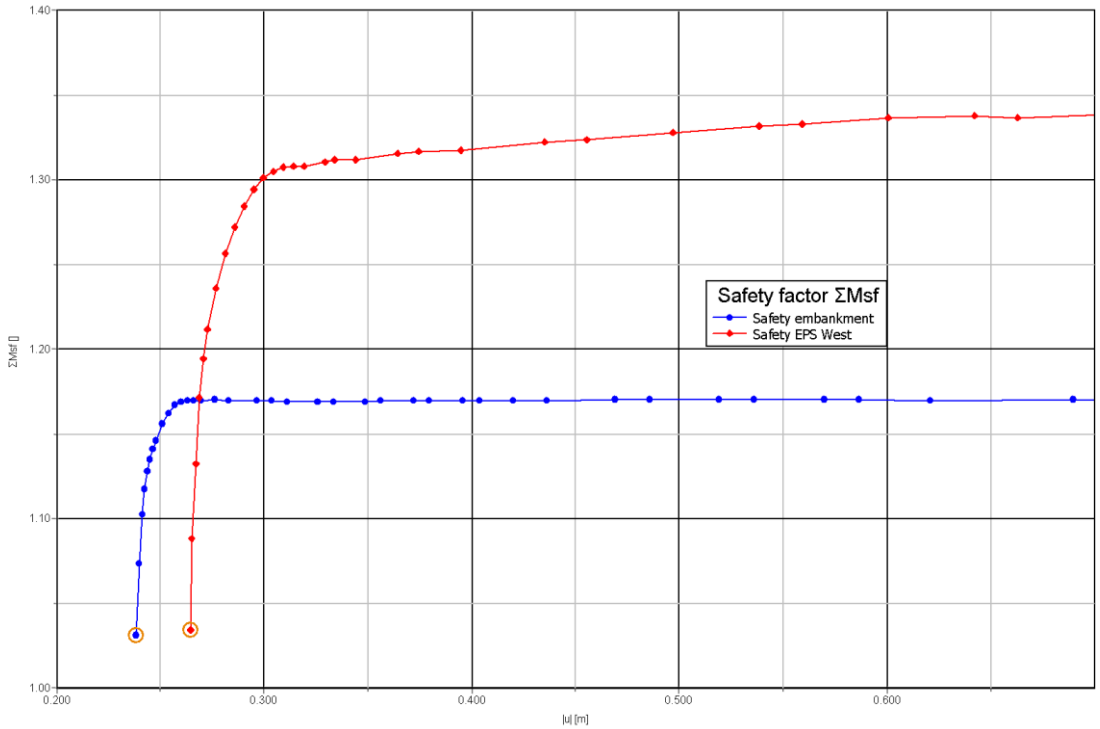

Figure 86 Msf safety factor calculation

15. Conclusion

In this chapter, 3 possible solutions have been tested in the Plaxis model to see the influence on results in the future. The three solutions are shown in Figure 87. All solutions are implemented after a consolidation time of 5000 days to visualize the results from implementing in the current structure of the case study. Both the sheetpile and the EPS in the western slope show positive results and will both lead to a stop of deformation after construction. The EPS in the eastern slope shows a negative result and is therefore not a solution.

The combination of EPS on both sides on the other hand shows very good results with almost no displacement on the long term.

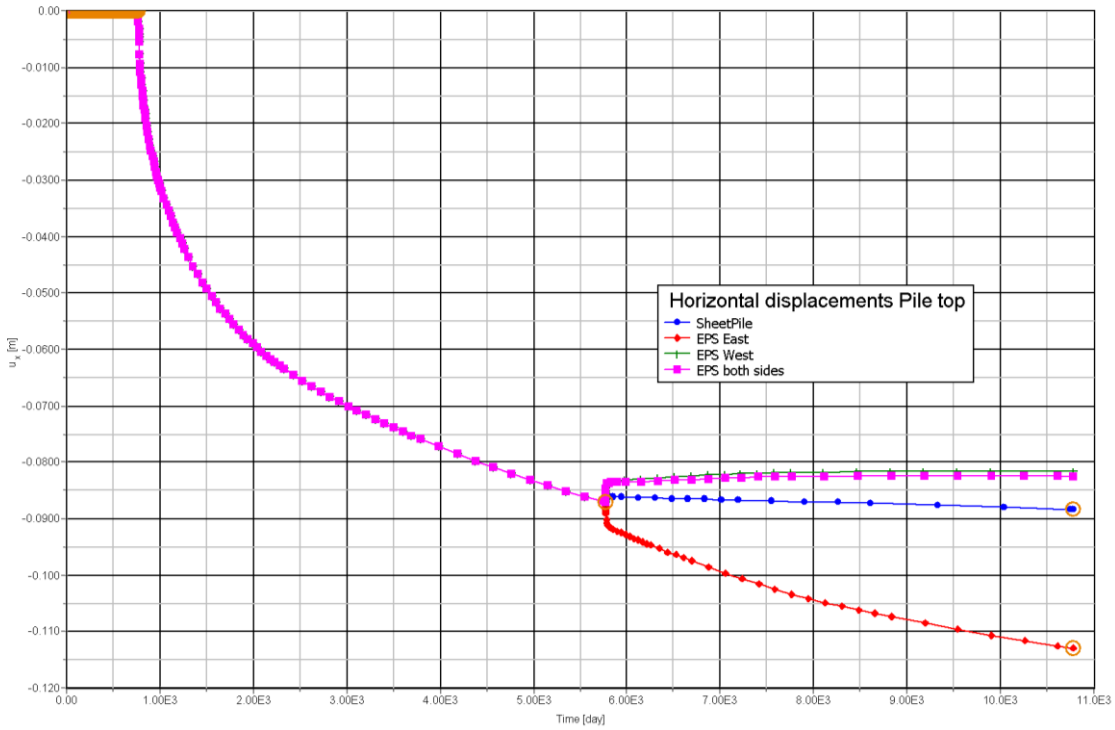

Figure 87 Incremental horizontal displacements of the 4 possible solutions

The sheetpile with the prestressed anchor gives the best result. The immediate recoil is very small and afterwards results are steady. The sheetpile is an already proven measure which is used at different sections of the track and the sheetpile and anchors have shown very effective results.

15.1 Practical considerations

The construction of the solution measures will lead to practical considerations which will be briefly addressed.

Sheetpile

Applying a sheetpile wall in infrastructural projects is a common practice and proven technology. Sheetpile walls are thin steel elements which are interconnected by interlocking. The elements form a flexible wall which is not fully rigid such as slurry walls. The sheetpile elements are driven in the soil by hydraulic pushing or vibration. Most main contractors have sufficient experience in the application of sheetpile walls.

Sheetpile walls can be installed aside the track and the construction has very limited effect on the rail track performance. The sheetpile elements can be driven in the soil without removing or affecting the surrounding track structure. But, by vibrating the sheetpile additional soil compaction can occur, so the structured needs to be monitored closely. Also, the grout anchor which needs to be installed underneath the track structure will be driven in from aside the embankment and does not interfere with the track occupation. For constructing the sheetpile of 14 meters deep a very large machine is required. This can be difficult to work from the relative small side road.

Sheetpile walls have a retaining function for the soil but also block the groundwater to flow. This could potentially lead to water accumulation on either side of the sheetpile. Water accumulation needs to be avoided since this could lead to additional problems. The water flow under the embankment needs to be managed in another way. This can be done by installing a culvert under the embankment through the wall or by creating punctures in the sheetpile to create a porous structure.

EPS

Applying EPS or other weight reduction materials is a less common practice. Because of the light weight of the material it should not interfere with the ground water level, since this could lead to drift of the structure.

To apply the weight reduction a part of the existing soil needs to be removed. With the removal of (part of) the embankment, the system assets will be changed. The works need to be performed partly on or close to the train track to replace the soil. During the works the train track can therefore not be used. Construction of a weight reduction measure will lead to significant closure of the track. The construction works of weight reduction on an existing structure are therefore less attractive. But application in a newly build structure have greater potential.

15.2 Cost approximation

In this chapter a simplified cost approximation of the 2 alternatives is given. This cost approximation is a simplified indication of the costs to compare the variants.

The data for the prices is based on the website library on bodemrichtlijn by Rijkswaterstaat [23]. The costs of the EPS material and stacking is based on practical knowledge of InfraDelft B.V..

Cost approximation			
Total length of measure	300	m	
Sheetpile wit prestressed anchor			
Depth	14	m	
Material	€ 120,00	per m2	
Installation	€ 35,00	per m2	
Groutanchor	€ 550,00	per anchor	(1 anchor per 2 meter)
Total	€ 2.445,00	per m	**€ 733.500,00**
EPS			
Volume	8,5	m3/m	
Material	€ 40,00	per m3	
Stacking	€ 60,00	per m	
Excavation and soil removal	€ 4,00	per m3	
Total	€ 580,00	per m	**€ 174.000,00**

Figure 88 Cost estimation (sources: Bodemrichtlijn RWS [23] and InfraDelft

The cost calculation is shown in Figure 88. From the approximation it's clear that the sheetpile is more than 4 times as expensive as the EPS variant. This is a large difference especially due to the large length over which the measure needs to be installed.

In the calculation there is accounted for the direct costs of the construction of both measures. The secondary costs are not included. Secondary costs will arise from the amount of traffic hindrance and track closure. Additional costs can arise from reconstruction of surrounding assets such as cables, ducts and systems which are not located on the concrete plate. The total amount of construction works cannot be foreseen in this initial study, this which will lead to the total required construction time. This construction time will be a significant factor in the total costs.

15.3 Risk assessment

In this chapter the expected risks of the 2 possible measures will be evaluated. Both measures show some risk and considerations during and after construction. The general influence of the risks will be shown and the risks will be assessed in a trade-off matrix.

The severity and the likelihood of the risk together brings the impact of the risk. This will be done according to the following risk assessment matrix as shown in Figure 89. The risks will be classified as low, medium or high risk.

Risk Assessment Matrix						
	SCALE OF SEVERITY					
SCALE OF LIKELIHOOD		1	2	3	4	5
	1	LOW	LOW	LOW	MEDIUM	MEDIUM
	2	LOW	LOW	MEDIUM	MEDIUM	MEDIUM
	3	LOW	MEDIUM	MEDIUM	MEDIUM	HIGH
	4	MEDIUM	MEDIUM	MEDIUM	HIGH	HIGH
	5	MEDIUM	MEDIUM	HIGH	HIGH	HIGH

Figure 89 Risk assessment matrix

First the prestressed sheetpile structured is considered and shown in Figure 90. The sheetpile installation is a well-known measure applied in lots of engineering practices. This makes the likelihood of the risks low since the contractors have a lot of experience.

The sheetpile leads to a slight deformation of the structure back to the origin. This will lead to some adjusting of the rails, but has low severity. The main risk comes from a possible failure of the tension anchors. There is always a risk that the anchors do not reach maximum capacity and thus the designed prestressing cannot be reached. Other risks include the water retainment of the sheetpile. If other means of drainage are not installed water accumulation can lead to stability problems of the embankment.

Risk Assessment List Sheetpile

RISK	Safety / Availability	AREAS AFFECTED	SEVERITY	LIKELIHOOD	RISK IMPACT	Cause	Consequence
Adjusting rail alignment	Availability	Rail fastening	1	4	Medium	Local displacements	Adjust the rail fastening
Replace fastening system	Availability	Rail fastening	3	2	Low	Local displacements exceed the adjustability	Replace the fastening system
Anchors fail	Safety	Sheetpile tension anchor	5	2	Medium	Anchors incorrectly installed	Sheetpile tension cannot be reached
Sheetpile rupture	Safety	Sheetpile tension anchor	3	2	Low	sheetpile interlocking fails	Sheetpile effectiveness is reduced
Train disruption	Availability	Train service	3	4	Medium	Construction works take long	Train service disruption for a week
Train speed restrictions	Availability	Train service	1	3	Low	Small deformations due to prestressing	As the structure is deforming slightly train speed has to be reduced during a week
Insufficient drainage	Safety	Soil instability	4	2	Medium	Water accumulation due to insufficient drainage	Soil instability if drainage is not sufficient

Figure 90 Risk assessment for sheetpile

The EPS construction risks are shown in Figure 91. Since the weight reduction leads to a larger bounce back of the structure. The likelihood of rail adjustments are higher, but still have a low severity. The main risks will consist of the excavation of the soil. Since surrounding rail assets are located in the soil slope. Assets like catenary poles, cables, ducts and signalling systems have to be either moved or stabilized during excavation and construction of the EPS.

Risk Assessment List EPS

RISK	Safety / Availability	AREAS AFFECTED	SEVERITY	LIKELIHOOD	RISK IMPACT	Cause	Consequence
Adjusting rail alignment	Availability	Rail fastening	1	5	Medium	Local displacements	Adjust the rail fastening
Replace fastening system	Availability	Rail fastening	3	2	Low	Local displacements exceed the adjustability	Replace the fastening system
Train disruption	Availability	Train service	3	4	Medium	Construction works take long	Train service disruption for a week
Train speed restrictions	Availability	Train service	1	3	Low	Small deformations due to prestressing	As the structure is deforming slightly train speed has to be reduced during a week
Stability of the surrounding structures (catenary, cables, systems)	Availability	Catenary, systems, cables etc.	3	3	Medium	Soil removal under/around the surrounding structures foundation	Surrounding systems could fail, require reconstruction

Figure 91 Risk assessment for EPS

To combine the results a trade-off matrix is composed. In this matrix the variants are evaluated on 5 aspects. The value is composed of a positive, medium or negative score. Depending on the value you give to the testing aspect a total score can be accumulated. Since structural safety is essential it gets the highest value, construction difficulty and time have a very large influence on the workability and on both costs and traffic hindrance.

Trade off matrix			
	Value	Sheetpile	EPS
Structural safety	5	-1	0
Construction difficulty	3	1	-1
Construction time	3	0	0
Costs	2	-1	0
Traffic hindrance	2	-1	-1
Total		-6	-5

Table 22 Trade-off matrix

In the trade-off matrix can be seen that the variants differ on 3 aspects. The sheetpile scores better on construction difficulty, but the EPS scores better on total structural safety and costs. Depending on which aspects have the highest value the correct decision can be made. With the current values the EPS scores slightly better than the sheetpile. Therefore the advice is to make a complete design of the EPS structure and construction works to create a better indication of construction difficulty and time.

V. Conclusion and recommendation

16. Conclusion

This chapter will give an overview of the conclusions that can be drawn from the results of the different studies in parts II, III and IV. Finally, the conclusion is given by answering the research questions as stated in part 0.

16.1 Part II

In this part the structure and measurements of the case study Rijpwetering are investigated. From the structure analysis of the case study it's clear that multiple soil investigations have been performed before construction. A main problem of these investigations is that most of these measurements have been performed on a linear length profile of the rail line. Problems have arisen from the asymmetrical soil structure in lateral profile. If at some sections multiple soil tests would have been performed a better 3-dimensional view of the soil structure would be at hand. This would have led to more accurate predictions at the design phase.

The GNSS measurements of the horizontal deformations show a very clear distinction between 2 different parts of the structure. The supported and the non-supported sections. Since application of the supported sheetpile structure the deformation rate has significantly dropped. It's clear from the study that the deformations caused by the asymmetrical soil can be obstructed by the supporting structure.

16.2 Part III

In part III the variant study has shown that the majority of the horizontal instability comes from the asymmetry of subsoil layers. The combination of different asymmetrical geometrical variants leads to the total displacement behaviour.

The embankment and the occurring displacements can very accurately be modelled with 2D finite element modelling. Especially the long-term displacement behaviour is very well modelled and fits well with the measurements.

The current displacement rate of the unsupported parts is currently in the order of 1.8 mm per year and this rate will only drop slightly in the coming years. That will lead to an incremental displacement of 14.68 mm in the coming 10 years leading to a total displacement of approximately 75 mm. This displacement is very close to the maximum at which structural safety is in danger. The values have already highly exceeded the maximum of 10 mm lateral displacement as stated in the High Speed Line guidelines.

The conclusion of this part is that for the supported sections the deformation is continuing but in a low rate and will damp out. Which means the deformations are safe, but monitoring is advised. For the unsupported sections the deformations are large and will continue at a high rate, therefore a solution needs to be applied.

16.3 Part IV

In part IV possible solutions are tested in the models from part III. The first option, to apply a pretensioned sheetpile wall in the western slope of the embankment gives very suitable results. The displacement rate is significantly reduced and can even be stopped with the correct amount of prestressing force. Aside from the results it's also a proven technology which can be implemented without changing or removing the current structure, leading to minimal nuisance to the traffic. The large size of the sheetpiles and length will make the construction process a difficult procedure.

The second option is to use weight reduction by replacing part of the embankment with a lightweight material such as EPS. If the weight reduction is performed in the eastern side of the embankment the displacement will enlarge. But if the weight reduction is implemented in the western slope the displacements can be stopped. A disadvantage is that applying weight reduction will cause a large bounce back, which requires additional adjustments and monitoring. Also the embankment needs to be partially removed which can cause difficulties with the surrounding rail assets.

16.4 Research questions

Is it possible to develop a suitable model to study the deformation behaviour of a settlement free plate structure on a sand embankment for a high-speed rail track?

With the correct data of the subsoil and the structure an accurate model can be made with 2D finite element modelling to predict the behaviour of the settlement free plate. The 2D finite element model has to consist of correct data from the subsoil and the structure but also about all geometrical disturbances surrounding the structure.

What is the influence of geometrical surrounding conditions on the deformation mechanism?

The geometrical surrounding conditions have a large influence on the horizontal deformations of the structure. If the surroundings are asymmetrical horizontal deformations will significantly increase. In soft soils these horizontal displacements will continue for a long term because of creep in the soil. Asymmetry underneath the structure will contribute most to the horizontal displacements and this will continue on the long term.

What is the main factor (mechanism) driving the horizontal deformations of the structure?

The main mechanism of the horizontal displacements is the asymmetry in the subsoil. This leads to a difference in the subsoil stiffness and the corresponding behaviour. The difference in settlement on either side results in a rotation mechanism leading to horizontal displacement of the top of the structure.

What engineering measures can be taken to stop the horizontal deformations?

There are two options assessed in this study. The first option is to apply compression to the side of the embankment which reduces the horizontal displacement. This is done by a prestressed sheetpile wall. This is a very effective solution to reduce or stop the horizontal deformations.

The second option is to stop the vertical settlement which leads to the rotation mechanism. This can be done by applying a weight reduction sufficient to stop the further displacements. Although the results are suitable to stop the deformations, the application of the weight reduction is more difficult and could result in temporary shut-down of the rail.

What are the main factors driving the horizontal deformation mechanism in the high speed rail settlement free plate structure and what measures can be taken to solve these horizontal deformations?

The main factor driving the horizontal deformations is the asymmetrical subsoil underneath the embankment.

There are two possible measures to stop the horizontal deformations. The embankment can be laterally supported, in this research analysed with a sheetpile wall. Or by stopping the vertical deformations and it's resulting rotation mechanism by applying weight reduction. Both measures are suitable for stopping the displacements and controlling the safety of the structure.

17. Recommendations

This chapter will give 3 types of recommendations. First the recommendations that have been learned from this study will be presented to what can be performed on the problems at the case study of Rijpwetering. Secondly for new projects with similar situations. Thirdly recommendations will be given for further research on this topic.

17.1 Case study Rijpwetering

- The section at Rijpwetering consists of 2 parts, the supported and unsupported parts. For the unsupported parts measures need to be taken to stop the continuing deformation of the structure.

- There are two possible solutions which have a similar positive effect on the resulting horizontal stability of the structure. Because of different practical considerations, risks costs and construction processes the solutions differ. Without a more detailed design it's impossible to advise a solution since the impact is yet unknown.

- The currently supported sections are still showing small deformations. Therefore, it is recommended to increase the prestressing force on the anchors simultaneously with the other sections.

- When the whole section will be supported and divided by a retaining wall the drainage capacity of the structure needs to be optimized. Since the original drainage system is blocked some extra drainage possibility need to be applied to prevent problems such as liquefaction.

17.2 Similar structures in the future

- For similar structures constructed parallel to an existing structure. It is advisable to perform multiple soil tests in both the longitudinal as the lateral plane of the field. In this way a better 3 dimensional modelling can be performed to decrease problems with asymmetry of the soil.

- In case of an asymmetrical soil layer it can be advisable to create a cunet underneath the embankment. A cunet is essentially canal like excavation which is filled up with a stable soil (sand). This way the embankment or structure will have a stable base and is less likely to show instability.

- For the current structure of the HSL it's difficult to excavate the embankment and apply a weight reduction. For future structures the EPS can easily be adopted in the design with a very low cost and almost no difficulty. The effect of weight reduction has shown great potential in this study.

- The calculation of the amount and rate of the long-term creep deformation is highly dependent on the modified creep index (μ^*) and the over consolidation ratio (OCR). These parameters can be roughly estimated but are not accurately determinable from the cone penetration tests. Therefore, it is advisable to conduct undrained creep tests from a local sample to determine more accurate values for long term behaviour prediction.

17.3 Further research

- Current research is performed to determine the lateral deformations in a 2D model. The modelling is divided in a supported and unsupported model. In reality the unsupported and supported sections will have interaction on the interface of the support edge. For the interface area a 3D model could give result regarding the influence area of the sheetpile structure.

- In the current study the effect of water level and possible water pressures have not been taken into account. The presence of the retaining sheet pile could lead to water accumulation in the soil which could add to the deformation behaviour. The effects of retaining a large area by the sheetpiles should be investigated.

- The part north of the Rijpwetering viaduct is also showing horizontal deformations which are eastbound in contradiction to the southern part. There is not an expected asymmetry in the soil and the structure seems to be rather symmetric. A study could be done to investigate the factors leading to these deformations, although they are less critical since deformations appear to have reduced in the last few years.

Bibliography

[1] Infraspeed Maintenance, “Onderzoeksrapport Rijpwetering (Instability substructure Rijpwetering),” 2016.

[2] Ex Aequo ingenieursbureau, “Externe toetsing baanverplaatsing rijpwetering,” 2017.

[3] GeoDelft, “Horizontale verplaatsing zettingsvrije plaat te Rijpwetering (oplossingsvarianten en prognose restverplaatsingen),” 2006.

[4] N. Speelman and R. van den Boom, “AC-178: HSL Rijpwetering,” 2014.

[5] C. Yu, L. Y. Pan, G. Y. Du, and C. Lei, “Numerical simulations on the lateral deformation in soft ground under embankments,” *ICEM 2008 Int. Conf. Exp. Mech. 2008*, vol. 7375, no. August 2009, p. 73750M, 2008.

[6] Bouwcombinatie Hollandse Meren, *Richtlijn zettingen en stabiliteit HSL baan Rijnstreek Noord tussen de Rijpwetering (km33.400) en het aquaduct (37.080)*. 2002.

[7] Fugro, “Geotechnische rapportage monitoring HSL KM 134.1,” 2016.

[8] Infraspeed Maintenance, “Risicodossier Rijpwetering,” pp. 1–4, 2016.

[9] J. L. Borges, “Three-dimensional analysis of embankments on soft soils incorporating vertical drains by finite element method,” *Elsevier, Comput. Geotech.*, vol. 31, no. 8, pp. 665–676, 2004.

[10] Arcadis, “Rapportage 1e herhalingsmeting Rijpwetering,” 2009.

[11] Gouda Geo, “Settlement beacon instruments.” [Online]. Available: https://www.gouda-geo.com/products/instrumentation/no-cat/settlement-beacon.

[12] RoyalHaskoningDHV, “ArcGIS HSL Rijpwetering visualisering monitoring- begeleidend document,” 2019.

[13] Plaxis, “Plaxis 2D reference manual V20.” 2019.

[14] B. Indraratna, A. S. Balasubramaniam, and N. Sivaneswaran, “Analysis of settlement and lateral deformation of soft clay foundation beneath two full-scale embankments,” *Int. J. Numer. Anal. Methods Geomech.*, vol. 21, no. 9, pp. 599–618, 1997.

[15] L. W. Schadee, “Paalfundaties onderworpen aan tijdsafhankelijke horizontale belastingen door zachte bodems,” TUDelft, 2012.

[16] Bouwcombinatie Hollandse Meren, “Zettingen en stabiliteit HSL baan Rijnstreek Zuid tussen de boortunnel (km 30.400) de Rijpwetering (km 33.350).” .

[17] P. A. Vermeer and H. P. Neher, “A soft soil model that accounts for creep,” *Beyond 2000 Comput. Geotech. Ten Years PLAXIS Int. Proc. Int. Symp. Amsterdam, March 1999.*, pp. 249–261, 1999.

[18] P. K. Aseeja, “Modelling Consolidation Behavior of Embankment Using Plaxis,” *Int. J. Sci. Eng. Res.*, vol. 7, no. 4, pp. 70–75, 2016.

[19] E. den Arend, “Schelpfactoren bij door grond horizontaal belaste palen,” TUDelft, 2010.

[20] Fugro, “Bestaande ontwerpmodellen door grond horizontaal belaste palen,” 2008.

[21] L. Schadee, “Soil Displacement Induced Laterally Loaded Piles Test Embankments

Bloemendalerpolder – GeoImpuls Program," *Geotech. Saf. Risk V*, pp. 625–629, 2015.

[22] Bouwcombinatie Hollandse Meren, "Detail Ontwerp HSL-A4 Noordelijk Holland, Paalfundering afdracht belastingen," 2013.

[23] Rijkswaterstaat, "Bodemrichtlijn Rijkswaterstaat." [Online]. Available: https://www.bodemrichtlijn.nl/Bibliotheek/bodemsaneringstechnieken/c-grondverzet/c3-ontgraven-met-een-grond-en-waterkerende-constructie.

[24] C. Esveld, *Modern Railway Track*. 2001.

[25] Rijkswaterstaat, *HSL Richtlijn*. 1999.

Appendices

A. Research background

High speed rail

A high speed rail track is constructed to achieve operating speeds of 300km/h. The track geometry has an enormous role in the influence of the vehicle reactions. The forces, running stability and car body accelerations of the train vehicle are bound to acceptable limits. Apart from safety concerns, the most strict guidelines in high speed operation are determined by the passenger comfort. The maximum value for lateral acceleration in limited to 1.5m/s^2. [24] To achieve these values for lateral acceleration the track must have a perfect alignment. All deviations of the normal should be limited to a maximum value of 5mm according to Table 23.

Table 23 Target and limit standard deviations for high-speed tracks operated at 300km/h [24]

Waveband	Level		Alignment	
	σ_{target} [mm]	σ_{limit} [mm]	σ_{target} [mm]	σ_{limit} [mm]
3 – 25 m	1.0	1.5	0.7	1.0
25 – 70 m	2.0	3.0	1.3	2.0
70 – 120 m	2.7	4.0	3.4	5.0

Lateral deformation of soil

To understand the observed lateral deformation of the high-speed rail structure the possible causes are reviewed. The lateral deformation results from deformation of the soil due to the pressure on the soil because of the embankment construction. Because of the embankment load there will always be a lateral deformation in soft soils. This deformation is not only affected by the load, but also by the presence of adjacent structures. [14] Finite element modelling of the a symmetrical embankment on soft soil has also shown that the lateral deformation at the foot of the embankment is linear proportionate to the vertical settlement. [5]

In the HSL guidelines[25] defined before construction the following deformation guidelines were stated:

- Lateral deformation of the entire structure and the settlement free plate should be smaller than 10 mm in 100 years.
- The substructure, at the moment of completion by the contractor, should be between +0 and -30 mm from the nominal design value.
- The vertical deformation of the settlement free plate should be less than 30 mm over a period of 100 years.
- The space under the settlement free plate should be less than 30 cm.

Analysis of soil structure

In September 2016 a geotechnical analysis is done by Fugro GeoServices B.V.[7] In the Geotechnical report multiple probes and 2 mechanical boreholes have been taken at the location km 134.1. This is very close to the problem area in the case study. It is estimated that the soil conditions will be approximately the same in the area. From the probe measurements an average value has been taken as a first indicator of the soil conditions. These values are given in Table 24.

Soil analysis KM 134.1			DKMP 4		
From	To	Material	Conusresistance	Frictionresistance	Frictionnumber
m	m	-	Mpa	Mpa	%
-2	-3.5	Sand	10	0.02	1
-3.5	-5	Sand (silt)	5	0.08	1.5
-5	-7	Peat	0.5	0.04	8
-7	-10.5	Clay	0.5	0.01	4
-10.5	-11.5	Peat	0.5	0.01	7
-11.5	-35	Sand (silt)	15	5	1

Table 24 Soil properties at KM134.1

Also a geotechnical analysis is performed before construction of the soil body.[6] The results of this soil composition at the location of interest is shown in Table 25.

Deel 3-1	km 32.58 - 32.71		Deel 3-2	km 32.71 - 33.04	
	Bovenzijde [m NAP]	onderzijde [m NAP]		bovenzijde [m NAP]	onderzijde [m NAP]
Veen, kleiig	-1,2	-5,6	Veen, kleiig	-1,4	-5,0
Klei, humeus	-5,6	-7,4	Klei, siltig	-5,0	-10,6
Klei, siltig	-7,4	-10,6	Veen, Basisveen	-10,6	-11,6
Veen, Basisveen	-10,6	-11,6	Zand, pleistoceen	-11,6	-35,0
Zand, pleistoceen	-11,6	-35,0			

Deel 3-3	km 33.04 - 33.11		Deel 3-4	km 33.11 - 33.19	
	bovenzijde [m NAP]	onderzijde [m NAP]		bovenzijde [m NAP]	onderzijde [m NAP]
Veen, kleiig	-1,6	-4,4	Veen, kleiig	-1,7	-2,4
Klei, humeus	-4,4	-5,2	Klei, humeus	-2,4	-3,8
Klei, siltig	-5,2	-10,8	Veen, kleiig	-3,8	-5,0
Veen, Basisveen	-10,8	-11,6	Klei, siltig	-5,0	-10,4
Zand, pleistoceen	-11,6	-42,5	Veen, Basisveen	-10,4	-11,4
			Zand, pleistoceen	-11,4	-42,5

Deel 3-5	km 33.19 - 33.22		Deel 3-6	km 33.22 - 33.33	
	bovenzijde [m NAP]	onderzijde [m NAP]		bovenzijde [m NAP]	onderzijde [m NAP]
Klei, siltig	-1,7	-10,8	Veen, kleiig	-2,0	-5,6
Veen, Basisveen	-10,8	-11,8	Klei, siltig	-5,6	-11,0
Zand, pleistoceen	-11,8	-42,5	Veen, Basisveen	-11,0	-11,8
			Zand, pleistoceen	-11,8	-42,5

Deel 3-7	km 33.33 - 33.50		Deel 3-8	km 33.50 - 34.26	
	bovenzijde [m NAP]	onderzijde [m NAP]		bovenzijde [m NAP]	onderzijde [m NAP]
Klei, humeus	-0,4	-3,6	Veen, kleiig	-4,0	-5,4
Veen, kleiig	-3,6	-5,6	Klei, siltig	-5,4	-10,6
Klei, siltig	-5,6	-10,6	Veen, Basisveen	-10,6	-11,6
Veen, Basisveen	-10,6	-11,4	Zand, pleistoceen	-11,6	-42,5
Zand, pleistoceen	-11,4	-42,5			

Table 25 Soil composition measurement (CPT) before construction [6]

B. Model simulation steps

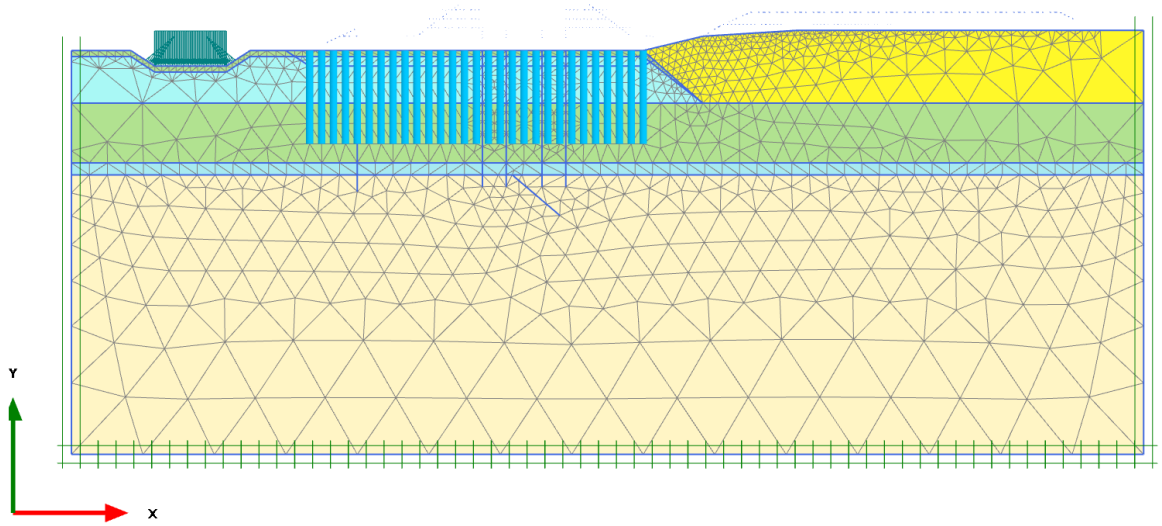

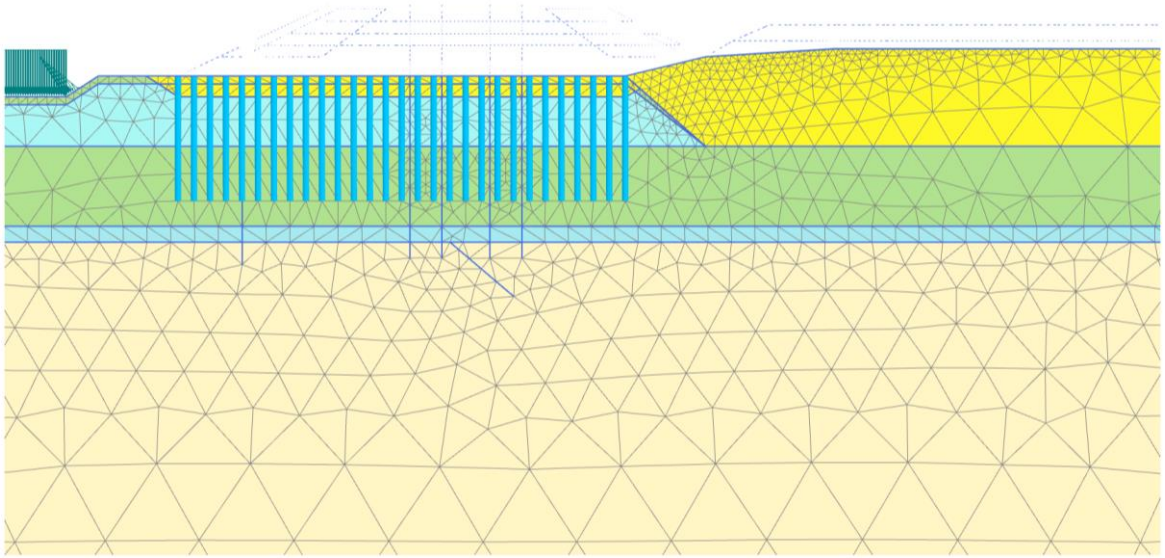

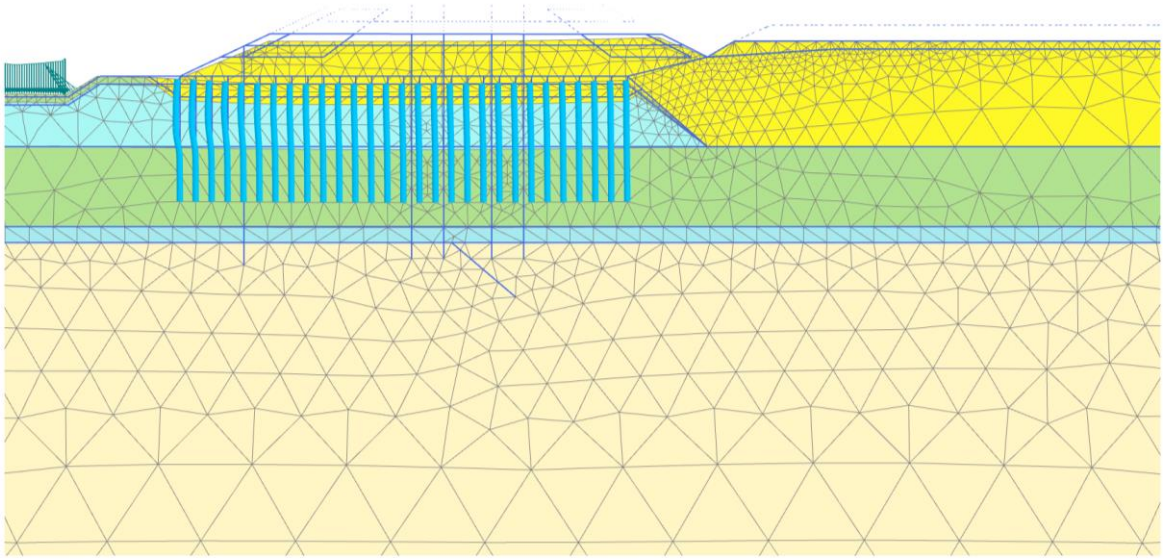

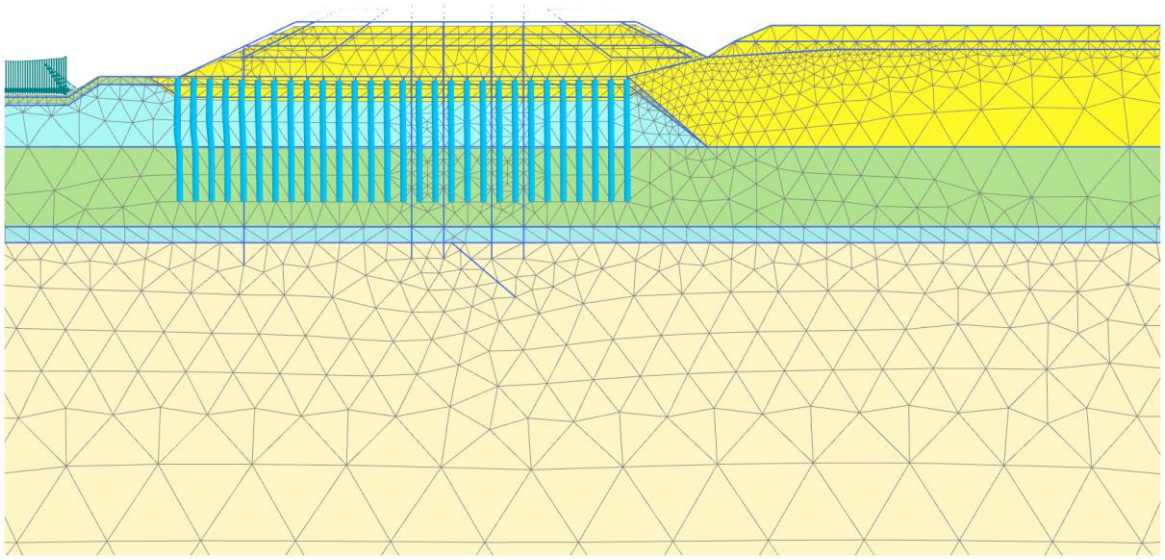

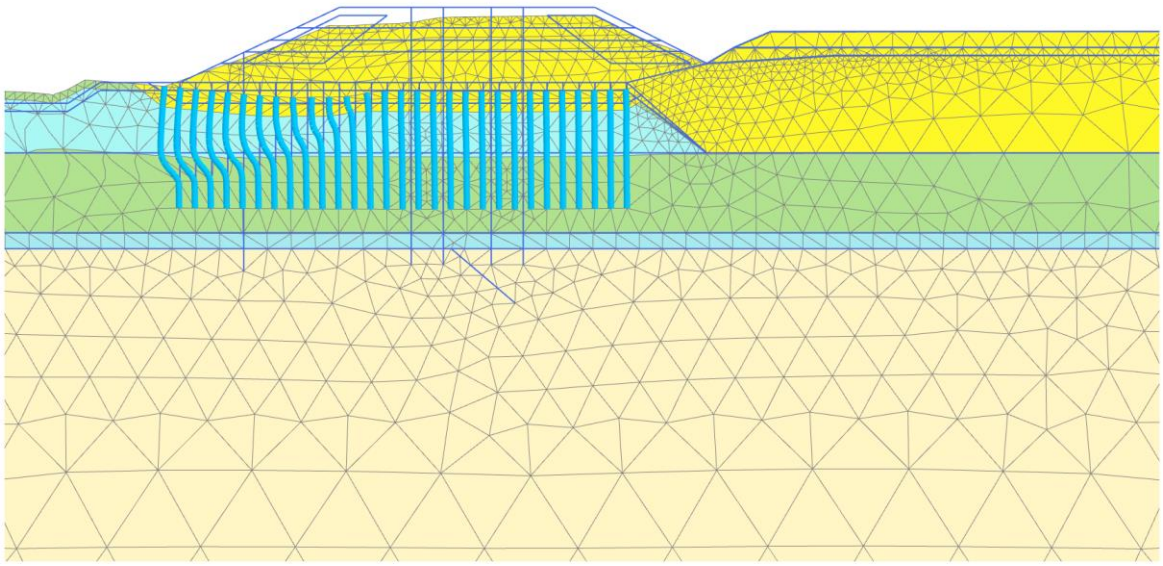

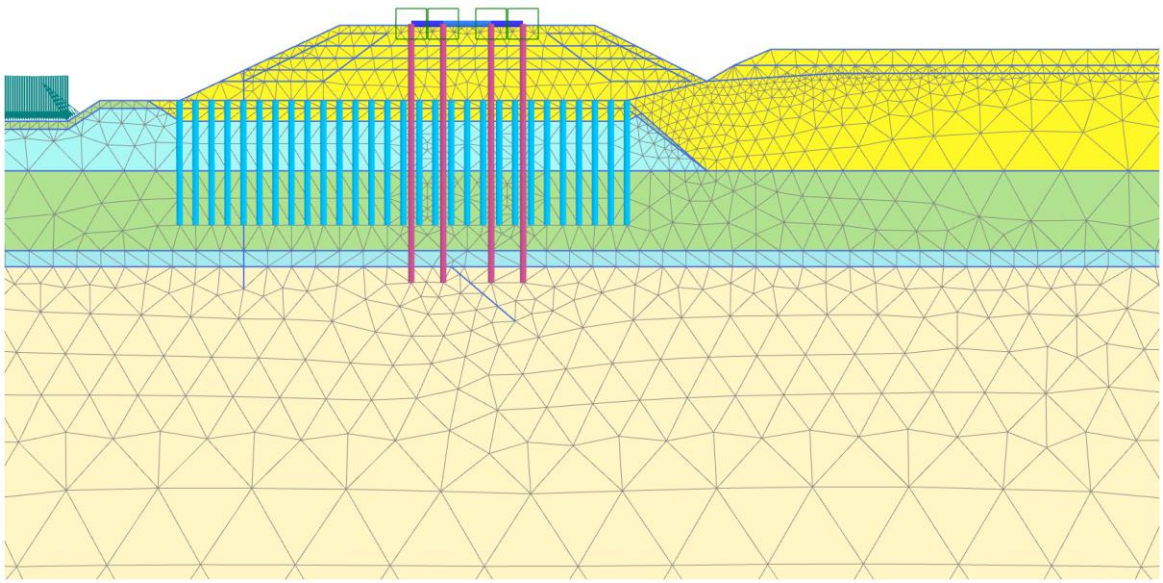

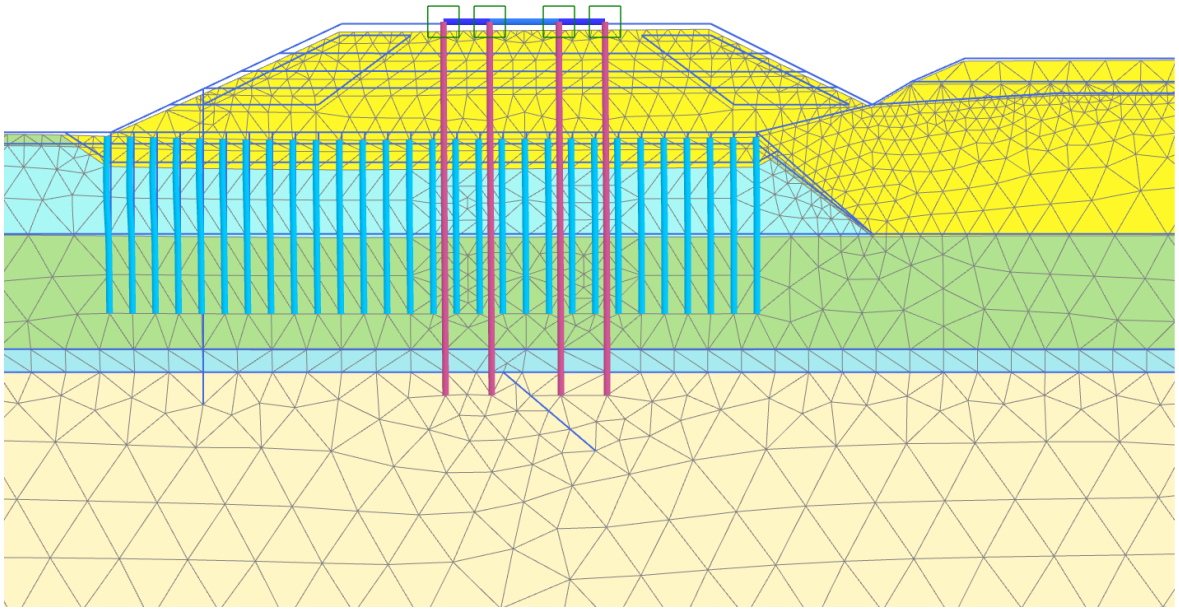

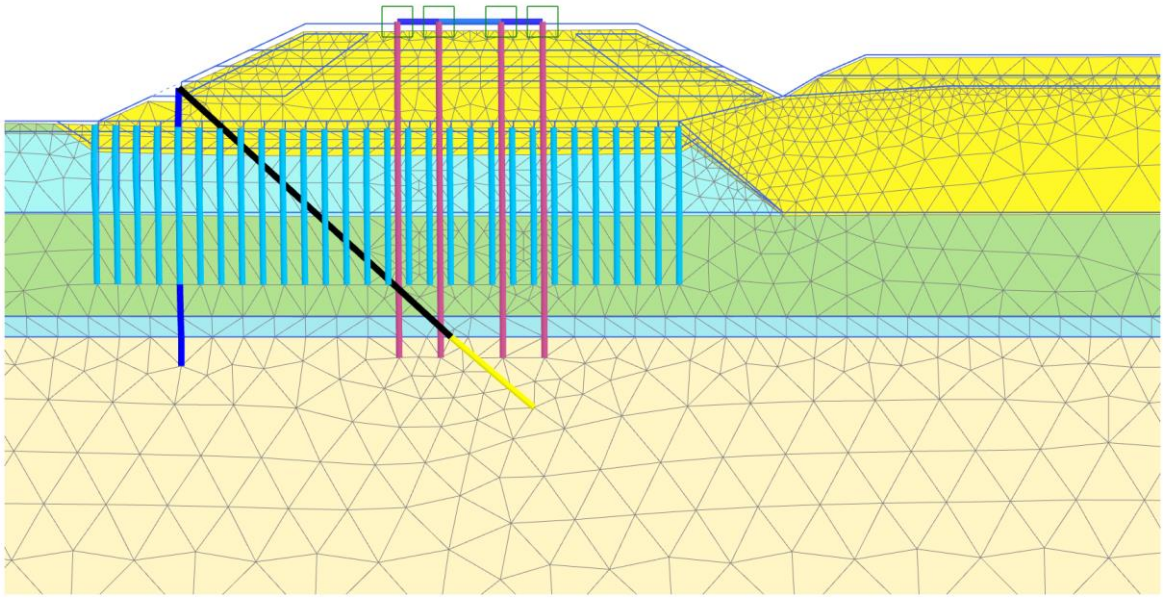

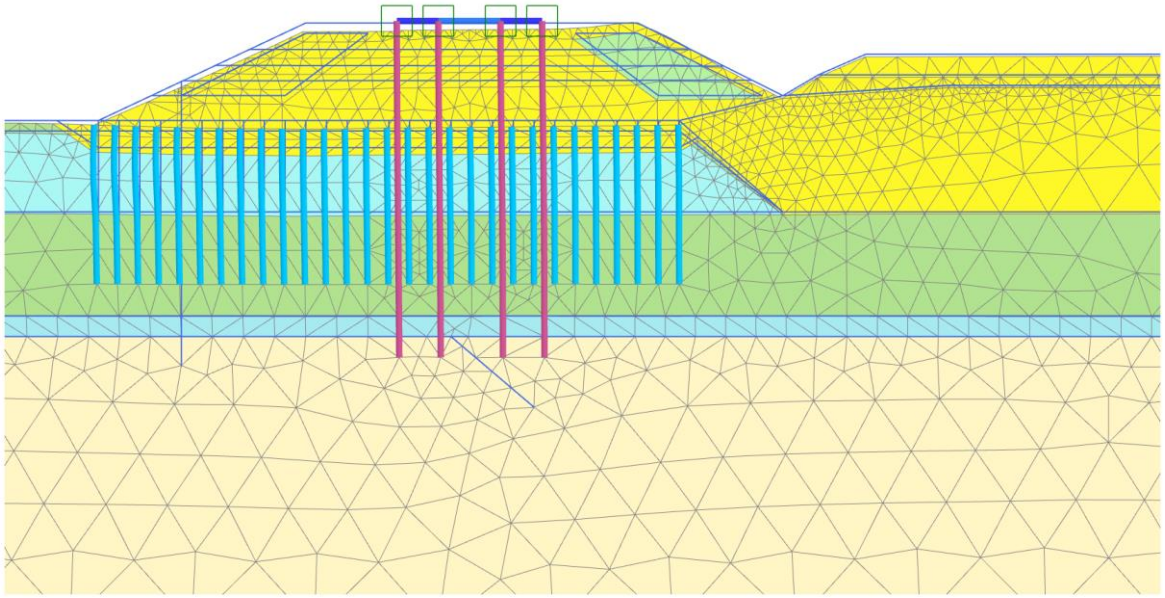

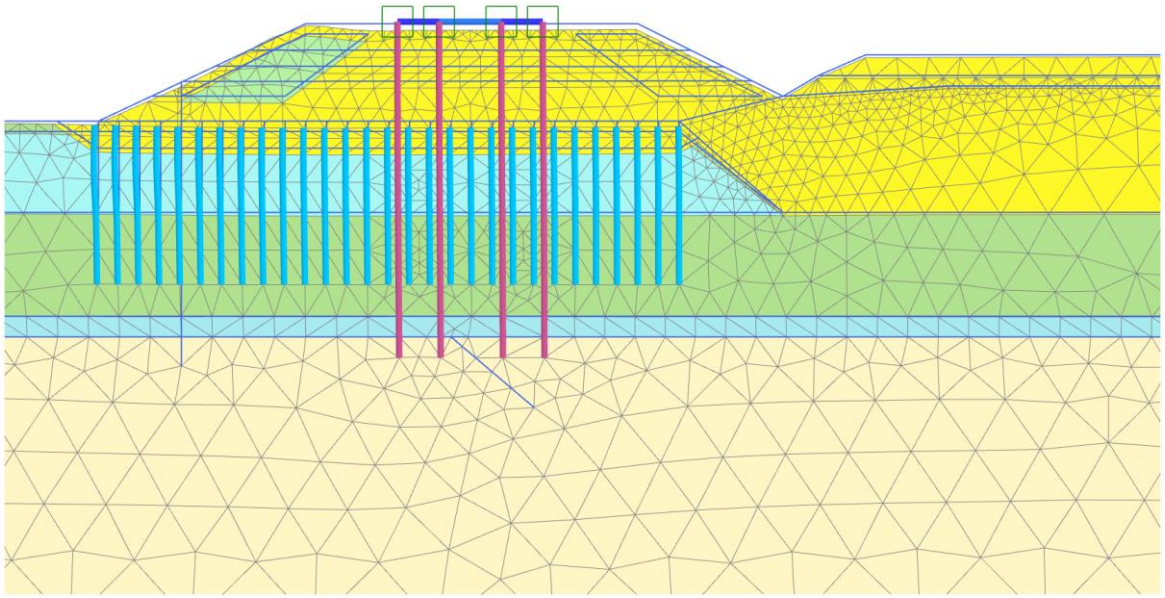

C. Comparison to inclinometers

In 2005 inclinometers have been installed in the embankment to measure the horizontal deformation of the soil. The inclinometer is a vertical tube which is bored in to the embankment from the top. Then an inclinometer is pulled through the tube from the bottom up. In that way the angle with relation to the gravity can be measured at each position. The inclinometers data can then be used to calculate the deformation of a section of the embankment.

For the FEM simulations of the asymmetrical soil layer the results are compared to the data of the inclinometers.

The top 4 measurements of the inclinometer are not suitable for the comparison since these measurements are very sensitive to small movements which do not relate to the embankments behaviour. One of the reasons is that the top of the inclinometers tube has been in collision with a vehicle and has therefore deformed the device top. The deeper located measurements on the other hand do give a representative value.

In the plaxis model a section is made at approximately the same location as the inclinometer. This is in the top of the embankment on the side of the concrete structure. This gives the horizontal displacement of the section in the following location. The section is taken from the top till a depth of 13m which is the depth of the inclinometer.

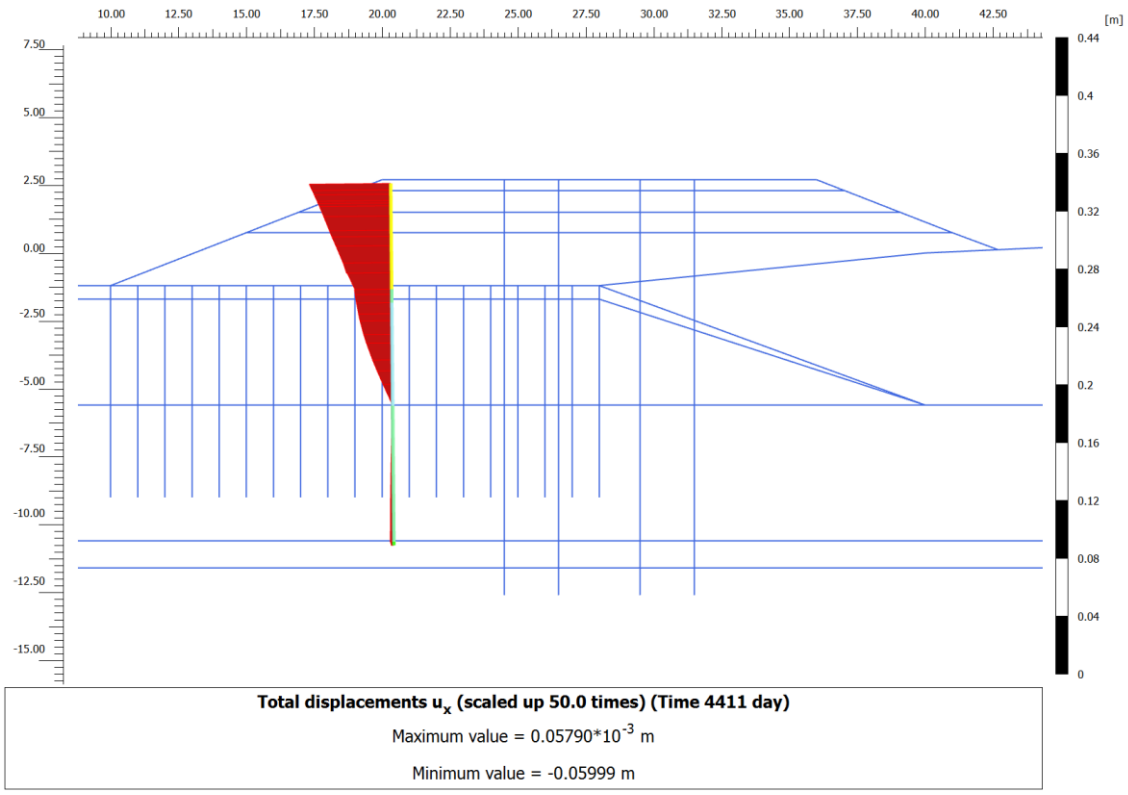

The measurements of the inclinometer and the section of the plaxis model are given in the following graph. The displacement from the inclinometer is taken at 6/9/2016 which is approximately 12 years after construction of the superstructure. The plaxis model is approximately 11 years (4000days) after the construction of the superstructure. The

displacement shows a very similar behaviour to a depth of -5m. Above this the measurements in the inclinometer are a bit higher than for the model. Nevertheless, the results give a decent comparison that the model is suitable the analysis

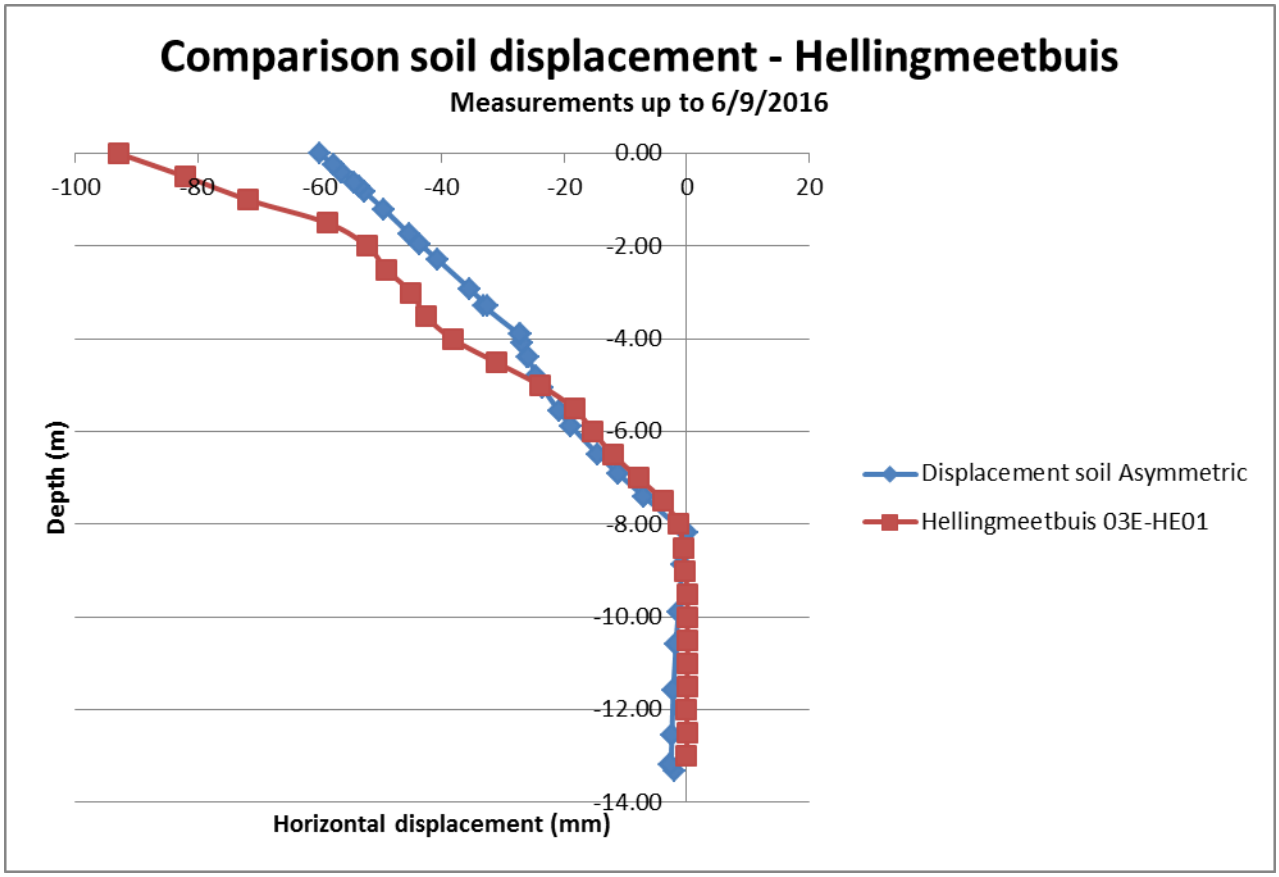

D. Horizontal displacement of foundation pile over depth

For the 4 different cases the results are plotted after a consolidation period of 4000 days after the construction of the foundation pile. The displacements are the residual displacements since construction and do not include immediate deformation. The graph shows the displacement of the most left foundation pile in the model. The horizontal displacement is shown over the depth.

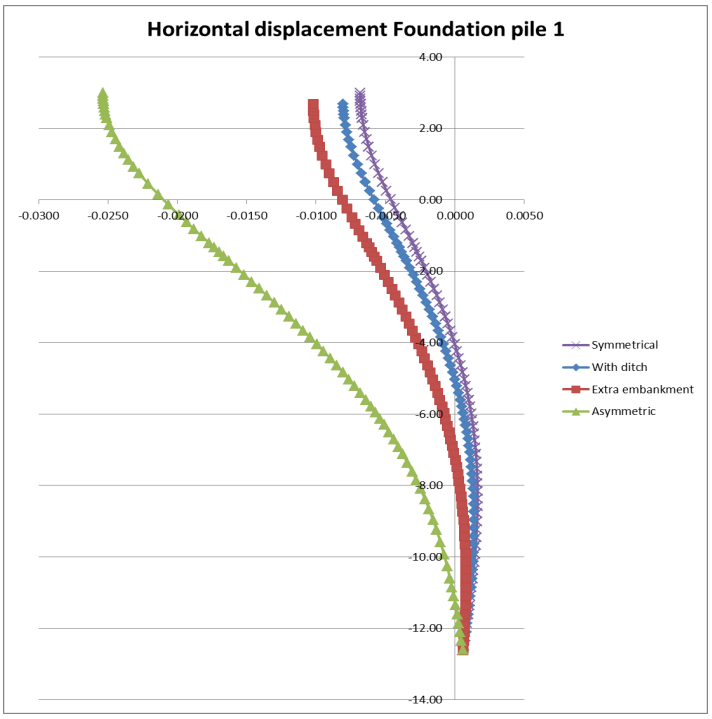

From the graph we see large differences in the total displacement, but similar shapes of the deformed pile. As expected the symmetrical basic case shows the smallest displacement, which means it's clear to see the impact of the changing surrounding conditions.

Case	Max displacement	Difference to Case 0 (mm)	difference Case 0 (%)
Symmetrical	-6.80755	0.00000	100%
With ditch	-8.09425	-1.28670	119%
Extra embankment	-10.20211	-3.39455	150%
Asymmetric	-25.35122	-18.54367	372%

The ditch on the western side of the embankment influences the deformation slightly by increasing the displacement with 1.29mm which is a difference of 119%.

The extra embankment on the eastern side of the structure has more influence on the deformations and causes an extra displacement of 3.39mm which is a difference of 150% to the symmetrical case. The asymmetric case has the largest influence as expected. The extra displacement is 18.54mm which is a difference of 372% with the symmetrical case.

E. Results unsupported model

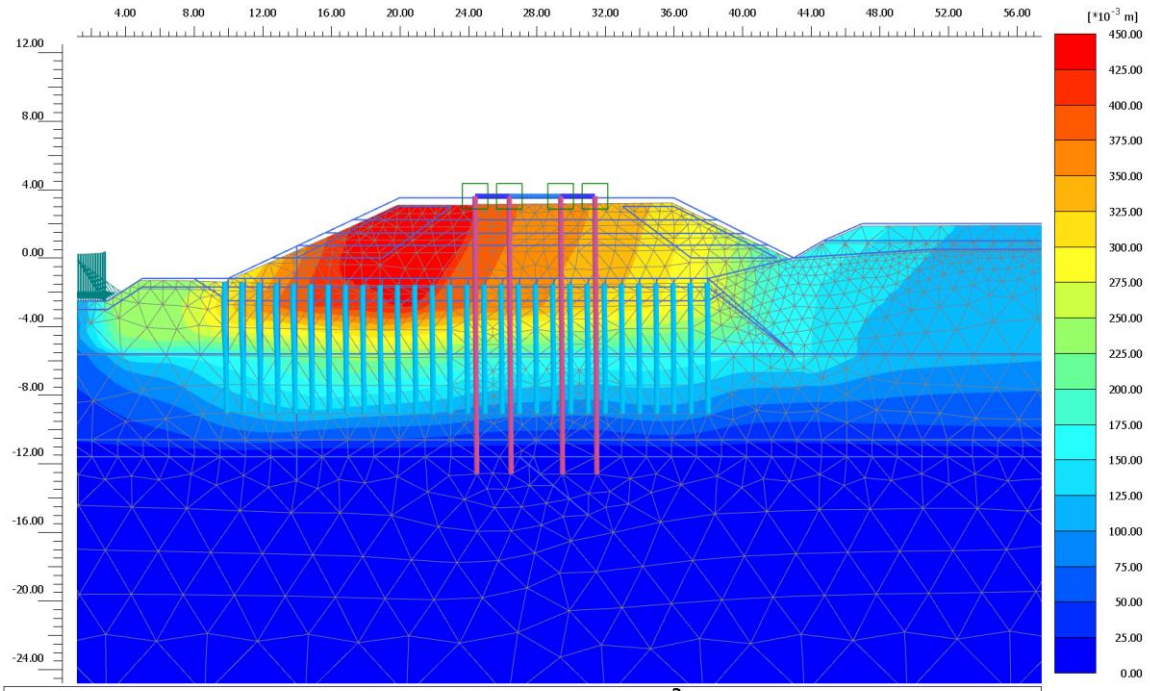

Total displacements |u| (Time 10.77*10^3 day)

Maximum value = 0.4454 m (Element 148 at Node 700)

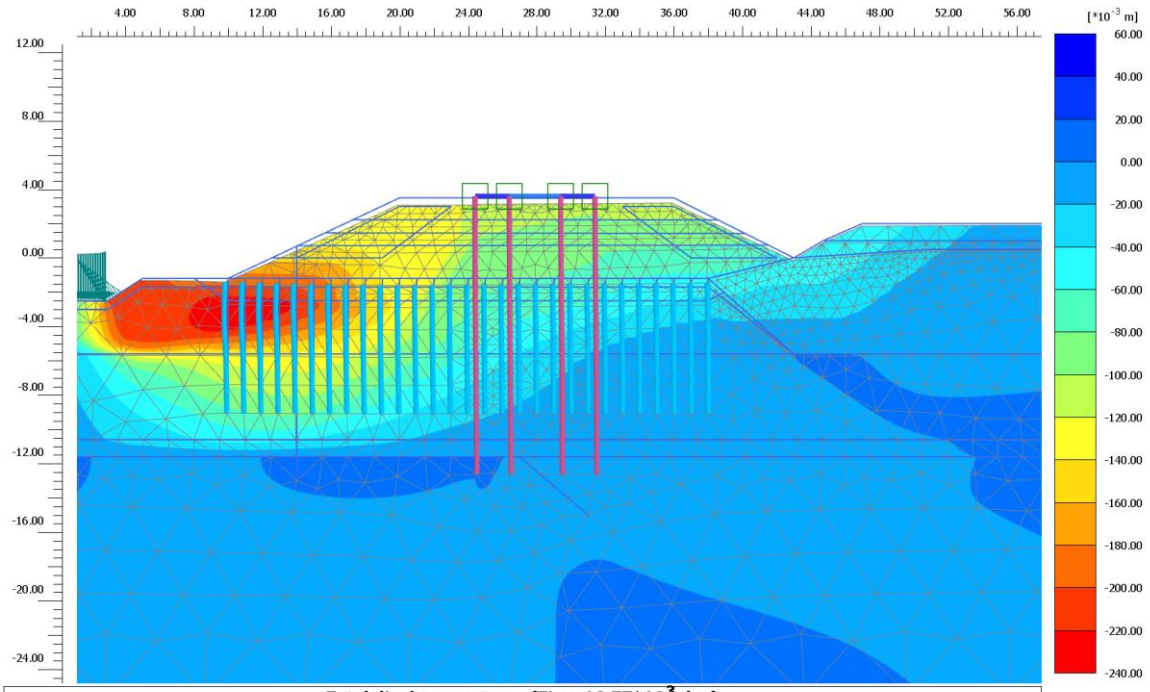

Total displacements u_x (Time 10.77*10^3 day)

Maximum value = 0.04110 m (Element 856 at Node 2271)

Minimum value = -0.2377 m (Element 1546 at Node 3744)

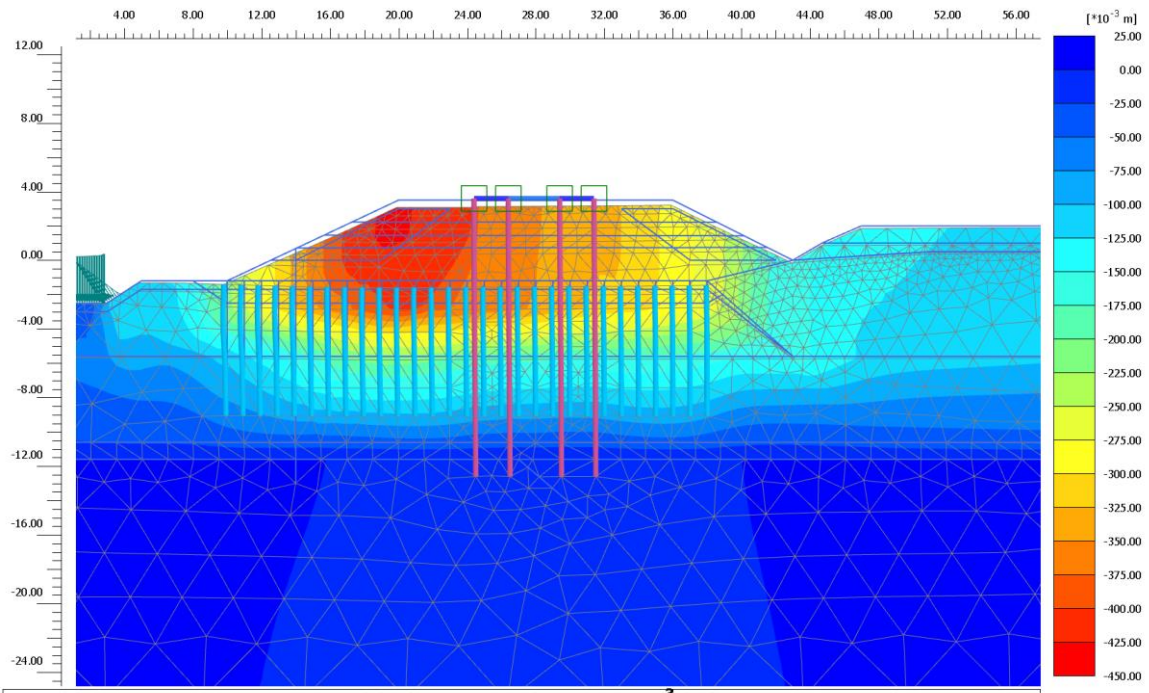

Total displacements u_y (Time $10.77*10^3$ day)

Maximum value = $0.2707*10^{-3}$ m (Element 2220 at Node 8348)

Minimum value = -0.4268 m (Element 118 at Node 539)

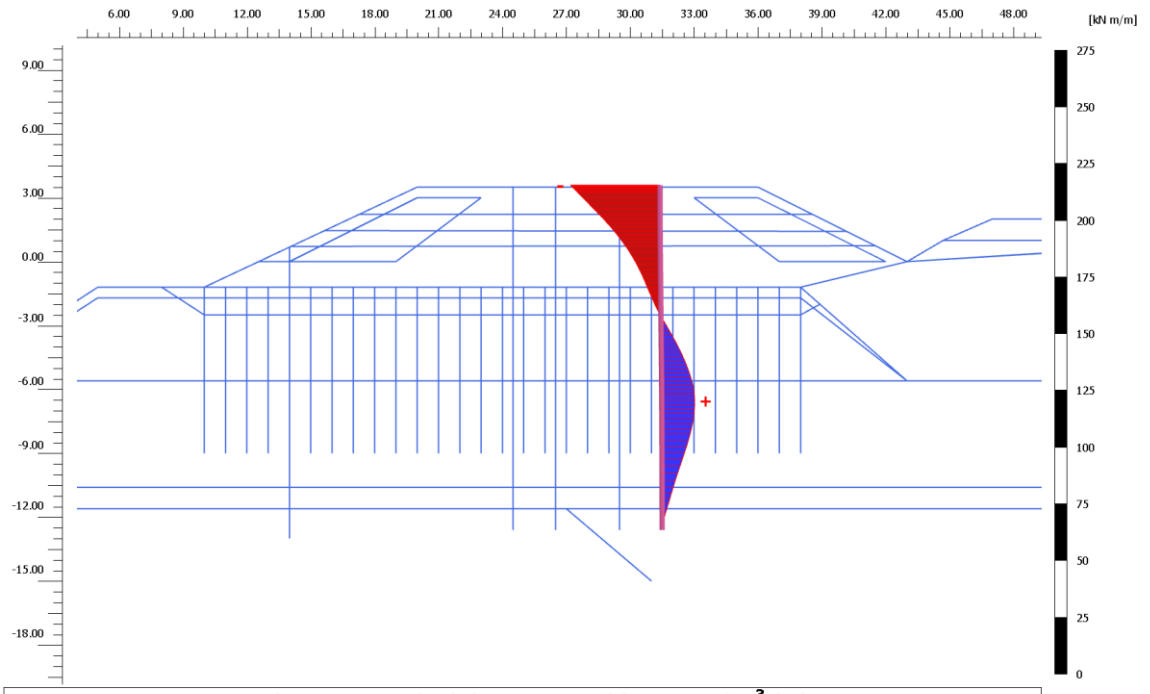

Bending moments M (scaled up 0.100 times) (Time $10.77*10^3$ day)

Maximum value = 15.49 kN m/m (Element 75 at Node 23557)

Minimum value = -41.98 kN m/m (Element 61 at Node 23500)

F. Results supported model

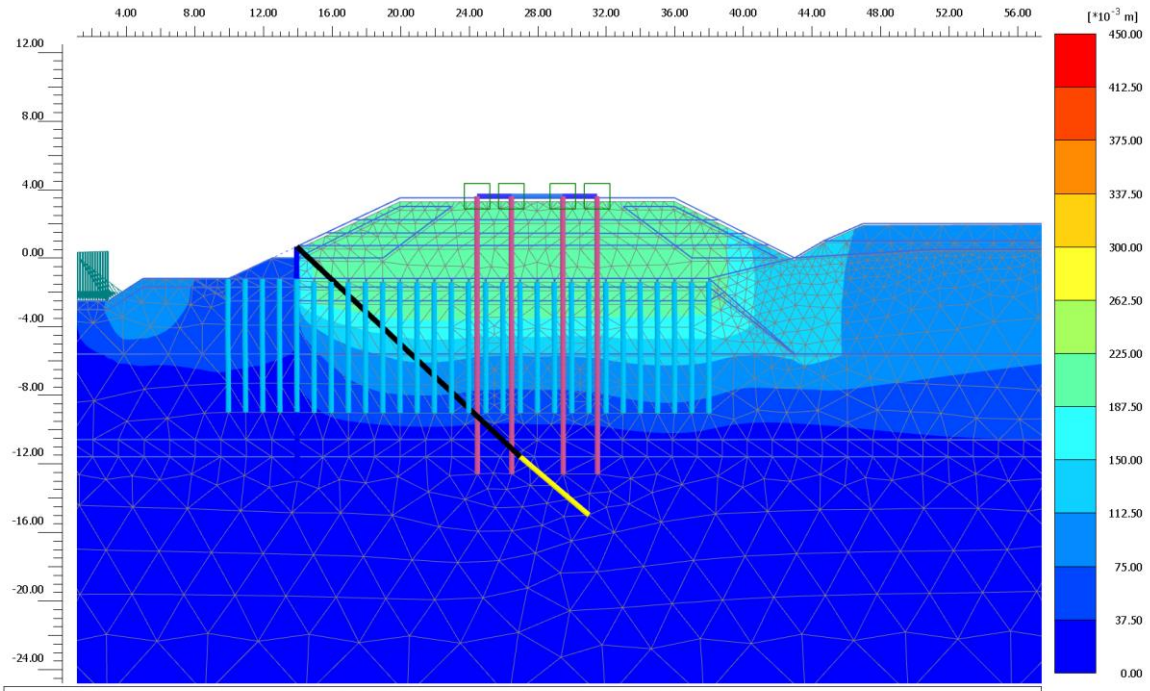

Total displacements |u| (Time 5773 day)

Maximum value = 0.2237 m (Element 291 at Node 676)

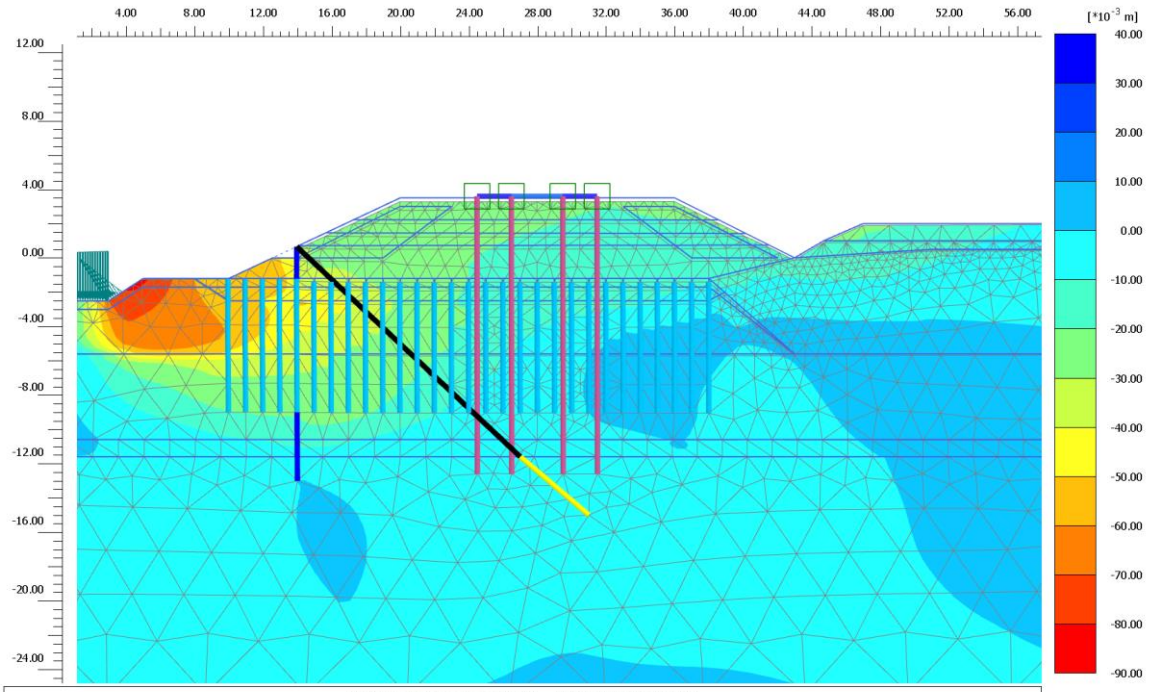

Total displacements u_x (Time 5773 day)

Maximum value = 0.03417 m (Element 856 at Node 2271)

Minimum value = -0.08321 m (Element 847 at Node 1970)

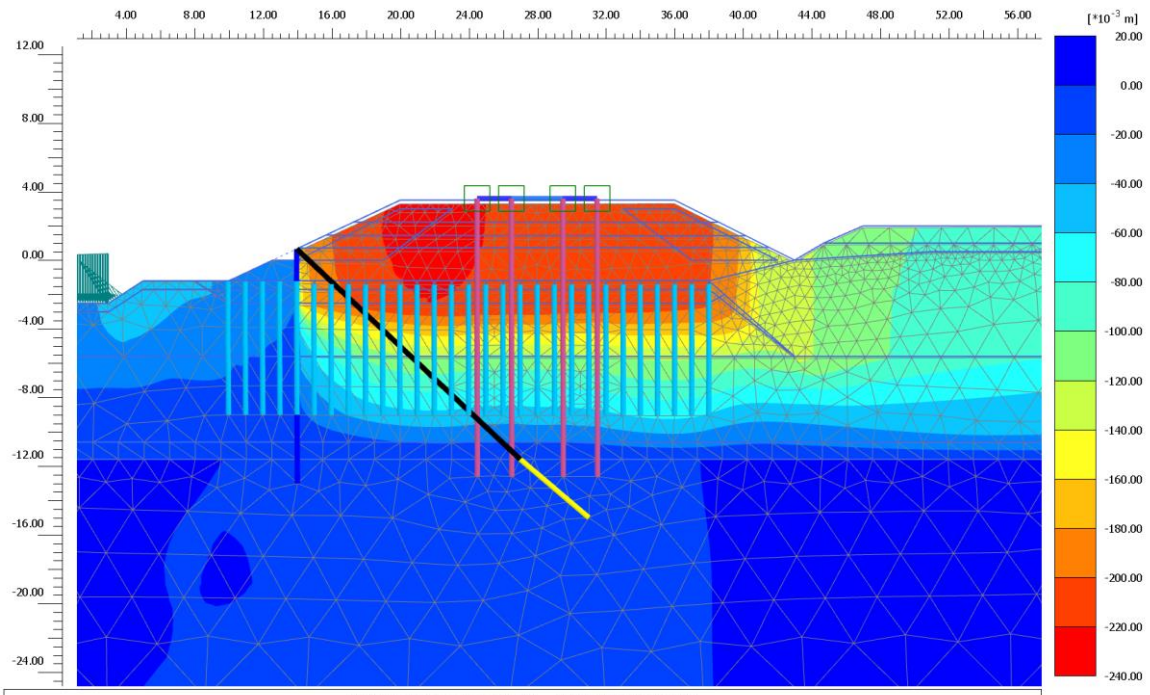

Total displacements u_y (Time 5773 day)

Maximum value = $0.3074*10^{-3}$ m (Element 2229 at Node 4972)

Minimum value = -0.2227 m (Element 291 at Node 677)

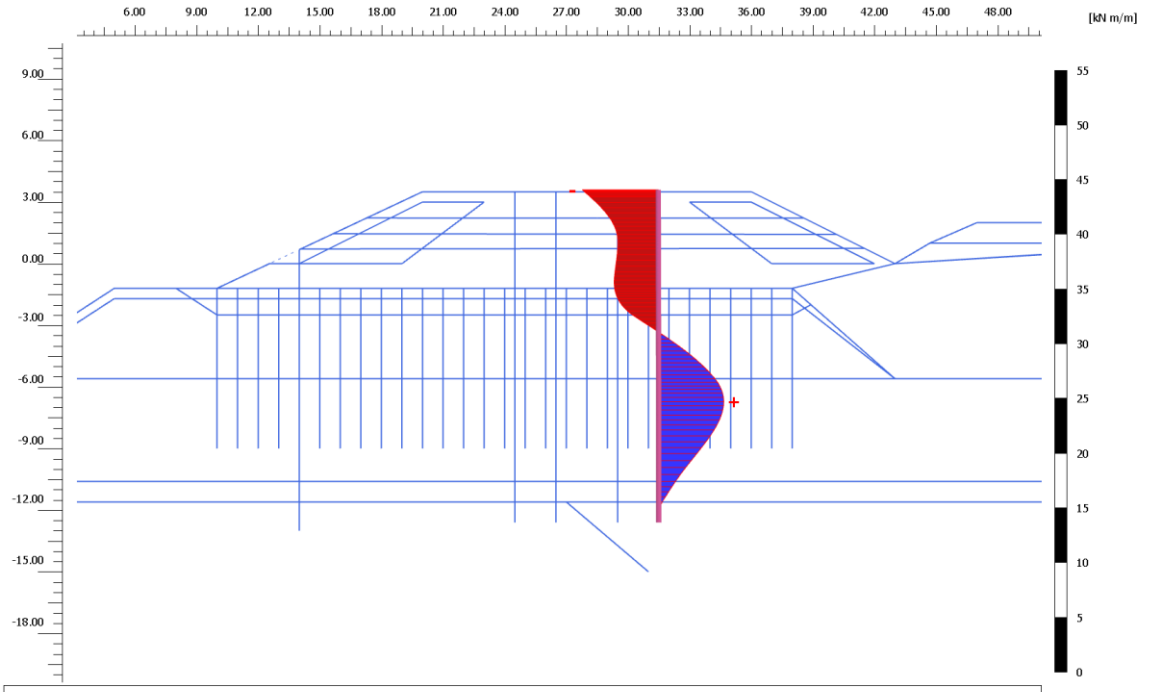

Bending moments M (scaled up 0.500 times) (Time 5773 day)

Maximum value = 6.338 kN m/m (Element 75 at Node 23558)

Minimum value = -7.404 kN m/m (Element 61 at Node 23500)

G. Results Sheetpile long term

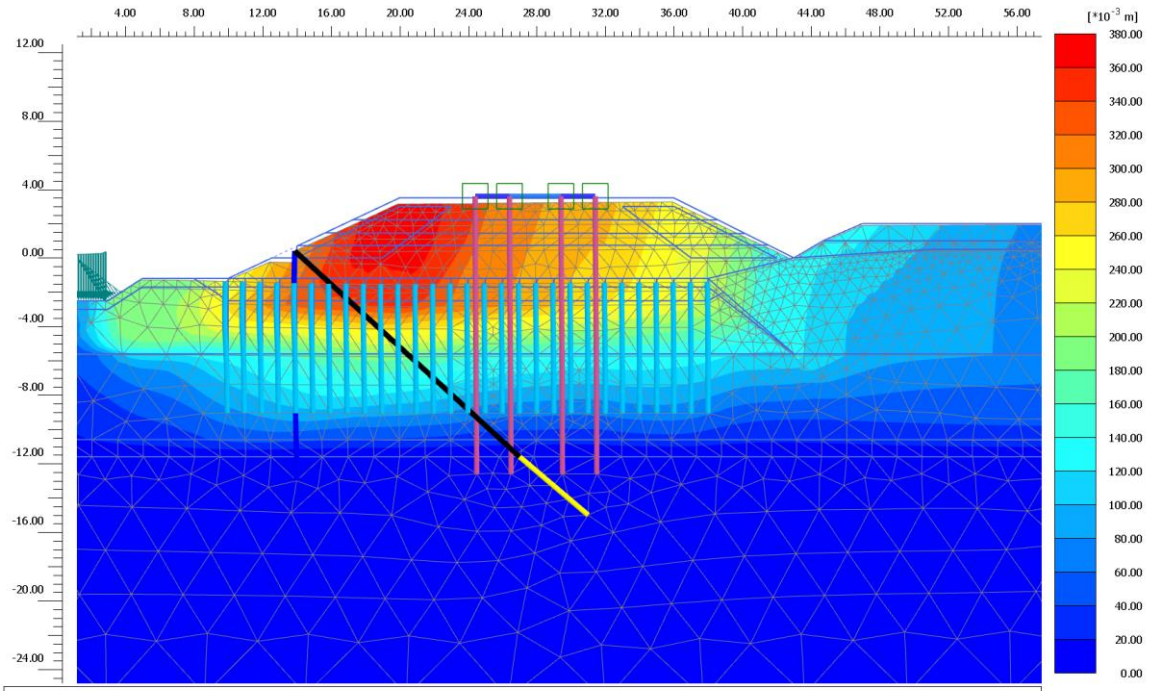

Total displacements |u| (Time 5773 day)

Maximum value = 0.3703 m (Element 34 at Node 269)

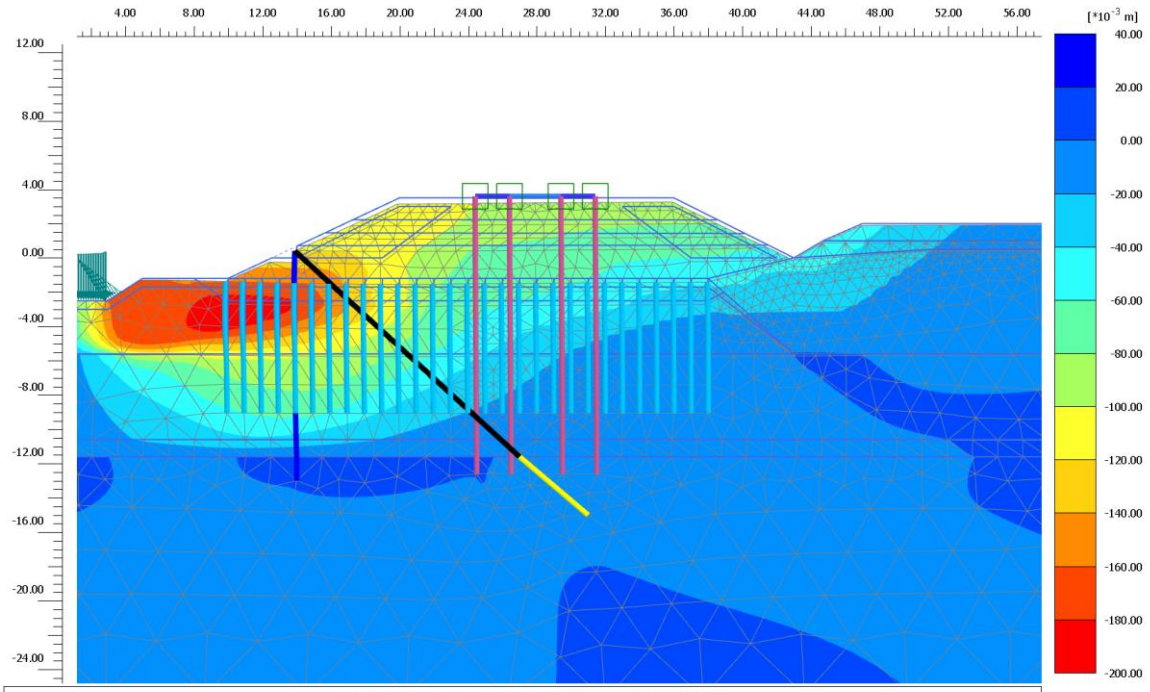

Total displacements u_x (Time 5773 day)

Maximum value = 0.03188 m (Element 856 at Node 2271)

Minimum value = -0.1962 m (Element 1546 at Node 3744)

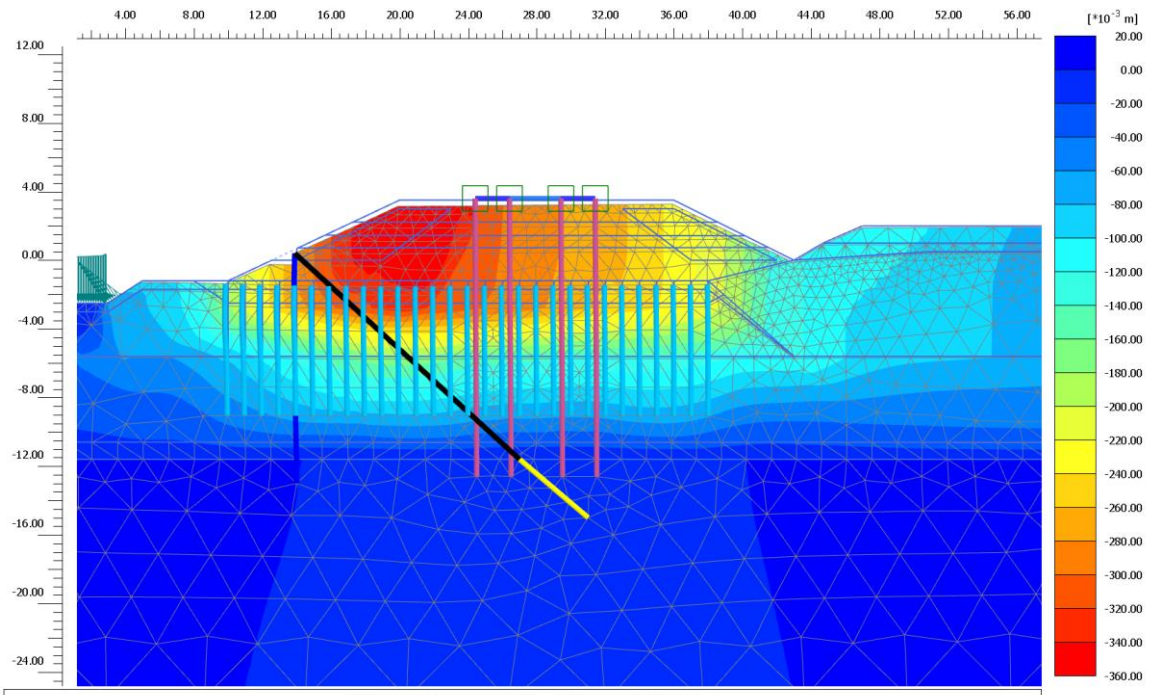

Total displacements u_y (Time 5773 day)

Maximum value = $0.2646*10^{-3}$ m (Element 2229 at Node 4972)

Minimum value = -0.3550 m (Element 117 at Node 369)

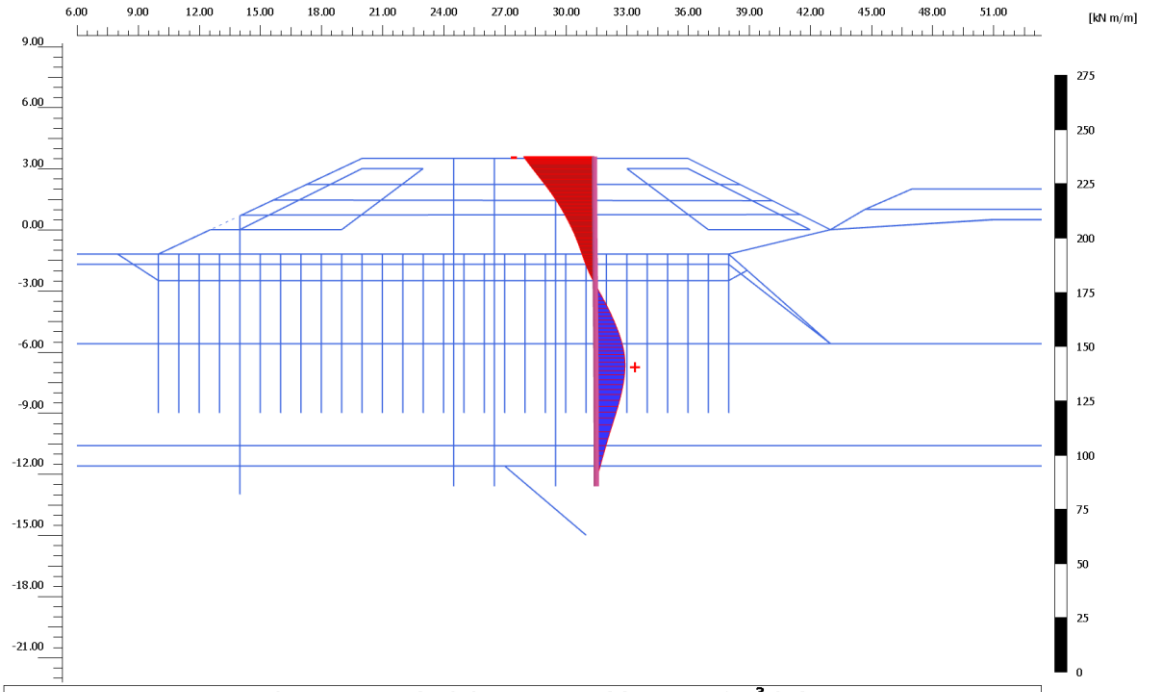

Bending moments M (scaled up 0.100 times) (Time $10.77*10^3$ day)

Maximum value = 14.26 kN m/m (Element 75 at Node 23558)

Minimum value = -34.90 kN m/m (Element 61 at Node 23500)

H. Results EPS East side

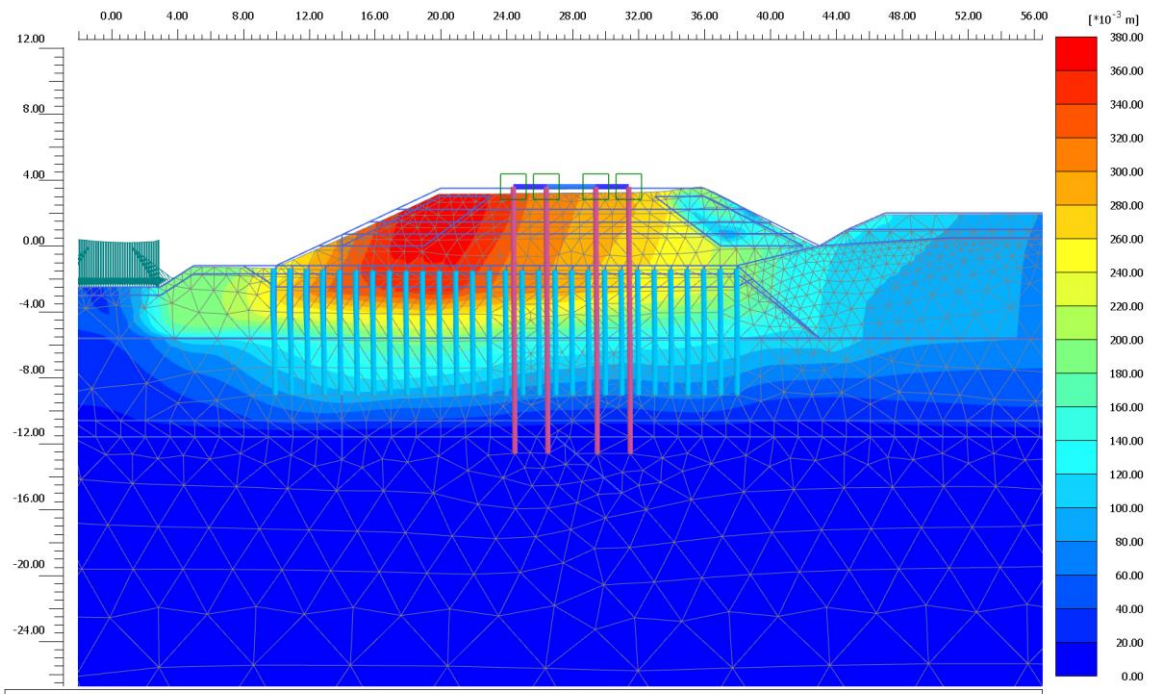

Total displacements |u| (Time 5773 day)

Maximum value = 0.3723 m (Element 34 at Node 269)

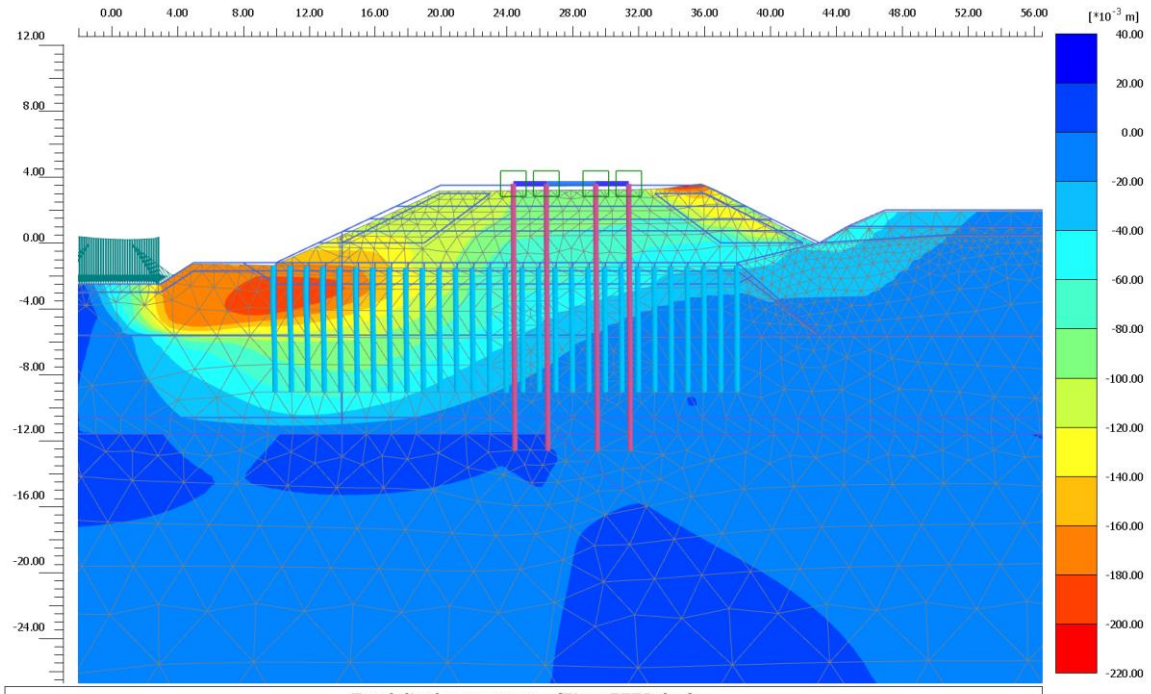

Total displacements u_x (Time 5773 day)

Maximum value = 0.03152 m (Element 856 at Node 2271)

Minimum value = -0.2103 m (Element 16 at Node 5082)

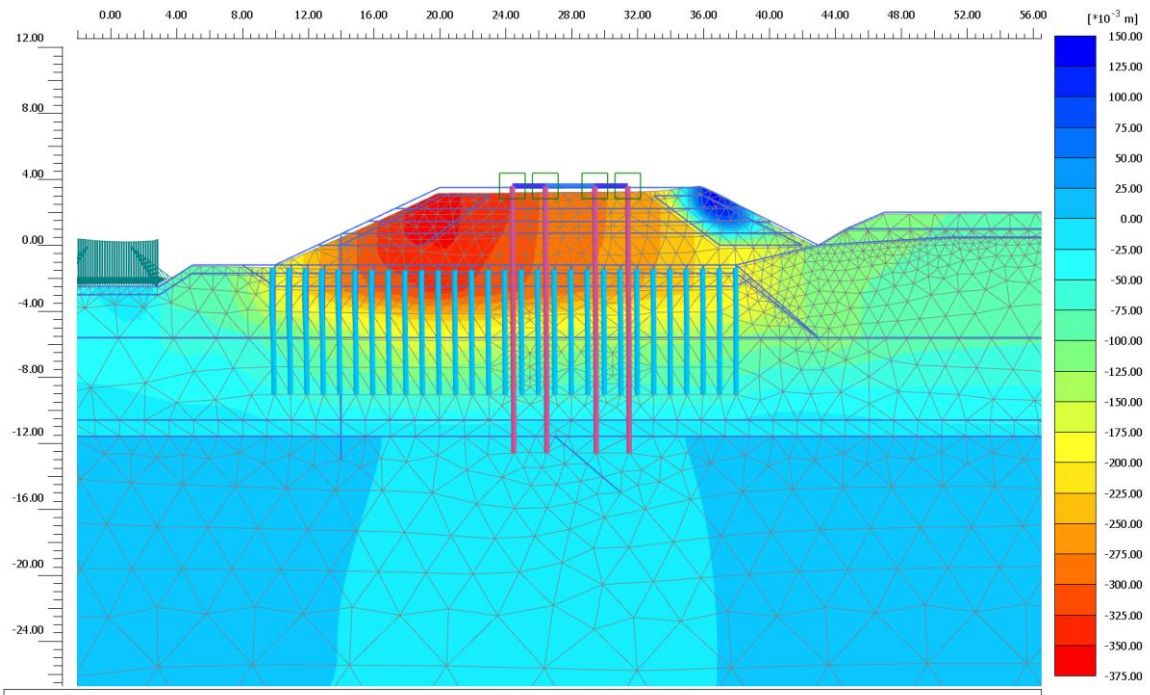

Total displacements u_y (Time 5773 day)

Maximum value = 0.1334 m (Element 128 at Node 6098)

Minimum value = -0.3563 m (Element 117 at Node 369)

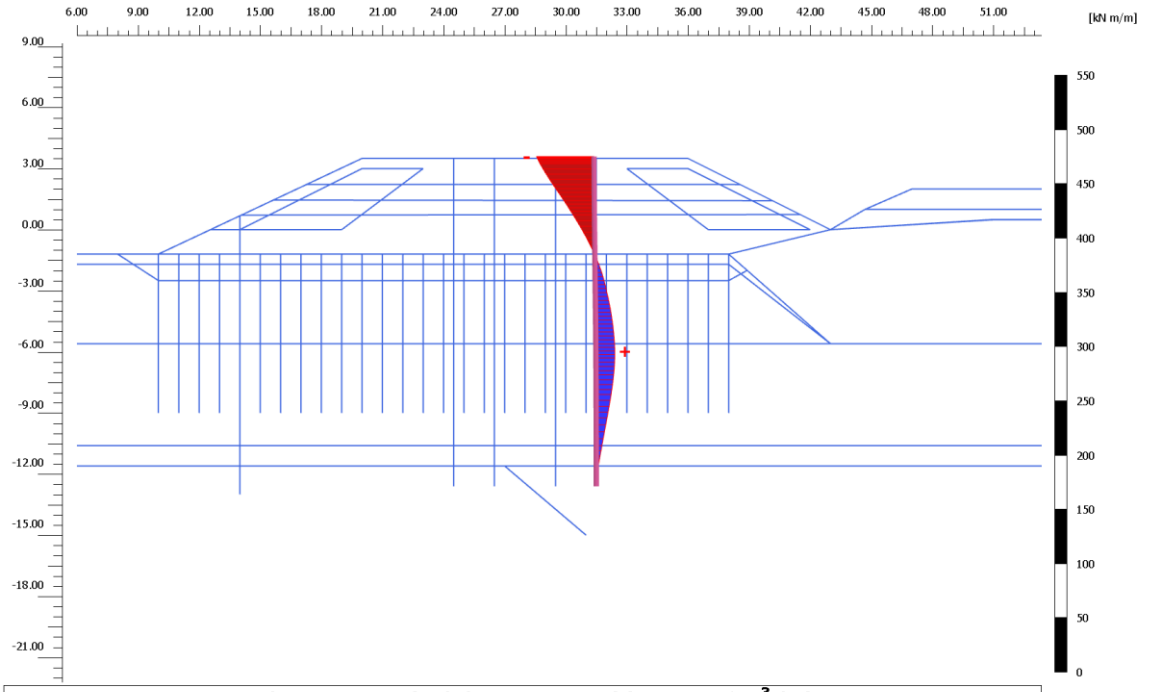

Bending moments M (scaled up 0.0500 times) (Time $10.77*10^3$ day)

Maximum value = 18.56 kN m/m (Element 74 at Node 23554)

Minimum value = -56.66 kN m/m (Element 61 at Node 23500)

I. Results EPS west side

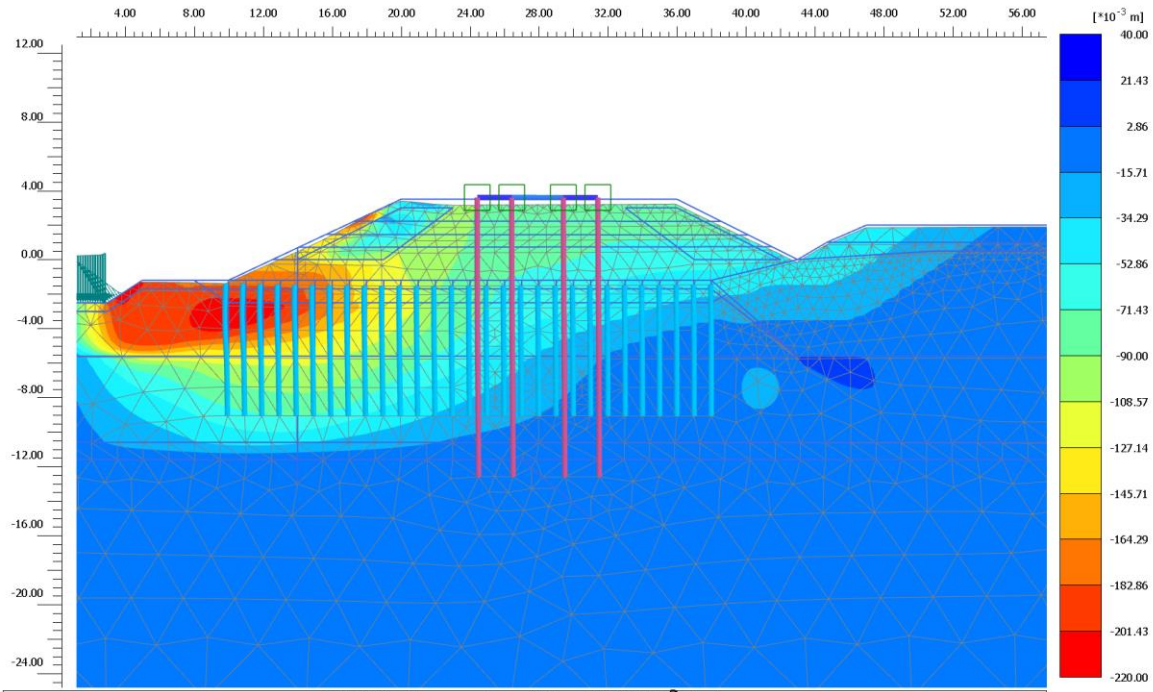

Total displacements u_x (Time $10.77*10^3$ day)

Maximum value = 0.04242 m (Element 856 at Node 2271)

Minimum value = -0.2145 m (Element 1508 at Node 3760)

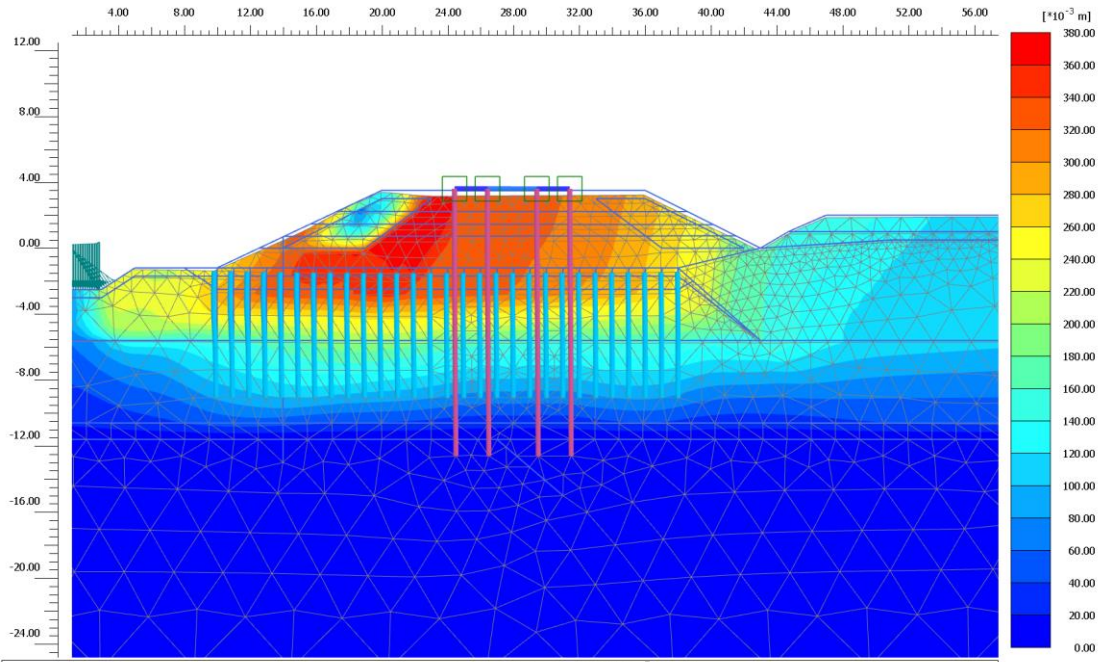

Total displacements |u| (Time $10.77*10^3$ day)

Maximum value = 0.3716 m (Element 47 at Node 120)

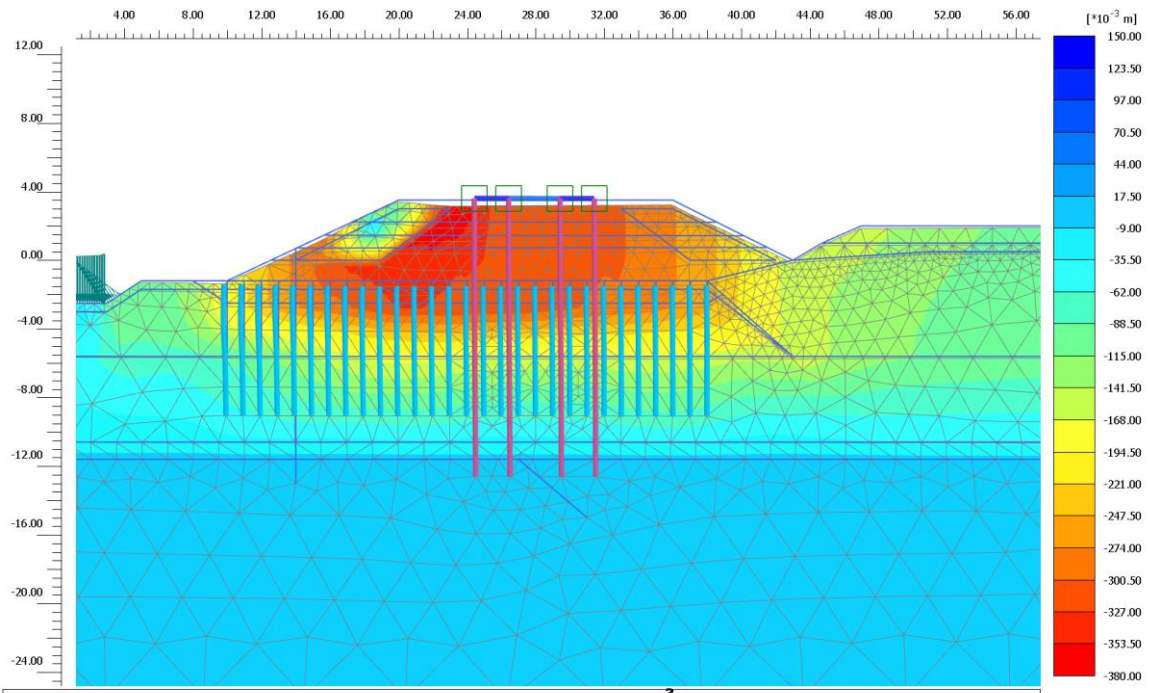

Total displacements u_y (Time $10.77*10^3$ day)

Maximum value = $0.4463*10^{-3}$ m (Element 2222 at Node 8342)

Minimum value = -0.3602 m (Element 47 at Node 120)

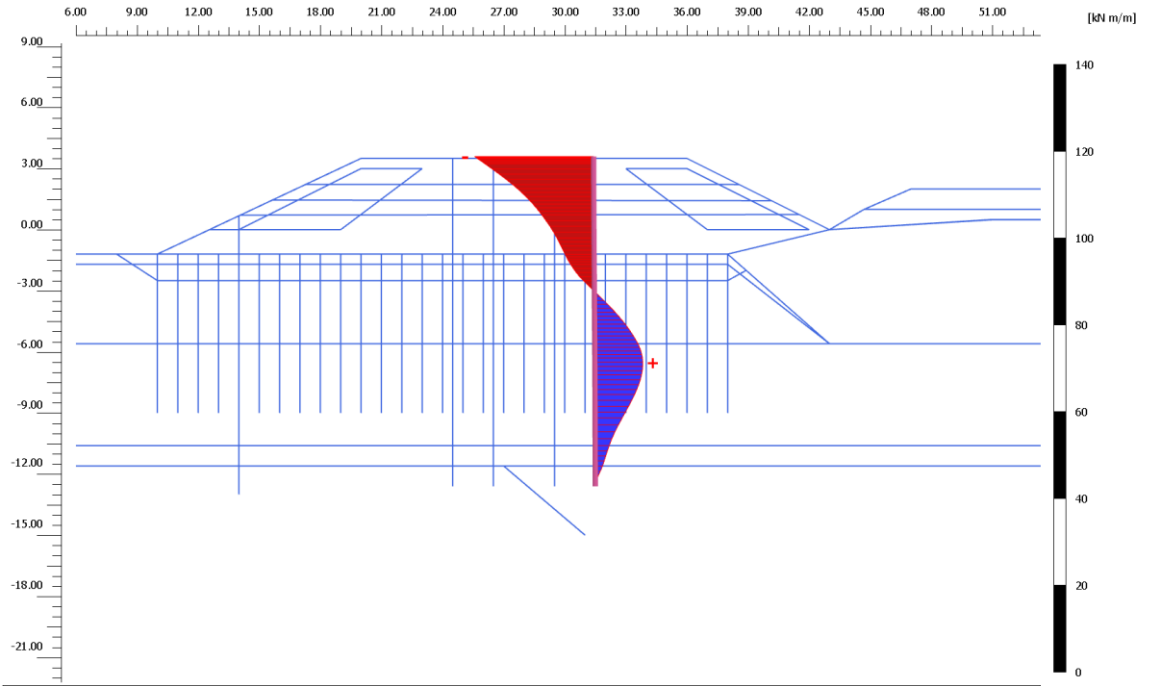

Bending moments M (scaled up 0.200 times) (Time $10.77*10^3$ day)

Maximum value = 11.75 kN m/m (Element 75 at Node 23557)

Minimum value = -29.23 kN m/m (Element 61 at Node 23500)

J.GNSS measurements

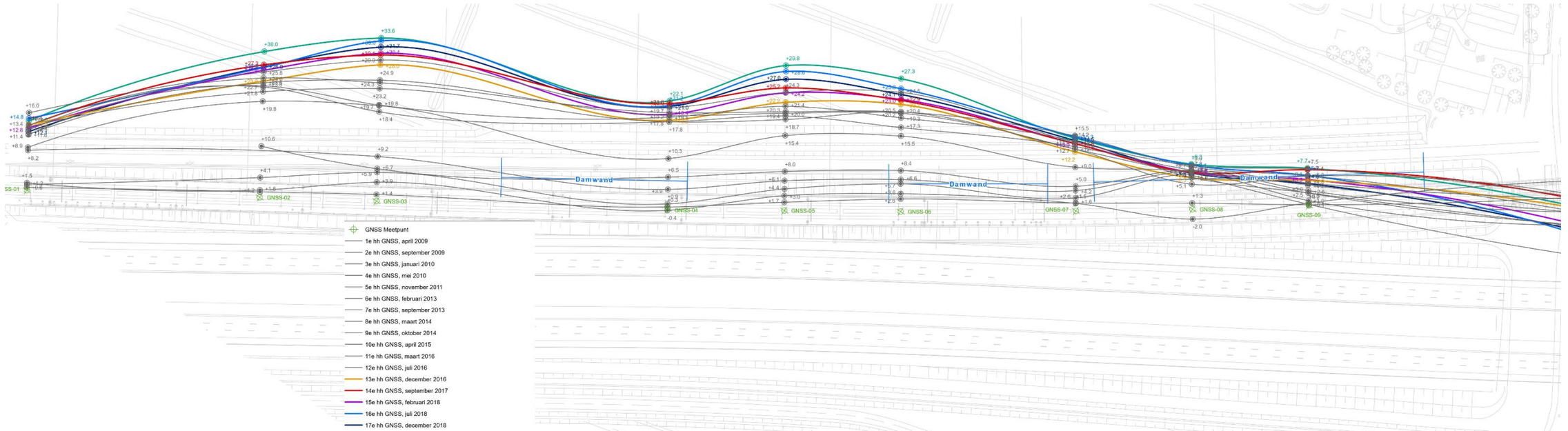

18th repetitive GNSS measurements Horizontal displacement (with regard to zero measurement 2009) (displacements perpendicular to the rail axis in mm)

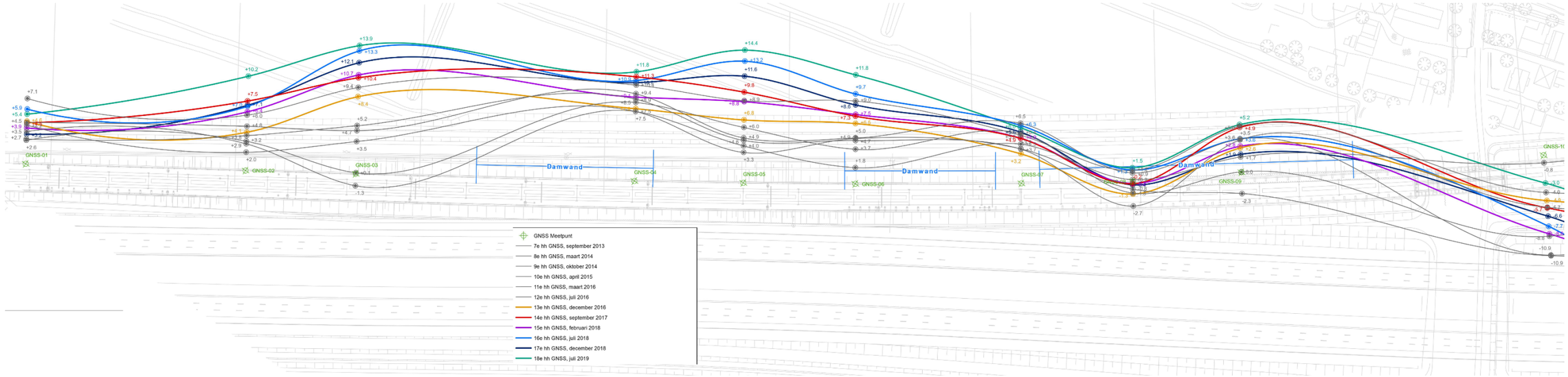

18th repetitive GNSS measurements Horizontal displacement (with regard to zero measurement 2013) (displacements perpendicular to the rail axis in mm)

K. Timeline case study Rijpwetering

PERIODE	DOOR	REFERENTIE	DATUM	BESCHRIJVING	AC-nr	TYPE
feb 2002;	Staat		28-2-2002	Ontwerp geaccepteerd door de Staat		ACC / OPLEVERING
Jul 2002- jul 2004	Bouwcomb	pag 144 blz 7	jul 2003 [zuid Rijpw]	Aanleg aardebaan		REALISATIE
jan 2003 - jul 2004	GeoDelft	pag 144 blz 8	nov 2006;	Metingen en analyses in opdracht van Bouwcomb		MONITORPROGRAMMA
Mrt 2003;	Bouwcomb	pag 144 blz 7	8-2-2003;	Afschuiving gevolgd door plaatsen deel ankerscherm [33.200-33.320] [langs Rijpwetering]		HERSTELMAATREGEL
aug-2003;	BeauDrains	pag 332 blz 5	8-1-2004	Vvrijgave Rijpwetering Noord [km 33.390-33.500]		ACC / OPLEVERING
Jan 2004;	Bouwcomb	pag 144 blz 7	20-01-2004;	Afschuiving gevolgd door plaatsen deel ankerscherm [33.000-33.200]		HERSTELMAATREGEL
Mrt 2004;	BeauDrains	pag 337 blz 6	14-9-2004;	Vrijgave deel [33.240-33.350]		ACC / OPLEVERING
Mrt 2004;	BeauDrains	pag 337 blz 6	14-9-2004;	Vrijgave deel [33.040-33.240]		ACC / OPLEVERING
jul 2004;	Bouwcomb	pag 257 pag 1	20-8-2010;	Vrijgave voor constructie van ZVP [Staat]		ACC / OPLEVERING
sept 2004;	BeauDrains	pag 337 blz 6	14/9/2004;	Eindrapportage BeauDrain [sept 2004]; => consolidatie nog lang niet voltooid		RAPPORT
aug 2004;	Bouwcomb	pag 178 pag 5	aug-2004;	Heien van palen voor de ZVP		HERSTELMAATREGEL
Okt 2004;	Deltares	pag 144 blz 8	1-8-2012	Aanbrengen EPS volgens rapport Deltares, eerder advies GeoDelft [33.045-33.339		HERSTELMAATREGEL
Okt 2004;	Bouwcomb	pag 316	okt 2004;	Storten ZVP		REALISATIE
Dec 2004;	Fugro	pag 178 pag 3	28-11-2006	Oplevering aardebaan aan de Staat		ACC / OPLEVERING
Dec 2005;	GeoDelft	pag 144 blz 8	nov-06	Oplevering van de totale onderbouwconstructie aan Staat.		ACC / OPLEVERING
Mrt 2005 - heden ???	Deltares	pag 257 pag 1	20-8-2010;	Zettings metingen door staat		MONITORPROGRAMMA
jan 2005 - jun- 2006	GeoDelft	pag 178 blz 3	28-11-2006;	Metingen horizontale vervormingen terp		MONITORPROGRAMMA
Apr 2005 - dec 2007	Deltares	pag 257 pag 2	feb-08	Waterspanningsmetingen door staat		MONITORPROGRAMMA
apr-2005;	Deltares	pag 257 pag 1	20-8-2010;	Plaatsen extentsiometers [km 33.170 en 33.300]		MONITORPROGRAMMA
apr-2005;	Deltares	pag 257 pag 1	20-8-2010;	Meting; km 33.170 damwand effect en km 33.300 damwand geen effect [> hor en vert verplaatsing].		METING
Mrt 2005 - sept 2007	Arcadis	pag 194 blz 4	28-3-2008	Metingen van verplaatsingen [Arcadis]		MONITORPROGRAMMA
Mrt 2006;	GeoDelft	pag 144 blz 9		Metingen; grotere zettingen en hogere waterspanningen.		METING
April + juni 2006	IFS	plattelloverzichter	1-4-2006	Platteln binnen km 131.900 en 134.150	AC?	HERSTELMAATREGEL
mei 2006 - jul 2006	Bouwcomb	pag 215	15-5-06 tot 15-07-06	Verankerde damwand geplaatst.		HERSTELMAATREGEL
aug 2006 - dec 2006	IFS	pag 215	26-11-2007;	vervangen van de bovenbouwconstructie [km 32.765 - km 33.561]		HERSTELMAATREGEL
nov-2006;	GeoDelft	pag 144 blz 9	nov-06	rapportage grotere verplaatsingen dan voorspellingen		RAPPORT
nov 2006;	Prof Verruijt	pag 190 blz 3	15/11/2006;	eindrapportage BeauDrain [sept 2004]; consolidatie nog lang niet voltooid		RAPPORT
28-11-2006;	Fugro	pag 167 e.v.	28-11-2006;	18 mnd na 2004 meting van te grote zettingen		RAPPORT
okt 2006 - nov 2006	IFS	pag 215	okt - nov 2006;	testritten 300 km/uur		COMMUNICATIE
nov 2007;	Staat	pag 331	23-11-2007;	Damwandscherm niet voor beheer Infraspeed		COMMUNICATIE
jan 2008;	Staat			overdracht aan Infraspeed muv damwandscherm		ACC / OPLEVERING
jan 2007;	IFS	plattelloverzichter	1-1-2007	Platteln binnen km 131.900 en 134.150		HERSTELMAATREGEL
mrt 2008;	Arcadis	pag 209 blz 34	28-3-2008;	ten zuiden van brug oplopende deformatie, door tweede aanspanning van ankers teruggedrongen, maar zet zich in laatste metingen in noordwesten weer door.		RAPPORT
mei 2008;	Staat	pag 226 blz 19		zijdelingse verplaatsingen groter dan verwacht, aanpassingen van bevestigingsconstructie. 32.765-33.561 en nastelbaarheid excentrisch 33.100-33.259		HERSTELMAATREGEL
mei-2008;	Staat	pag 226 e.v	29-5-2008	(1) rapportage damwand- historie en maatregelen (2) onderdeel aanvullende maatregelen.		RAPPORT
aug-2009;	Staat	pag 289 blz 3	8-8-2009;	opname einde garantie termijn, vaststelling paalbreuk.		RAPPORT
aug 2010;	Deltares	pag 257 e.v.		analyse zettingsmeting		RAPPORT
mrt 2011 - mei 2011;	Bouwcomb	pag 268 blz 7		Herstel randbalk en paal nabij KW Zuidweg (KW1408)	AC0147	HERSTELMAATREGEL
apr-2012;	DHV	pag 252 blz 2	20-4-2012	zettingen zetten nog steeds lineair door. Blijven monitoren		ZETTING
dec-2011;	DHV	pag 342	13-12-2011;	onderzoek verplaatsing oplegblokken kunstwerk		RAPPORT
aug-2012;	Deltares	pag 321 blz 9	1/8/2012;	Landhoofd; analyse buigendemomenten in palen; opneembaarheid van de belasting maakt geen deel uit van de opdracht		RAPPORT
okt 2012;	Bouwcomb	pag 289 e.v.	5-10-2012;	Controle berekening palen;		RAPPORT
nov 2006;	Staat	pag 294	28/11/2006;	Inspectiepad; Melding aan IFS verwachting grotere zettingen, mogelijk herleggen kabelkokers noodzakelijk. Indien > 30 cm, zal dit in overweging worden genomen		COMMUNICATIE
apr-2011 mrt 2012	expertoverleg	pag 45 e.v.	27-4-2011;			RAPPORT
nov-2011;	expertoverleg	pag 294	1-6-2012	Melding van incidentele zakkingen kabelgoten en randbalken over lengte 1500 m.		RAPPORT
okt, nov-2011 + apr 2012;	IFS	pag 306	15-11-2011+26-4-2012;			COMMUNICATIE
mei 2012;	Staat	pag 309	16 + 30 mei 2012	Inspectiepad; Afwijzing claim		COMMUNICATIE
aug 2012;	IFS	pag 313	23/8/2012;	Inspectiepad; Herindienen claim met volledige onderbouwing historie		COMMUNICATIE
sept	Staat	pag 315 blz 2	26-9-2012	Inspectiepad; Zetting in 2030 beperkt tot 30 cm.		RAPPORT
sept - okt 2012	Staat	pag 315	26/9/2012 - 1/10/2012	Inspectiepad; Afwijzing claim		COMMUNICATIE
apr-2011;	expertoverleg	pag 45 e.v.		Overschrijding hor verplaatsing baan [km 133.250]		< > HOR. VERPLAATSING
nov 2011, mrt 2012;	expertoverleg	pag 45 e.v.		Hor verplaatsing baan [km 133.240-133.250]		< > HOR. VERPLAATSING
jul-2012 + okt 2012;	expertoverleg	pag 48		overschrijd intervent. hor verplaatsing baan [km 133.240-133.250]		< > HOR. VERPLAATSING
okt 2012;	IFS			Aanvulling porfier en ophalen leidingen en goten.		HERSTELMAATREGEL
dec 2012 + sept 2013 + dec 2013;	expertoverleg	pag 49		Overschrijd intervent. hor verplaatsing baan [km 132.6-133.6]		RAPPORT
jun 2014;	Bouwcomb	6164-ZVP-ALG-	1-7-2014	Aanpassing randelement zuidelijk landhfd KW Zuidweg (KW14	AC0356	HERSTELMAATREGEL
aug 2014;	Expo_Geo_HSL	12-09-2014	wk 33 2014	Opvulling holle ruimtes onder ZVP [132.850-133.600]. Tot 40 cm zand aangebracht, vooral tpv damwanden is veel zand		HERSTELMAATREGEL
sept 2014;	Expo_Geo_HSL	plattelloverzichter	1-9-2014	Geometrie in gebied km 131.4 – km 132.4 geplatteld		HERSTELMAATREGEL
sept 2014;	Expo_Geo_HSL	plattelloverzichter	1-9-2014	Geometrie in gebied km 132.6 – km 133.6 geplatteld		HERSTELMAATREGEL
sept 2014;	Expo_Geo_HSL	plattelloverzichter	1-9-2014	Geometrie in gebied km 133.8 – km 134.8 geplatteld		HERSTELMAATREGEL
jan-2016	IFS	IAV(IMC#CIVSTM&WOD # 000845		Scheurvorming paalkoppen km 132.800 tot 133.400	AC0178?	RAPPORT